Western University

Scholarship@Western

2009

ENCAPSULATION AND CONTROLLED RELEASE OF rh-ERYTHROPOIETIN FROM BIOPOLYMER NANOPARTICLES

Mehrdad Bokharaei

ENCAPSULATION AND CONTROLLED RELEASE OF rh-ERYTHROPOIETIN FROM BIOPOLYMER NANOPARTICLES

(Spine title: ENCAPSULATION AND CONTROLLED RELEASE OF rh-ERYTHROPOIETIN)

(Thesis Format Monograph)

By

Mehrdad <u>Bokharaei</u>

Graduate Program in Engineering Science

Department of Chemical and Biochemical Engineering

A thesis submitted in partial fulfillment
of the requirements for the degree of

Master of Engineering Science

The School of Graduate and Postdoctoral Studies

The University of Western Ontario

London, Ontario, Canada

THE UNIVERSITY OF WESTERN ONTARIO
SCHOOL OF GRADUATE AND POSTDOCTORAL STUDIES

CERTIFICATE OF EXAMINATION

Supervisor

Examiners

_____

_____

Dr. Argyrios Margaritis

Dr. Dimitre Karamanev

_____

Dr. David J. Freeman

_____

Dr. Mita Ray

The Thesis by

Mehrdad Bokharaei

Entitled

Encapsulation and Controlled Release of rh-Erythropoietin from Biopolymer Nanoparticles

is accepted in partial fulfillment of the
requirements for the degree of
Master of Engineering Science

Date_____

_____
Chair of the Thesis Examination Board

ABSTRACT

Recombinant human erythropoietin (rhEPO) is a glycoprotein, which is produced commercially from Chinese hamster ovary (CHO) cells. It is used for chronic therapy of renal anemia and chemotherapy-induced anemia in cancer patients. Recent evidence suggests that rh-EPO exerts tissue protective effects via multiple mechanisms which include inhibition of apoptosis, promotion of angiogenesis and decreased inflammation. After Intra Venus (I.V.) injection, the blood concentration of rh-EPO rapidly decreases due to proteolysis with a short half-life of 8.5 h, which makes treatment expensive. It is desirable to develop an encapsulation method which will provide a controlled release of rh-EPO and maintain the desirable concentration levels in the blood for longer time. Nanoparticles encapsulated rh-EPO can also be used for direct injection to specific tissues/organs, where sustainable concentration of rh-EPO are desirable

In this thesis, we report the production of biopolymer nanoparticles (BNP) with the following methods: (a) emulsification-evaporation (b) ionotropic gelation of the biopolymer chitosan with tripolyphosphate (TPP). The nanoparticle size distribution in aqueous solution was measured using Dynamic Light Scattering system. Three different methods were used and compared for the measurement of rh-EPO concentration in PBS aqueous solution, namely, Enzyme Linked Immunosorbent Assay (ELISA), High Performance Liquid Chromatography (HPLC), and Fluorometry. A series of experiments were performed on the encapsulation of rh-EPO in chitosan biopolymer nanopartciles using the iontropic gelation method with TPP. Rates of release of rh-EPO encapsulated in chitosan-TPP nanoparticles were measured in Phosphate Buffered Saline solution (PBS).

The concentration versus time release data were used with second order diffusion equation to estimate the effective diffusivity of rh-EPO in chitosan-TPP nanoparticles. It was concluded that the chitosan-TPP biopolymer nanoparticles were the best method for the encapsulation of rh-EPO.

Keywords: Erythropoietin, rh-EPO, encapsulation, nanoparticles, biopolymers, controlled release, drug delivery, diffusivity of rh-EPO, chitosan, tripolyphosphate, alginate, poly(lactic-co-glycolic acid), polyvinyl alcohol, dynamic light scattering, ELISA, HPLC, Fluorescence.

.

ACKNOWLEDGEMENTS

I wish to thank my thesis supervisor, Professor Argyrios Margaritis for suggesting this research topic and his enthusiastic support and guidance throughout the course of this research, and for corrections in this M.E.Sc thesis.

Special thanks to Dr. David Freeman, Department of Physiology and Pharmacology, for the training and allowing me to use the HPLC system, Dr. Anargyros Xenocostas, Department of Hematology, for providing the rh-EPO and the use of the ELISA system available at Victoria Hospital, London Health Sciences Centre. Special thanks also to Dr. Ben Hedley for helping with the ELISA analyses of rh-EPO controlled release samples.

I would also like to thank Professor John deBruyn, Department of Physics for allowing me to use of the Dynamic Light Scattering facility to measure the size distribution of nanoparticles. I would also like to thank Dr. Stanley Dunn and Lee-Ann Briere, Department of Biochemistry, for helping me with the fluormetric assay of rh-EPO.

Finally, I would like to thank my parents for their support and for encouraging me to acquire higher education.

TABLE OF CONTENTS

List of Tables

List of Tables in Appendices

List of Figures

NOMENCLATURE

a_0 = Initial radius of sphere, cylinder or half-thickness of slab (m)

A_s = Particle surface area, (m)

C_0 = Initial concentration of drug in the matrix (g.mL^{-1})

C_l = Concentration of solute in liquid phase (g.mL^{-1})

C_s = Concentration of solute in solid phase (g.mL^{-1})

C_l^∞ = Solute concentration in liquid phase at equilibrium, (g.mL^{-1})

C_s^∞ = Solute concentration in solid phase at equilibrium, (g.mL^{-1})

d = Diameter of stirrer, (m)

D_e = Effective diffusivity of solute in polymer (m^2.s^{-1})

k_0 = Erosion rate constant (g.m^{-2}.s^{-1})

K_p = Partition coefficient

M_l^t = Amount of drug released from the particle at time t, (g)

M_l^∞ = Total amount of drug released after polymer disintegration or at equilibrium (g)

M_s^0 = Amount of solute in the sphere at the beginning, (g)

M_s^t = Amount of solute in the sphere at time t (g)

q_n = Eigen values defined by equation 2-10

r = Distance from the centre of the sphere (m)

R = Radius of the particle (m)

Re = Reynolds number

t = Time, (s)

U = Velocity of stirrer, (m.s^{-1})

V_l = Volume of liquid in diffusion vessel, (mL)

α = Final fraction of drug uptakes by sphere

μ = Viscosity of liquid in diffusion vessel, (g.m^{-1}.s^{-1})

ρ = Density of liquid in diffusion vessel, (g.mL^{-1})

CHAPTER 1

INTRODUCTION

Erythropoietin (EPO) is a glycoprotein hormone which is exclusively produced in the renal interstitial cells of kidneys. EPO is the main hormone that regulates the number of red blood cells in plasma (Mocini *et al.*, 2007). As shows in figure 1-1, it has 165 amino acids and its molecular weight is in the range of 30-36 kDa (Lai *et al.*, 1986; Walsh, 2003). EPO contains 40% carbohydrates, three N-linked acidic oligosaccharides located at asparagines 24-, 38- and 83- and one O-linked oligosaccharide at serine 126. The oligosaccharides are identified as fucose, mannose, N-acetylflucoseamine, galactose and N-acetylneuraminic (Walsh, 2003; Jelkmann, 1992; Lai *et al.*, 1986; Mocini *et al.*, 2007). Carbohydrates are responsible for *in vivo* biological activity of EPO and in two independent reports by Takeuchi *et al.* (1992) and Jelkmann (1989), it has been shown that removal of galactose or N-acetylneuraminic acid causes the rapid clearance of EPO from the blood by the liver.

Erythropoietin was first identified in 1906, but due to limitation in its availability, its structure has not been studied thoroughly (Lai *et al.*, 1986). Homogenous human EPO was first purified from the urine of aplastic anemia patients by Miyake *et al.* (1977), using a 7-step procedure, which included the following: ion exchange chromatography, ethanol precipitation, gel filtration and adsorption chromatography.

Figure 1-1: Primary structure of human erythropoietin

(Romanowski and Sytkowski, 1994)

The EPO gene was cloned in 1985 and expressed into the mammalian cell line, which was used to produce 32 mg recombinant human Erythropoietin (rh-EPO) per liter of culture medium. Analysis of the rh-EPO shows that its polypeptide sequence and carbohydrate moieties are identical to human EPO and has full biological activity *in vitro* and *in vivo* (Broudy *et al.*, 1988; Lin *et al.*, 1985).

Recombinant human EPO is used for chronic therapy of renal anemia, zidovudine therapy of HIV infection and chemotherapy (Morlock *et al.*, 1997; Pistel *et al.*, 1999). Recent evidence also suggests that rh-EPO exerts tissue protective effects via multiple mechanisms that include, inhibition of apoptosis, promotion of angiogenesis, and decreased inflammation (Boogaerts 2006; Arcasoy 2008; Vander Meer *et al.*, 2004). rh-EPO has a short half-life of 8.5 h, and it is susceptible to proteolysis and it is cleared from the blood rapidly after Intra Venus (I.V) administration. This results in multiple injection which is inconvenient to patients and increases the treatment cost (Piestel *et al.* 1999). Moreover, for non-hematological effects, high doses of rh-EPO are required which may elevate blood pressure, increase haematocrit, induce thrombosis, chronic heart dilation, ventricular edema, compromise exercise performance and acute cardiac failure (Boogaerts, 2006). Therefore, it is advantageous to prepare a delivery system to apply high doses of rh-EPO to the site of injury while preventing the excessive erythropoiesis. For hematological effects, it is desirable to design a delivery system with long term drug release in order to reduce the number of injections. Drug encapsulation in biopolymer nano or microparticles is a promising new system that can meet all the requirements. Different methods and polymers for encapsulation of rh-EPO have been reported in the

scientific literature. However, the main problems that were encountered were the rh-EPO aggregation, due to use of harsh organic solvents, and high initial release rate in first 48 hours of drug delivery (Morlock *et al.,* 1997; Hahn *et al.*, 2006).

The first objective of this research is to encapsulate rh-EPO in chitosan nanoparticles which is a biodegradable and biocompatible biopolymer, and secondly, study the kinetics of drug release *in vitro*. Chitosan is a natural, hydrophilic, biocompatible, nontoxic and noncarcinogenic biopolymer, which has received extensive attention as a carrier for hydrophilic drugs. Chitosan has many free amine groups, which give a total positive charge to the biopolymer molecule; therefore, ionic interaction can take place between chitosan and rh-EPO at pH greater than 4.3, which is the iso-electric point of rh-EPO. Moreover, chitosan has great affinity toward sialic acid (Sinah *et al.*, 2004) which is found in the rh-EPO molecular structure.

CHAPTER 2

LITERATURE REVIEW ON ENCAPSULATION

2-1. Encapsulation Methods

Encapsulation of a compound in a polymeric material is defined as the immobilization of this compound within the polymer and formation of particles. Based on the size of the particles they are divided into microparticles (1 $\mu m < d < 1mm$) and nanoparticles ($d < 1$ μm). To produce particles of desired size and with desired properties, many different encapsulation methods have been developed, which include the following: (1) coacervation, (2) polymer-polymer incompatibility, (3) interfacial polymerization in liquid media, (4) in-situ polymerization, (5) spray drying, (6) fluidized bed coater, (7) centrifugal extrusion, (8) rotational suspension separation, (9) heat denaturation, (10) solvent evaporation, and (11) ionotropic gelation.

The following section describes the different methods of encapsulation reported in the scientific literatures.

2-1-1. Coacervation

This method is the first encapsulation method which was commercialized and used for carbonless copy papers. Coacervation is defined as "the separation of two liquid phases in

colloidal systems" (De Kruif *et al.*, 2004). Coacervation can be divided into two types: simple coacervation and complex coacervation.

In simple coacervation colloidal phase separation takes place by addition of an agent whereas in complex coacervation, phase separation and particle formation occurs by interaction between two oppositely charged water-soluble polymers. The polymer rich phase, named complex coacervate, is in equilibrium with the supernatant (Thies, 1996; Gosh, 2006). First investigation of complex coacervation method was done by Bugenberg de Jong who used gelatin and Arabic gum, primarily because of their abundance and biodegradability (Prata *et al.*, 2008; Mayya *et al.*, 2003). Since that time, many different polymers have been used such as poly(acrylic acid), whey protein, chitosan, alginate hyaluronate. The encapsulation method used was the same and was based on the interaction between two charged polymers (Liu *et al.*, 2007; Weinbreck et al, 2003; Espinosa-Andrews *et al.*, 2007; Mathieu *et al.*, 2005; Baruch *et al.*, 2006).

2-1-2. Polymer-Polymer Incompatibility

This method is based on polymer phase separation, and it is mainly used for water insoluble core materials (Magadassi and Yelena, 1996). Two oppositely charged polymers dissolved in the same solvent. Under appropriate temperature, pH and concentrations, they interact with each other and form a complex with low solubility in the solvent and result in phase separation. By reducing the temperature, the complex starts precipitation and forms a shell around the core material, which has already been dispersed in the solution (Bakan and Anderson, 1976; Magadassi and Yelena, 1996).

2-1-3. Interfacial Polymerization

In contrast to the aforementioned methods which were using the polymers to form particles, in this method, the starting compounds are monomers and polymerization occurs at the interface between two phases. First, the liquid core material contains a multifunctional monomers dispersed in an aqueous phase contains dispersing agents, then by addition of co-reactant (cross-linker) to this mixture, a rapid polymerization reaction takes place at the interface which leads to the formation of the capsule shell. Dispersion of organic phase in the liquid phase is a very important step which will affect the particle size distribution. Moreover, hydrodynamic conditions in the vessels and agitation rate have significant effect on the particle size and particle size distribution (Alexandridou and Kiparissides, 1994; Benita *et al.*, 1984; Thies, 1994). The method is feasible mainly for the production of polyamides and polyesters which are formed by polymerization of amines with chlorides, i.e. sebacoyl dichloride, terephetaloyl chloride, etc (Alexandridou and Kiparissides, 1994).

This method is not suitable for encapsulation of fragrances, drugs and flavors because polymerization always requires a chemical or physical initiator and complete removal of these chemicals is a question (Alleman *et al.*, 1993), but it can be used for the encapsulation of agrochemicals such as pesticides and herbicides (Thies, 1994).

2-1-4. In-Situ Polymerization

Similar to interfacial polymerization, encapsulation process starts with polymerization of monomers .Polymerization takes place in the continuous phase, not at the interface.

2-1-5. Spray Drying

This is one of the oldest methods for encapsulation, where the materials encapsulated are dispersed into a water-soluble polymer and fed as droplets into a heated chamber where they are dried and micron-sized particles are formed (Thies, 1996; Magadassi and Vinetsky, 1996).

Although the spray-drying technology is well established, the problems of this method are the formation of irregular rough and non-uniform size particles, fractured microcapsules, incomplete encapsulation, low loading capacity and availability of limited number of water-soluble biodegradable polymers (Magadassi and Yelena, 1996; Li et al., 2008a; Tsifansky et al., 2008).

2-1-6. Fluidized Bed Coater

This technique is used for the coating of solid or porous particles and it is widely used in pharmaceutical industries. Solid particles are suspended in a gas stream inside a chamber, by spraying the coating material onto them a layer of polymer is formed around the solids. They are moved into the drying zone and recycled back into the coating area. This cycle is repeated several times until the desired thickness is obtained. The main advantage of this method is its ability to use a wide range of coating materials, but the particles shape is not spherical and the size distribution is broad (Ghosh, 2006; Thies, 1996).

2-1-7. Centrifugal Extrusion

Core and shell materials are passed through a concentric feeding tube and pumped to nozzles which are located on the outer surface of a rotating device. When the shaft rotates around its axis, the core material is covered with a layer of shell polymer which extrudes out of the orifices in the rotating nozzles due to centrifugal force. The droplets change into the solid capsules by air cooling or immersing into a gelling bath, depending on the nature of the shell polymer (Desai and Park, 2005). This method is suitable for polar liquids as core materials, and shell materials are usually hydrophilic polymers such as, gelatin, sodium alginate, cellulose derivatives, etc (Desai and Park, 2005; Thies, 1996).

2-1-8. Rotational Suspension Separation

This method is used for encapsulation of solid materials. Core and shell materials are mixed till a uniform dispersion obtained. They are fed onto a rotating disk. Upon leaving the edge of the disk, droplets are formed, and then by solidification, capsules are formed. To obtain an optimum encapsulation, shell material must be cooled rapidly. (Gosh, 2006)

2-1-9. Heat Denaturation

This is a novel method which uses a shell around core materials by denaturing the proteins. In the first step, the core material is emulsified in a protein solution and then by increasing the temperature, the protein denaturation process is initiated. The protein denaturation makes it insoluble in water. The process should be controlled in such a way that the denatured protein forms a layer around the core materials (Magadassi and Vinetsky, 1996).

This process was first used in 1972, and the researchers produced human serum albumin (HSA) particles. They emulsified human serum albumin in water at room temperature then added the emulsion into hot cotton seed oil which caused HSA denaturation and particles formation (Allemann *et al.*, 1993). Although this process is simple, but the drawbacks of this process are using heat for denaturation of protein and necessity of organic solvent to wash the oil.

2-1-10. Solvent Evaporation

This technique is based on the differences in degree of solubility of a polymer in two miscible solvents. It can be categorized in different ways based on: (a)The nature of the dispersing phase (aqueous or nonaqueous), (b) The fusion of active agents into the organic solution (dissolved, dispersed and emulsified), and (c) Drug solubility in water.

Since emulsification is the most investigated method for encapsulation of therapeutic agents, for the rest of the discussion, emulsification-solvent evaporation for hydrophobic and hydrophilic drugs is explained a little more.

2-1-10. (a) Oil-in-Water Emulsification (Single Emulsion)

This method is mostly appropriate for lipophilic agents such as: Ibuprofen, steroidal hormones, cytostatics, anti-inflammatories and narcoleptics (Benoit *et al.*, 1996; Tamilvanan and Sa, 1999). In this method, water immiscible polymer and the drug are dissolved in an appropriate organic solvent, such as, methylene chloride or chloroform, and mixed well, then emulsified in water containing a surfactant. By diffusion of solvent

into the aqueous phase, micro or nanoparticles are formed and solvent is removed under reduced or atmospheric pressure.

2-1-10. (b) Water-in-Oil-in-Water Emulsification (Double Emulsion)

For encapsulation of water soluble drugs by emulsification, the aforementioned method was modified and a multiple emulsion system was used. In this method, first the agent is dissolved in an aqueous medium and then emulsified in an organic solvent that contains the polymer (water-in-oil). The whole emulsion is emulsified again in a larger volume of an aqueous solution (water-in-oil-in-water), where the particles are formed by diffusion of organic solvent from the first emulsion into the second aqueous phase. The organic solvent also acts as a partition between the two aqueous phases and prevents the agent to diffuse toward the second aqueous medium (Benoit *et al.*, 1996; Cohen *et al.*, 1991).

There are several factors that have great influences in particle size and other physicochemical characteristics of particles. Effects of some of the major process and formulation parameters in particle size, encapsulation efficiency and drug release are shown in Tables 2-1 and 2-2 for single emulsion and double emulsion, respectively. The type of mechanical mixer and rotational speed are major factors that control the rate of mixing between phases and the size of particles produced.

2-1-11. Ionotropic Gelation

A novel method utilizes hydrophilic polymers, such as, alginate and chitosan. The main principle of this method is gelation process, due to ionic crosslinkage between an anion

11

Table 2-1: Effect of process parameters on physicochemical properties of particles prepared by emulsification-evaporation method (Single Emulsion)

Process parameter		Effect	Reference
Stirring rate	Increase	Particle size decrease.	Patrickand McGinity, 1997
Organic solvent	Low water solubility	Complete partitioning. Better drug loading efficiency.	Tamilbanan and Sa, 1999
	Increase volume	Decrease the particle size. Decrease drug loading efficiency.	Patrickand McGinity, 1997
Volume of aqueous phase	Increase	Increase drug loading efficiency	Bodmeier and McGinity, 1987
Polymer concentration	Increase	Particle size increases. Drug loading Increases.	Mao *et al.*, 2008
Temperature	Increase	Decrease drug loading efficiency. Increase particle size.	Bodmeier and McGinity, 1987 Jalil and Nixon, 1990

Table 2-2: Effect of process parameter on physicochemical properties of particles prepared by emulsification-evaporation method (Double Emulsion)

Process parameter		Effect	Reference
Polymer Concentration	Increase	Particle size increase. Encapsulation efficiency increase.	Ghaderi *et al.*, 1996 Li *et al.*, 2008b
External aqueous phase	Increase	Encapsulation efficiency increase. Particle size increase.	Li *et al.*, 2008b
Stabilizer concentration	Increase	Particle size decrease. Polydispersity decrease.	Capan *et al.*, 1999 Li *et al.*, 2008b

13

or cation and its counter ion. Since particles are formed in an aqueous solution without any harsh organic solvent, this method has received extensive attention for encapsulation and delivery of therapeutic agents such as, peptides, proteins, DNA, Vaccines, etc.

2-1-11. (a) Alginate Particle Production

Alginate is a polysaccharide which is extracted from the brown seaweed. It is copolymer of α-L-guluronic and β-D-mannuronic acid (Figure 2-1). The amount of guluronic and mannuronic acid varies and it depends on the source of alginate (Herrero *et al.*, 2006; Wells and Sheardown, 2007).

Alginate can form gel when it reacts with a multivalent cation such as Ca^{2+}, Ba^{2+}, Al^{3+}, according to Eq 2-1 (Aoyagi *et al.*, 2005; Bao *et al.*, 2002; Briens *et al.*, 1997; Herrero *et al.*, 2006; Kilonzo *et al.*, 2007; Manocha and Margaritis, 2008; Margaritis and Kilinzo, 2005; Merchant and Margaritis, 1987; Pilkington *et al.*, 1998a; Pilkington *et al.*, 1998b).

$$2NaAlg(l) + CaCl_2 \rightarrow Ca(Alg)_2(s) + 2\ NaCl \qquad (2\text{-}1)$$
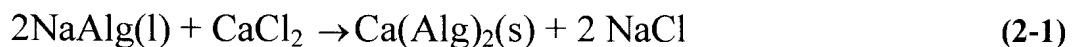
Where 'Alg' represents alginate.

Alginate capsules are formed by drop wise addition of Na-alginate to an aqueous solution of calcium chloride ($CaCl_2$), or other cations, while it is mixing (fig 2-2). Size and geometry of capsules depends on sodium alginate concentration, calcium chloride concentration and dropping velocity. It has been reported that particle size will decrease by increasing sodium alginate concentration and alginate solution flow rate and it will
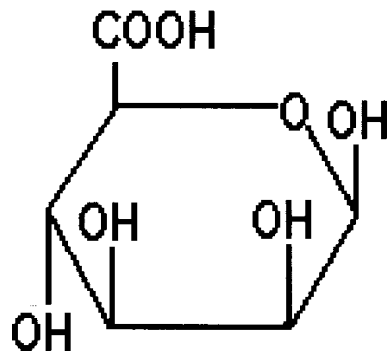
14

A

ß-D-mannuronic acid

α-L-guluronic acid

B
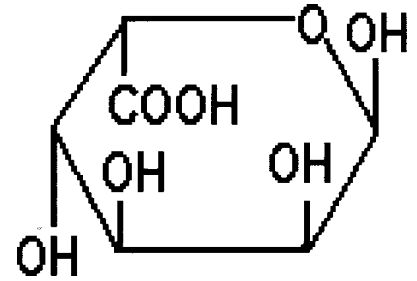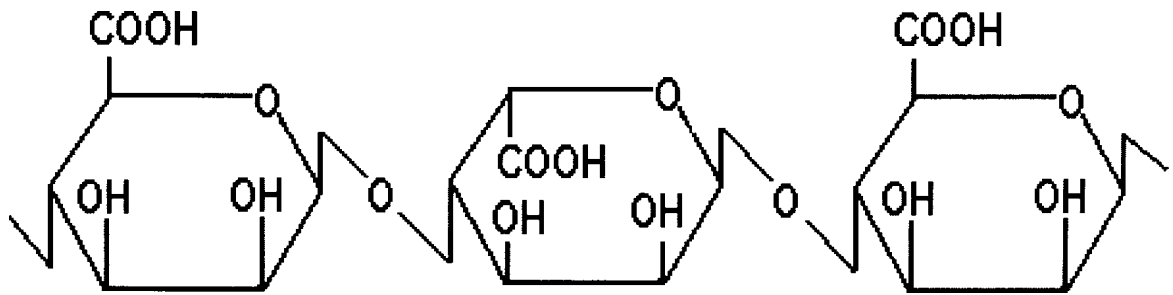
ß-D-mannuronic acid   **α-L-guluronic acid**   **ß-D-mannuronic acid**

Figure 2-1: Alginate molecular structure (B) and its monomers (A).
Adapted from Millman 1992.
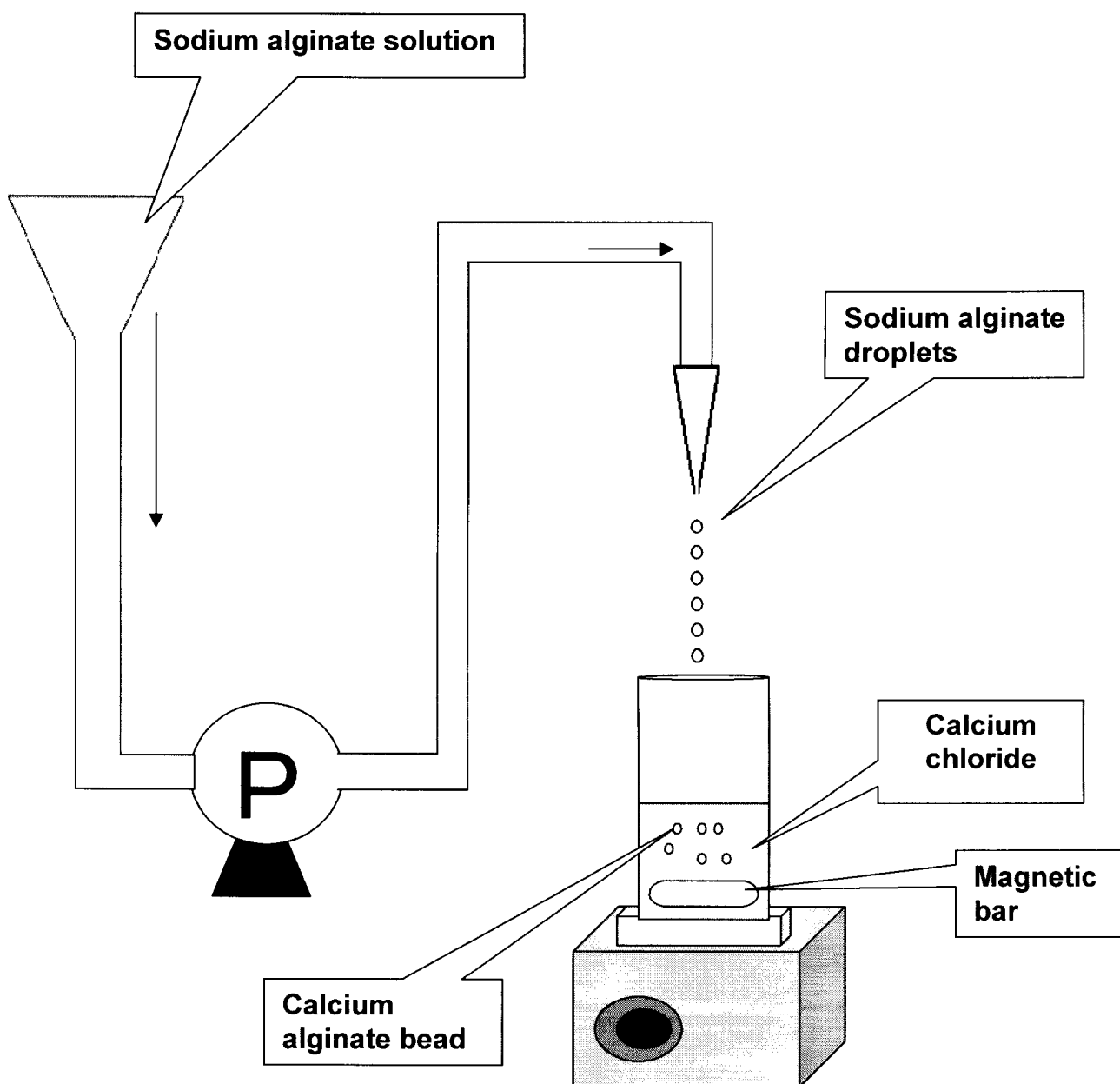
Figure 2-2: Schematic diagram of alginate bead production without air atomization.

increase by increasing calcium chloride concentration (Chai *et al.*, 2004; Blandino *et al.*, 1999). To decrease the particle size at constant sodium alginate and calcium chloride concentration, some researchers utilized air flow to break down the droplet size. It has been shown that average particles diameter decrease when the air flow rate increases and alginate particles as small as 5 μm can be produced by this method (Herrero *et al.*, 2006; Kwok *et al.*, 1991).

2-1-11. (b) Chitosan Particle Production

Chitosan is a natural linear polysaccharide synthesized by alkaline deacetylation of chitin obtained from exoskeleton of crustaceans. It is a copolymer of N-acetyl-D-glucosamine and D-glucoseaimine (Fig 2-3). It is a hydrophilic polymer which is dissolved in acidic solution, pH below 6.5 and it can form gel in acidic solution if it comes in contact with a polyanion (Sinha *et al.*, 2004).

Chitosan molecular structure consists of free amine groups which gives the molecule an overall positive charge and consequently a good mucoadhesive property. In addition, it has been reported that chitosan can reduce the drug clearance rate in blood when it is added as an excipient to the drug formulation (Sinha *et al.*, 2004). There are also several reports on the safety and lack of toxicity of chitosan (Sinha *et al.*, 2004; Rao and Shrma, 1997; Guliyeva *et al.*, 2006; Borchard, 2001).

Rao and Sharma (1997) did a systemic *in vivo* toxicity test and injected chitosan in mice, and no toxicity was observed during the test period. They also tested the polymer for eye

17
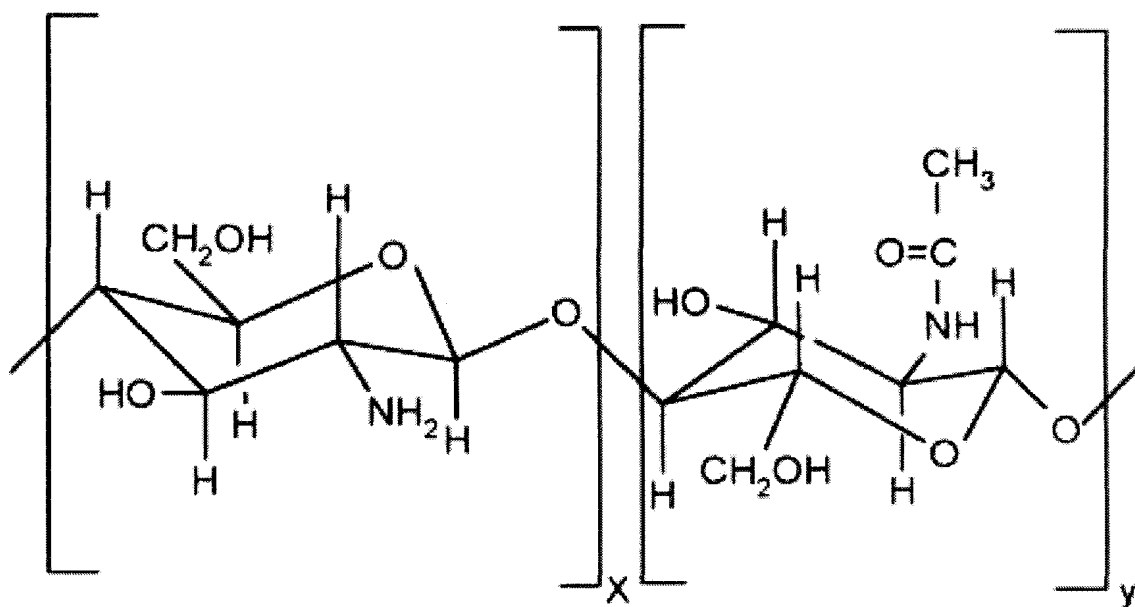
Figure 2-3: Chitosan Molecular Structure. Adapted from Lee et al, 1998

18

irritation and skin irritation in rabbit and guinea pig, respectively, and it was not reported any un-expected result. Chitsoan also degrades by general lysozymes and converts to carbon dioxide via glycoprotein pathway (Gan and Wang, 2007). Hence, due to its biocompatibility, low-toxicity, biodegradability and mucoadhesive properties, chitosan is considered a good candidate for drug carrier.

Chitosan particle formation by ionotopic gelation involves dissolution of chitosan in an aqueous acidic solution and addition of a negatively charged molecule such as sodium tripolyphosphate, sodium alginate, κ-carragenan, hexadesyl sulphate, to it. Sodium tripolyphosphate (TPP) is the most common negatively charged molecule which is used due to its non-toxicity and its ability to form gel quickly. In addition, chitosan-TPP particles form under mild conditions, have positive surface charge, and associate with peptides and proteins in a great capacity (Fernandez-Urrusuno et al, 1999; Gan and Wang, 2007; Gan et al., 2005). These features can be adjusted easily to produce particles with specific characterization.

Chitosan particle formation, particle size, and particle size distribution depend on the ratio of the chitosan to TPP. Nanoparticles are formed when chitosan:TPP artio is 3:1 to 6:1. At lower ratio, chitosan precipitates out of the solution as aggregates and at higher ratio nanoparticles hardly forms (Clavo et al., 1997; Fernandez-Urrusuno et al., 1999). Encapsulation efficiency and drug release rate depend on the chitosan molecular weight and its degree of deacetylation. Utilizing chitosan polymer with higher molecular weight

and higher degree of deacetylation increases encapsulation efficiency and decreases drug release rate (Xu and Du, 2003; Gan *et al.*, 2005).

2-2. Mechanisms of Drug Release

To design a controlled drug delivery system, it is beneficial if one can predict the release profile of the drug from the desired polymeric systems by understanding the mechanism of drug release. The drug release mechanisms from polymeric nano and microparticles are complicated and depends on the composition and geometry of the delivery system. It can be zero-order, variable or bioresponsive (Siepmann and Peppas, 2001; Hilary, 2001). Diffusion and polymer dissolution are the most important parameters that control the drug release form the particles.

2-2-1. Diffusion –Controlled Drug Release

This case is applied to the system when the non-degradable polymer is used or when the rate of diffusion of solute is much greater than the rate of polymer degradation. The driving force for transferring of solute from inside the particles to the liquid media is the difference between the concentration of solute inside and outside the particle. For such a system, Fickian diffusion law is applicable which can be expressed as equation 2-2 for a spherical geometry.

$$\frac{\partial C_s}{\partial t} = \frac{1}{r^2}\left[\frac{\partial}{\partial r}(D_e r^2 \frac{\partial C_s}{\partial r}) + \frac{1}{\sin\theta}\frac{\partial}{\partial\theta}(D_e \sin\theta \frac{\partial C_s}{\partial\theta}) + \frac{D_e}{\sin^2\theta}\frac{\partial^2 C_s}{\partial\phi^2}\right] \quad (2\text{-}2)$$

Equation 2-2 is a general form when diffusion takes place in all directions. But, in most analytical solutions, it has been assumed that diffusion takes place only in radial direction and the diffusion coefficient is constant. Figure 2-4 shows a spherical coordinate for radial diffusion and equation 2-2 for this system can be re-written as:

$$\frac{\partial C_s}{\partial t} = D_e \left(\frac{\partial^2 C_s}{\partial r^2} + \frac{2}{r} \frac{\partial C_s}{\partial r} \right) \tag{2-3}$$

To find the final solution to this equation it is necessary to define two different immersing conditions and apply appropriate initial and boundary conditions for each case.

2-2-1. (a) Spherical Particles Immersed into a Finite liquid Volume

Finite liquid volume is considered when drug has limited solubility in liquid medium or when the drug concentration in the liquid reaches to substantial level, which can happen when liquid volume is small or the fluid flow is low (Abdekhodaie and Cheng , 1997). For this system, initial and boundary conditions are defined as:

1. **Initial conditions**

   - Solute distributed homogenously throughout the particles

   $$t = 0 \quad , \quad 0 < r < R \quad , \quad C_s = \text{Constant} \tag{2-4}$$

   - Solute concentration in liquid is zero at the beginning

   $$t = 0 \quad , \quad r > R \quad , \quad C_l = 0 \tag{2-5}$$

21
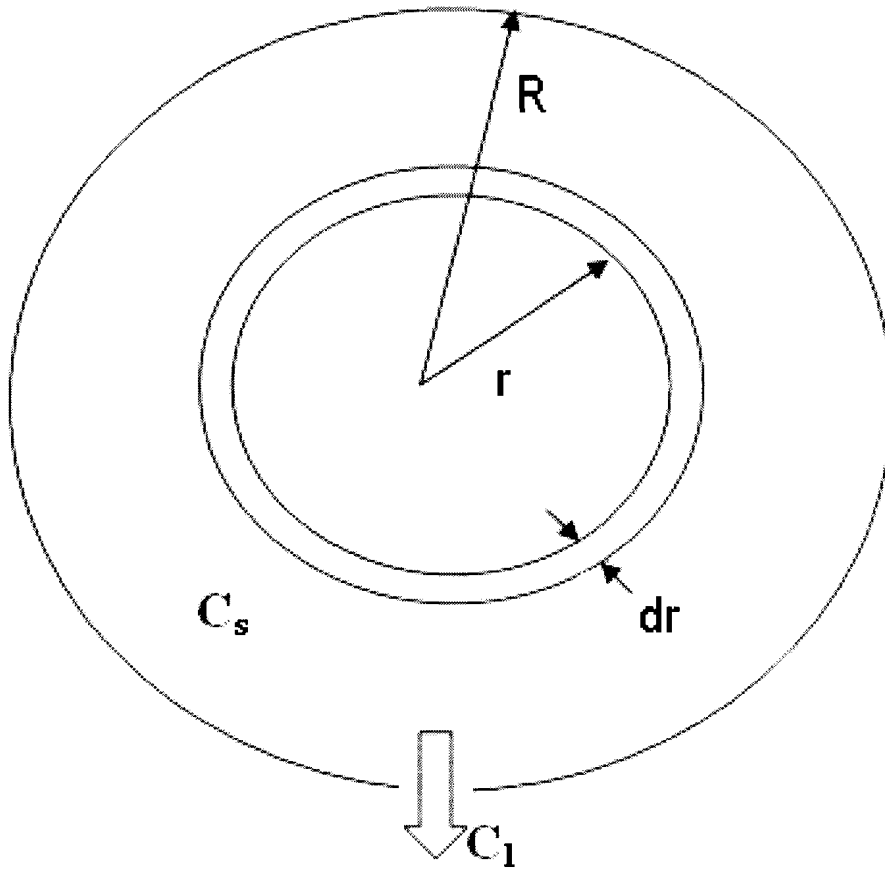
Figure 2-4: Spherical coordinate system for solute diffusion, Adapted from

Merchant *et al.* **(1987)**

2. Boundary Conditions

- No angular dependence of the solute

$$t > 0 \quad , \quad r = 0 \quad , \quad \frac{\partial C_s}{\partial r} = 0 \qquad \text{(2-6)}$$

- There is no mass transfer resistance in bulk liquid.

$$t > 0 \quad , \quad r = R \quad , \quad V_l \frac{\partial C_l}{\partial t} = K_p A_s D_e \frac{\partial C_s}{\partial r}\bigg|_{r=R} \qquad \text{(2-7)}$$

Applying the above initial and boundary conditions, Crank (1975) used Laplace transform and found the following solution for equation 2-3:

$$\frac{M_l^t}{M_l^\infty} = 1 - \sum_{n=1}^{\infty} \frac{6\alpha(1+\alpha)}{9 + 9\alpha + \alpha^2 q_n^2} \exp\left[\frac{-D_e q_n^2 t}{R^2}\right] \qquad \text{(2-8)}$$

Terms K_p, q_n, and α are the system characteristics. 'K_p' is called partition coefficient. It shows the solubility of solute in solid and liquid phase, and it is the ratio of solute concentration in solid to solute concentration in liquid at equilibrium.

$$K_p = \frac{C_s^\infty}{C_l^\infty} \qquad \text{(2-9)}$$

'α' shows the correlation between liquid volume, solid volume and partition coefficient. It shows the ultimate fraction of solute which can be absorbed or remained in the particles.

$$\alpha = \frac{V_l}{4\pi R^3 K_p}$$

$$(2\text{-}10)$$

'q_n' is a mathematical term. It is positive and non zero roots of the following equation:

$$3\tan(q_n) + \alpha q_n^2 \tan(q_n) - 3q_n = 0 \qquad (2\text{-}11)$$

2-2-1. (b) Spherical Particles Immersed into an Infinite Liquid Volume

Opposite to the finite volume, when particles are immersed in a large volume of liquid, drug concentration in liquid phase will remain far below its maximum level of solubility and the change of solute concentration in liquid phase with time is negligible. Therefore, initial and boundary conditions can be written as follow:

1. **Initial conditions**

   - Solute distributed homogenously throughout the particles

   $$t = 0 \qquad , \qquad 0 < r < R \qquad , \qquad C_s = \text{Constant} \qquad (2\text{-}12)$$

   - Solute concentration in liquid is zero at the beginning

   $$t = 0 \qquad , \qquad r > R \qquad , \qquad C_l = 0 \qquad (2\text{-}13)$$

2. **Boundary Conditions**

   - No angular dependence of the solute

   $$t > 0 \qquad , \qquad r = 0 \qquad , \qquad \frac{\partial C_s}{\partial r} = 0 \qquad (2\text{-}14)$$

24

- Change of solute concentration in liquid is negligible

$$t > 0 \qquad , \qquad r = R \qquad , \qquad C_s = C_l = 0 \tag{2-15}$$

Merchant and his co-workers (1987) found a solution to the equation 2-3 by using the above initial and boundary conditions (Eq 2-16)

$$\frac{M_s^t}{M_s^0} = 1 - \frac{6}{\pi^2} \sum_{n=1}^{\infty} \frac{1}{n^2} \exp\left(-\frac{D_e n^2 \pi^2 t}{R^2}\right) \tag{2-16}$$

Equations 2-8 and 2-16 show the correlation between the mass of drug released and the release time when diffusion controlled the drug release. It can be concluded from the equations that drug release from spherical particles, in both immersing conditions, when diffusion controls the release change exponentially. Therefore, when drug release mechanism is studying by plotting $\frac{M_l^t}{M_l^\infty}$ or $\frac{M_s^t}{M_s^0}$ vs time based on the immersing condition, by matching these equations to the experimental data, one can determine whether diffusion is controlling the drug release or not.

2-2-2. Dissolution – Controlled Drug Release

This mechanism of control release is seen only in biodegradable polymers when rate of polymer disintegration is greater than rate of drug diffusion through the pores of particles. Particle dissolution can be homogenous or heterogeneous. Homogenous erosion happens

25

when degradation takes place in the whole area of the particles and it is also called bulk erosion. In contrast, heterogeneous erosion occurs when molecules are only separated from the surface of the particles. Polymer characteristic dictates the type of erosion which might take place in particles. In drug delivery, heterogeneous dissolution is more applicable where drug release from such a system is zero order (Sah and Chien, 2001; Lee, 1980).

Surface dissolution involves separation of an atom, molecule or ion from the surface of the particle and then diffusion of detached molecule through the stagnant boundary layer of liquid adjoined to the particle surface. This can happen by cleavage of polymer backbone, cross link cleavage, ionization and hydolysis (Cooney 1972; Heller et al, 1978)

For surface erosion when the particles are immersed in infinite liquid volume, Hopfenberg model (Eq 2-17) is applicable if drug release controls only by polymer dissolution (Katzhendler et al, 1997; Lee, 1980):

$$\frac{M_l^t}{M_l^\infty} = 1 - \left[1 - \frac{k_0 t}{C_0 a_0} \right]^n \qquad (2\text{-}17)$$

In the above equation 'n' depends on the geometry of the matrix and it is 1 for slab, 2 for cylinder, and 3 for sphere.

CHAPTER 3

MATERIALS AND METHODS

3-1. Chitosan Solution Preparation

Chitosan solution was prepared by mixing chitosan flakes (Sigma Aldrich, Canada) with 2% acetic acid solution (Glacial acetic acid). For complete dissolving, chitosan and acetic acid solution were mixed over night (10 – 12 hours) and then it was filtered by using Whatmann filter paper number 2 (Pore size = 8 μm). Then the pH was adjusted to 5 by using 10 M sodium hydroxide solution.

3-2. Sodium Tripolyphosphate Solution Preparation

Sodium tripolyphoasphate solution (TPP), 1 mg/mL was prepared by dissolving measured amount of sodium tripolyphosphate powder in deionized water. The pH was adjusted to the desired pH (5, 7, 9) by using glacial acetic acid.

3-3. Nanoparticle Production

For each set of experiments, 10 mL of chitosan solution (1 mg/ml, 2 mg/mL and 3 mg/mL) at pH 5 was mixed with 1 mg/ml of TPP solution at different volumes (2 mL, 2.5 mL, 3.34 mL, 4 mL, 5 ml, 6 mL, 6.67 mL, 7.5 ml, and 10 mL) at 400 rpm using magnetic stirrer. The stirrer speed was reduced to 100 rpm and the suspension was mixed for 30 min, then centrifuged at 105,000 x g for 30 min and pellets were collected for further study. Fig 3-1 shows the schematic diagram for the process.
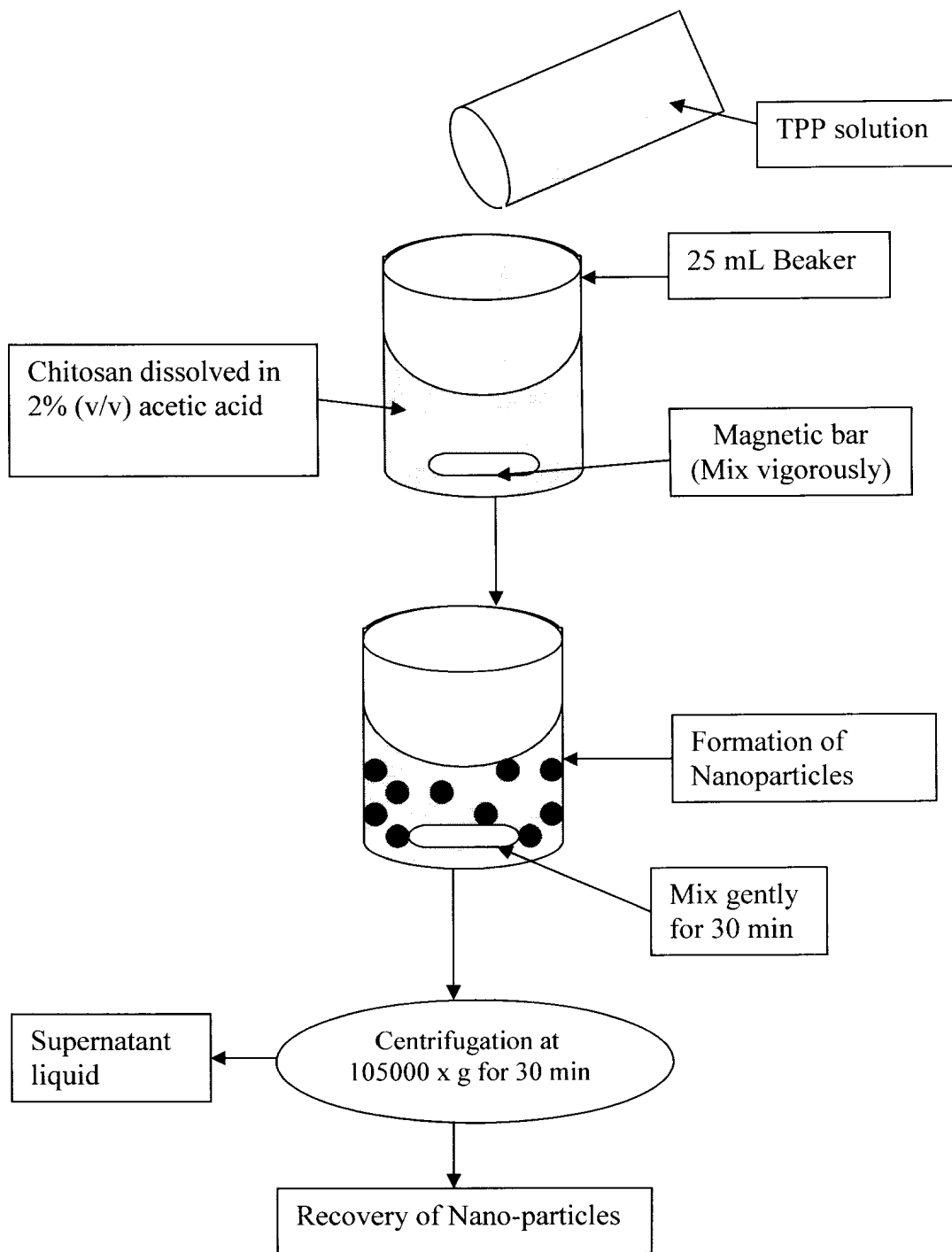
Figure 3-1: Schematic diagram of chiotosan-TPP nanoaprticle production by ionotropic gelation method.

3-4. Particle Morphology

Particle morphology was studied by transmission electron microscope (TEM) CM-10 (Philips) in Biotron Imaging Centre at the University if Western Ontario. Samples were placed on carbon grit, air-dried at room temperature for 1-2 min.

3-5. Particle Size Determination

chitosan –TPP particles were suspended in distilled water. 2 mL of the suspension was placed in a test tube and Chitosan-TPP particle size and particle size distribution was determined by dynamic light scattering system (AlV/CGS 3000, Langen, Germany).

3-6. Erythropoietin Encapsulation

Two hundred microliter (200 μL) of 320 μg/mL(40000 IU/ml) recombinant human Erythropoietin was mixed with 10 mL of 1 mg/mL chitosan solution at pH 5, at 400 rpm. Then 2 mL of 1 mg/mL TPP solution at pH 5 was added to this mixture and stirrer was set at 100 rpm and suspension was mixed for 30 min, after that the suspension was centrifuged at 105000 x g for 30 min and pellets and supernatant were separated and stored for further studies.

3-7. Erythropoietin Measurement Methods

rh-EPO concentration was measured using three different methods, namely, ELISA, Fluorometry, and HPLC.

3-7-1. Enzyme-Linked Immuno Sorbent Assay (ELISA)

ELISA test was done by using Human erythropoietin ELISA kit (StemCell Technology). The solutions, reagents and components of the kit listed in table 3-1. Measurement was done according to the assay procedure manual from the StemCell technology

ELISA Procedure

Before starting the procedure, 10 X wash buffer was diluted to 1 X by deionized water and stored at 2-8°C until used.

Twenty five microliter (25 μL) of buffer A was added to each well of plate, then 50 μL of standard, buffer or sample in duplicate and 50 μL of biotinylated anti-EPO antibody was added to each well. Plate was covered and incubated on a microplate shaker at 500 rpm for 1 hour. After incubation, wells were washed five times with 200 μL of 1 X wash buffer.

Plate was blot dried and immediately, 100 μL of streptavidin-HRP conjugate added to each well. Plate was covered again and incubated at room temperature on microplate shake (500 rpm). After 15 min, plate was washed 5 times with 1 X wash buffer and blot dried. Then 100 μL of the TMB Substrate solution added to each well and incubated on the bench top for 15 min at room temperature. Wells with EPO became blue. Then 100 μL of stop solution added to each well and blue colors changed to yellow. 15 min after addition of stop solution light absorbance at 450 nm was measured by a microplate reader. Wells with substrate and stop solution only were used as blank.

Table 3-1:List of components provided with ELISA kit.

Component	Description
Microplate	96-well plate pre-coated with anti-EPO monoclonal antibody
Buffer A	Phosphate buffered Saline containing protein, detergent and preservative
Buffer B	Phosphate buffered Saline containing protein, detergent and preservative (diluent for test samples)
EPO standard	100 mU/mL, 50 mU/mL, 25 mU/mL, 6.25 mU/mL, 3.12 mU/mL, 1.56 mU/mL, and 0 mU/mL
Biotinylated anti-EPO antibody	Biotinylated monoclonal antibodt against human EPO diluted in buffer B
Streptavidin-peroxidase conjugate	Streptavidin conjugated to horseradish peroxidase (HRP) and diluted in HRP stabilizing buffer
TMB substrate solution	Ready-to-use buffered solution of Tetramethylbenzidine (TMB) and hydrogen peroxide
Stop solution	0.5 N sulphuric acid
10X wash buffer	Concentrate of phosphate buffered saline containing detergent
Adhesive covers	To cover plate for incubation

* 1 U = 8 ng rh-EPO.

3-7-2. Fluorometric Assay

rh-EPO is an endogenous fluorescence compound because of the existence of 3 tryptophan in its structure. Therefore, it is possible to measure its concentration in solution by measuring its fluorescence intensity. This is applicable only for measuring EPO concentration *in vitro* and when other fluorescence compounds do not exist. 600 μL of each sample was placed in a cuvette and its fluorescence intensity was measured by fluormeter Flourolog3 (John-Yvan). Samples were excited at 280 nm and the fluorescence emission was recorded at 340 nm.

3-7-3. rh-EPO Assay Method Development Using HPLC

For rh-EPO assay development, Hewlett-Packard (hp) 1090 High Performance Liquid Chromatography (HPLC) system attached with a fluorescence detector (Waters 474) was used. A Jupiter C4 column (150 x 4.6 mm, 5 μm particles with pores size = $300^{o}A$) was purchased from Phenomenex. Mobile phase A was 60% HPLC grade methanol and 0.1% Trifluoroacetic acid (TFA) and mobile phase B was 100 % HPLC grade methanol with 0.1% TFA. Flow rate was set at 0.5 mL/min and column temperature was fixed at $35^{o}C$. Gradient was varied from 0% A to 100% B over 10 min. Injection volume was 15 μL.

3.8 rh-EPO Loading Efficiency

Loading efficiency is defined as the ratio of the amount of drug loaded in particles to the initial amount of drug. To determine mass of drug loaded in chitosan-TPP nanopartciles the rh-EPO concentration in supernatant was measured by fluormetric assay, and by

writing a mass balance the amount of drug which was encapsulated was determined and drug loading efficiency was calculated form the equation 3-1:

$$Drug\ Loading\ Efficiency = \frac{Mass\ of\ Encapsulated\ rh - EPO(\mu g)}{Initial\ Mass\ of\ rh - EPO(\mu g)} \qquad (3\text{-}1)$$

3-9. rh-EPO Release Study from Chitosan -TPP Nanoparticles

Loaded nanoparticles were prepared according to the method explained in section 3-6. Nanoparticles were suspended in 4 mL of phosphate buffered saline (PBS) solution at pH 7.4 and placed in shaker at 200 rpm and $37^{O}C$. At different intervals, it was centrifuged at 105000 x g for 30 min and the whole supernatant was replaced with fresh buffer. The supernatant was analyzed by fluorometer (fluoroLog 3) for rh-EPO concentration measurement.

3-10. rh-EPO Diffusivity Estimation in Chitosan Nanoparticles

Ninety six microgram (96 µg) of rh-EPO was encapsulated in chitosan nanoparticles according the method explained in section 3-6. The particles were suspended in 10 mL phosphate buffered saline (PBS) at pH 7.4 and mixed with a 5 cm magnetic bar at 200 rpm. The temperature was controlled by circulating hot water around vessel to keep the temperature constant at $37^{o}C$. After 6 hours the suspension was centrifuged and the whole supernatant was replaced with fresh 10 mL PBS. 14 hours after that, the suspension was centrifuged and supernatant was separated and stored for rh-EPO assay by ELISA.
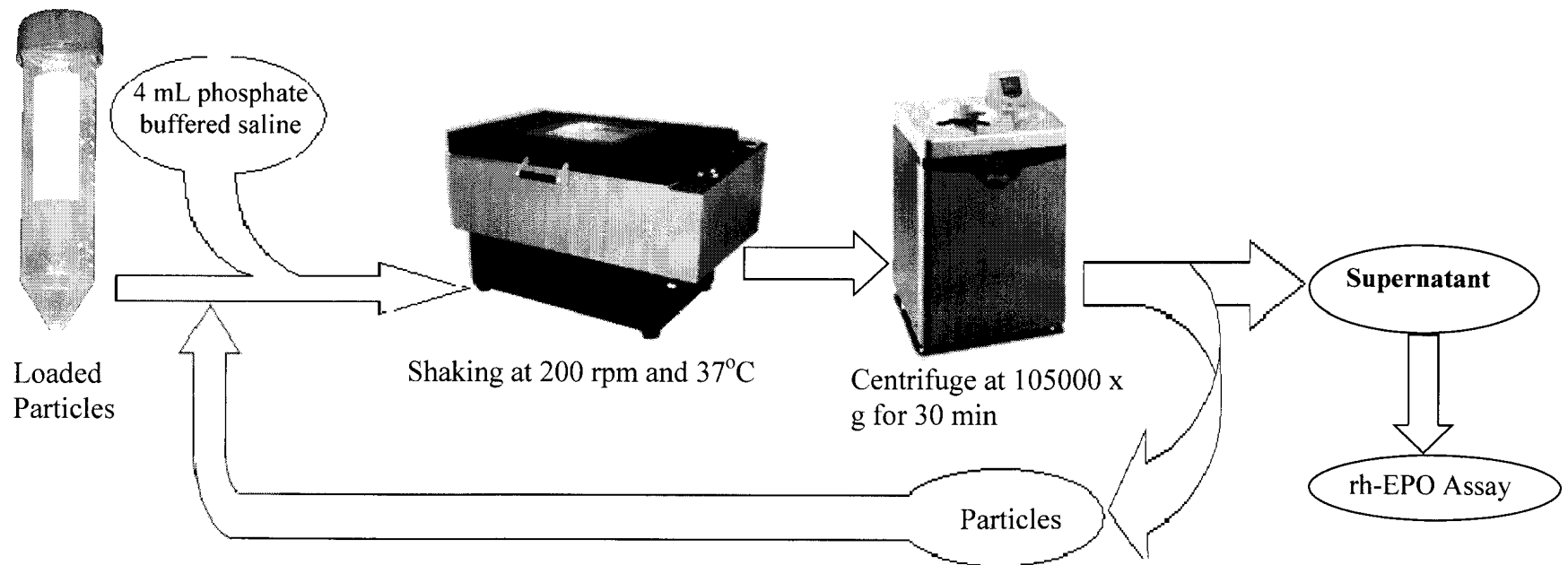
Figure 3-2: Schematic diagram for rh-EPO controlled release study in PBS solution

3.11.Emulsification-Evaporation Method for PLGA Particle Production

Two hundred milligram (200 mg) of poly(lactic-co-glycolic acid) (PLGA) was dissolved in 2 ml of dichloromethane, and it was rapidly poured into 20-25 mL of 1% (w/v) polyvinyl alcohol solution and homogenized at 8000 to 24000 rpm. Homogenization was done at different times to investigate the effect of homogenization time on particle size. This emulsion was added to a beaker contains 200 mL of 0.1% (w/v) polyvinyl alcohol and stirred at 200-300 rpm by a magnetic stirrer for solvent removal at atmospheric pressure. After that the mixture was centrifuged at 20000 x g for 45 min, supernatant was removed and particles were stored for further study. Figure 3-3 shows a schematic diagram for rh-EPO encapsulation in PLGA by emulsification-evaporation method.
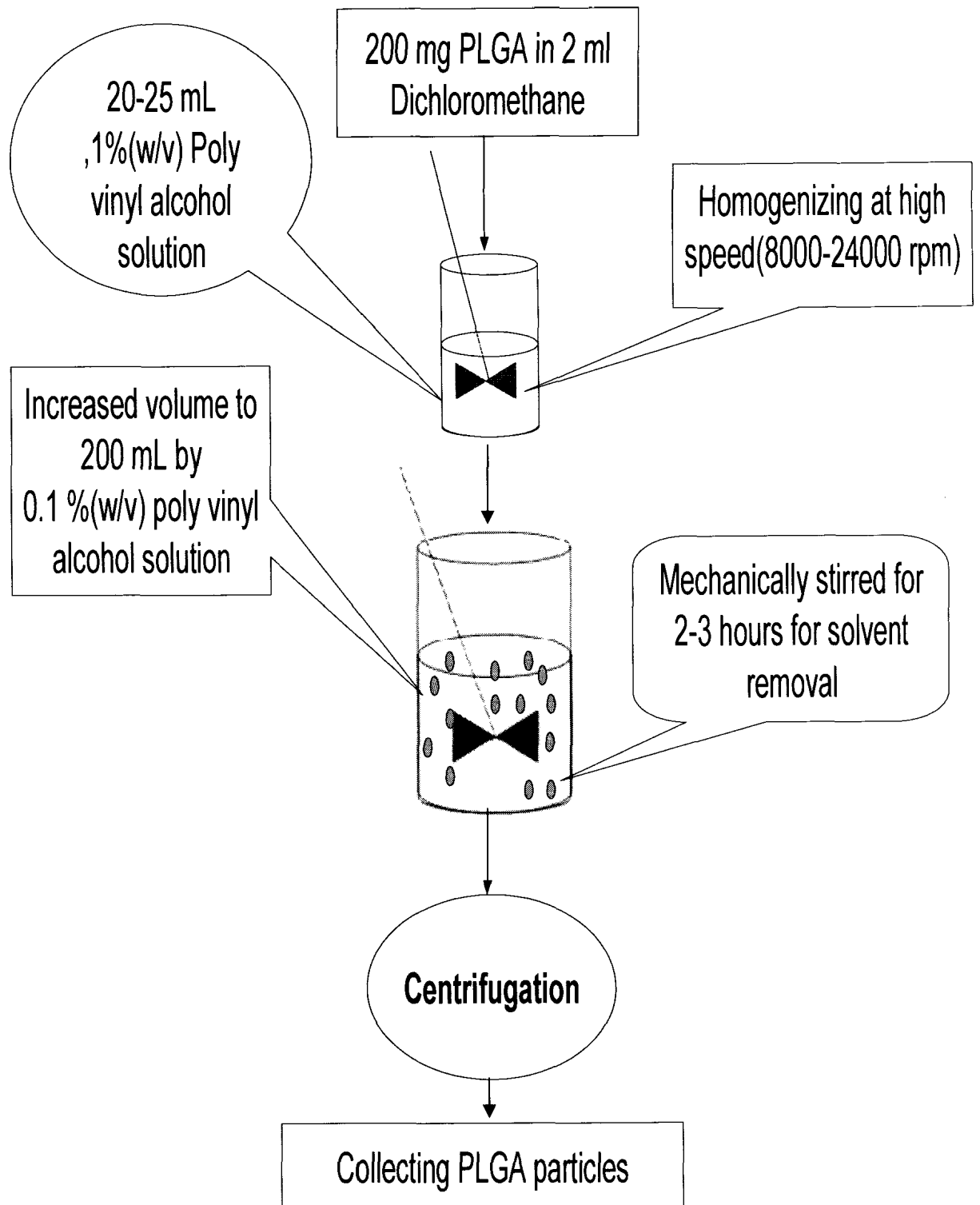
Figure 3-3: Schematic diagram for microparticle formation by emulsification-evaporation method. Adapted from Morlock *et al.*, (1997)

CHAPTER 4

RESULTS AND DISCUSSION

Chitosan nanoparticle production, recombinant human erythropoietin (rh-EPO) encapsulation and drug release profile of rh-EPO from chitosan nanoparticles were examined *in vitro*. In addition, an assay method by HPLC was developed to measure rh-EPO concentration in PBS solution.

Chitosan was selected as the drug carrier for rh-EPO encapsulation for two main reasons. First, chitosan is a natural hydrophilic biopolymer and it has been approved safe, non-toxic and non-carcinogenic for medical and pharmaceutical applications. Second, because of free amine groups in its structure, it has a positive charge and also, it has been shown that chitosan has a great affinity toward sialic acid. Availability of 11-14 sialic acid on the rh-EPO molecular structure can increase the absorption of rh-EPO by chitosan molecule and consequently increase the encapsulation efficiency. In addition, by adjusting the pH of gelling liquid above rh-EPO isoelectric point which is 4.3, an ionic interaction between rh-EPO and chitosan takes place. Since chitosan is only soluble in water at pH below 6, and the rh-EPO isoelectric point is 4.3, the operating pH window is very narrow. Therefore, operating pH was fixed at 5 for chitosan solution and in all the experiments, chitosan first dissolved in 2% acetic acid solution then pH was adjusted to 5.

Before encapsulating rh-EPO in chitosan nanoparticles, it was necessary to find the

optimum nanoparticle production conditions. So, the effect of chitosan concentration, chitosan to sodium tripolyphosphate (TPP) mass ratio and pH of TPP solution on particle size, particle size distribution and morphology was examined.

4-1) Standard Curves

rh-EPO concentration was measured using fluorometric assay and ELISA for rh-EPO release study and estimation of rh-EPO diffusion coefficient, respectively. Therefore, it was necessary to generate standard curves for each assay.

4-1-1) Enzyme- Linked immuno Sorbent Assay (ELISA)

ELISA standard curve was prepared by using 8 standard EPO samples (800ng/L, 400 ng/L, 200 ng/L, 50 ng/L, 24.96 ng/L, 12.48 ng/L, and 0 ng/mL) contained in the ELISA purchased kit and followed the recommended procedure which was described in section 3-7-2. Standard curve was generated by plotting concentration vs the absorbance of EPO standard samples (Fig 4-1)

4-1-2) Fluorometric Assay

Fluorescence intensity of 8 samples of rh-EPO (16 µg/mL, 8 µg/mL, 4 µg/mL, 2 µg/mL, 1.6 µg/mL, 1.2 µg/mL, 0.8 µg/mL, and 0.4 µg/mL) was measured and used for standard curve preparation. Standrad curve was created by plotting rh-EPO fluorescence intensity vs its corresponding concentration (Fig 4-2)
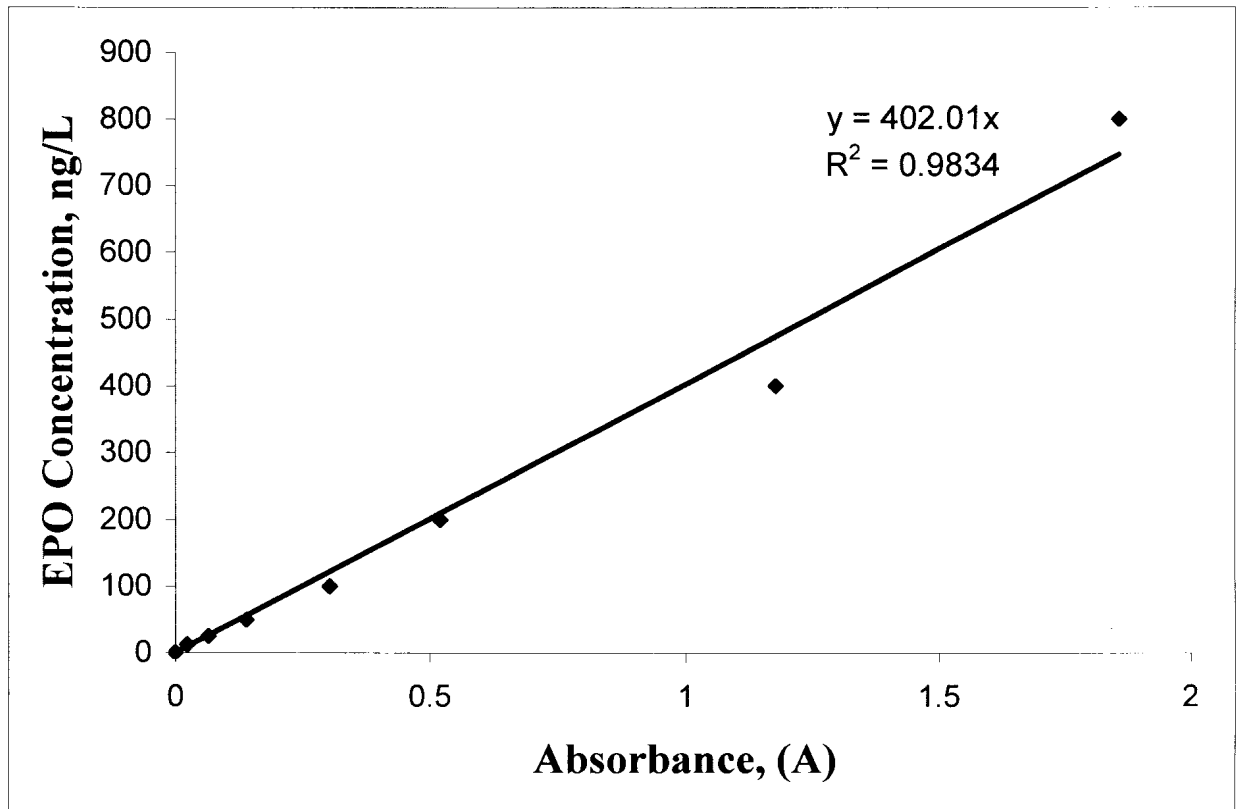
Figure 4-1 EPO standard curve using ELISA assay technique; (■) Experimental points, (—) Line of best fit.
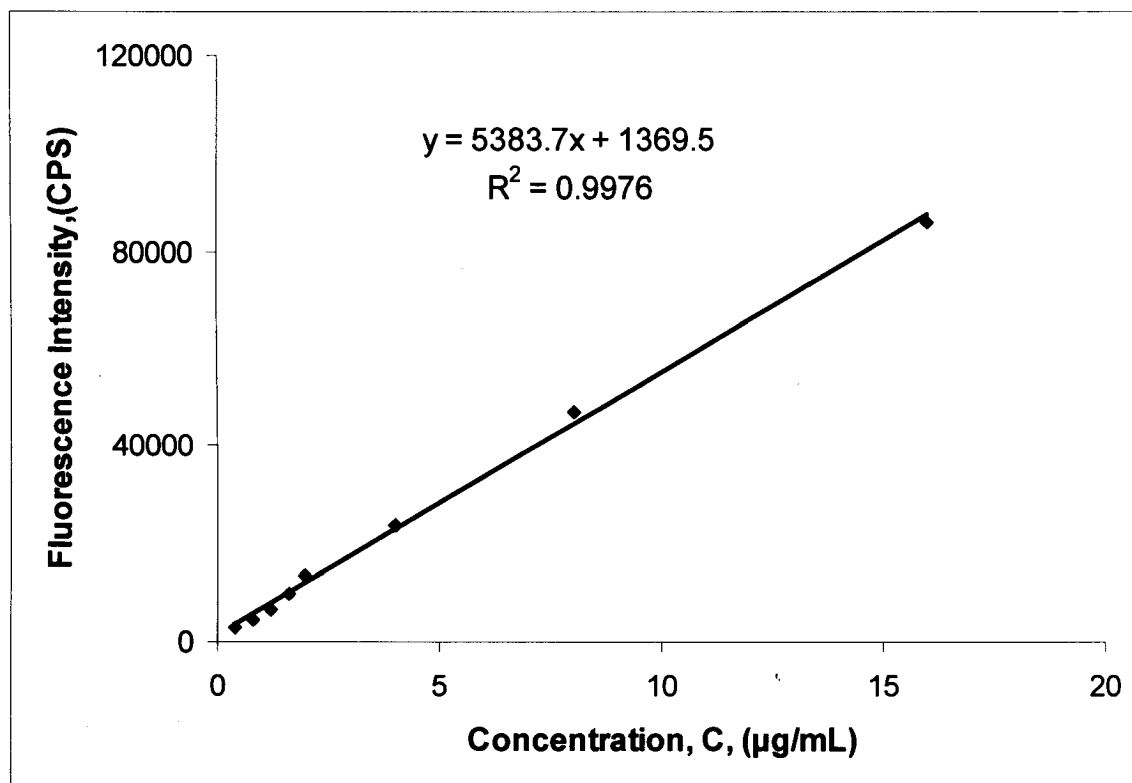
Figure 4-2: Standard curve of fluorescence intensity versus concentration for rh-EPO;(■) experimental points, (—) line of best fit (Flourometric assay). (Data are the average of three values)

4-2) Experimental Results

4-2-1) Effect of chitosan concentration and chitosan to TPP mass ratio on particle size

Chitosan concentration was varied from 1-3 mg/mL. Lower than 1 mg/mL chitosan particles hardly formed and higher concentration, over 3 mg/mL, was not operational due to high viscosity of the solution.

Figures 4-3 to 4-12 show the effect of chitosan concentration on particle size and particle size distribution at different chitosan to TPP mass ratio. The data are the average of 3 sets of measurements. It was observed that chitosan particles size at constant chitosan to TPP mass ratio will increase when chitosan concentration increases. This can be due to the increase in viscosity of the chitosan solution.

Particle formation by ionotropic gelation is due to interaction between phosphate ions of TPP with free amine groups in chitosan molecule. Therefore, the availability of amine group and uniform distribution of TPP molecule throughout the solution is a crucial parameter. When the viscosity of the solution increases at constant stirring speed and geometry of the mixing vessel, the Reynolds number will decrease according to equation (4-1):

$$Re = \frac{Ud\rho}{\mu} \qquad (4\text{-}1)$$

Consequently, by decreasing the Reynolds number of the liquid, it will take longer time for TPP molecule to be distributed uniformly throughout the solution. Therefore, mixing of the anion molecule (TPP) with cation molecule (chitosan) is not done properly. Therefore it causes the formation of larger molecule and increase the particle polydispesity of chitosan-TPP nanopartciles.

Figure 4-13, which is generated from figures 4-4 to 4-12, shows that at constant chitosan solution concentration, when chitosan to TPP mass ratio increases, the average particle size decreases. This can be explained by comparing the mass of TPP added to the vessel for particle formation. When chitosan to TPP mass ratio is decreased, the mass of TPP added to the chitosan solution at a fixed concentration increases, as a result, high TPP mass may raise the pH of solution and cause amine group in chitosan to lose their hydrogen ion. This will decrease chitosan solubility and its overall positive charge. Therefore, some chitosan particles which are formed will not be dense enough and will have larger diameter.

Reviewing the effect of chitosan concentration and chitosan to TPP mass ratio, it can be concluded that when chitosan concentration was 1 mg/mL and chitosan to TPP mass ratio was fixed at 5, average particle size is smaller, and particle size distribution is narrower in compare to the conditions where higher chitosan solution concentration and lower chitosan to TPP mass ratio were used.
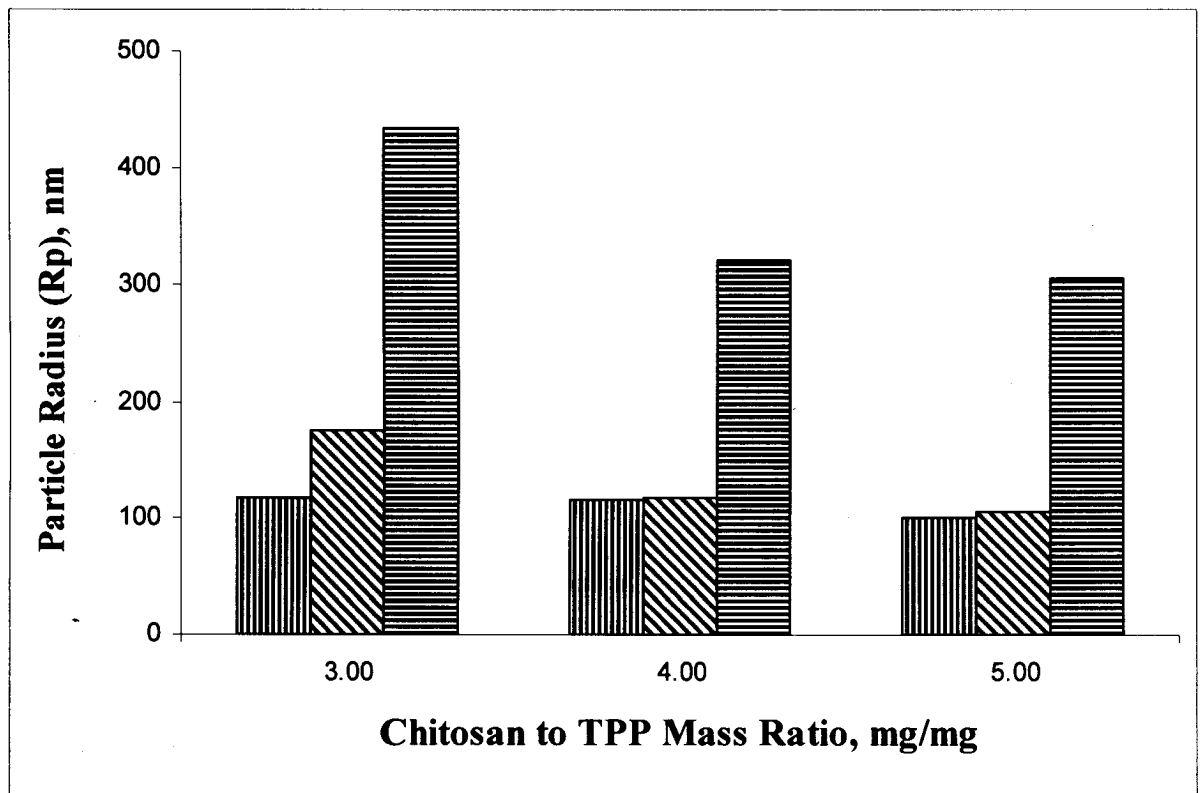
Figure 4-3; Effect of chitosan solution concentration on particle size at different chitosan (CS):TPP mass ratio (Data are the average of three sets of measurement).

▉ : Chitosan concentration = 1.00 mg/mL

▧ : Chitosan concentration = 2.00 mg/mL

▤ : Chitosan concentration = 3.00 mg/mL
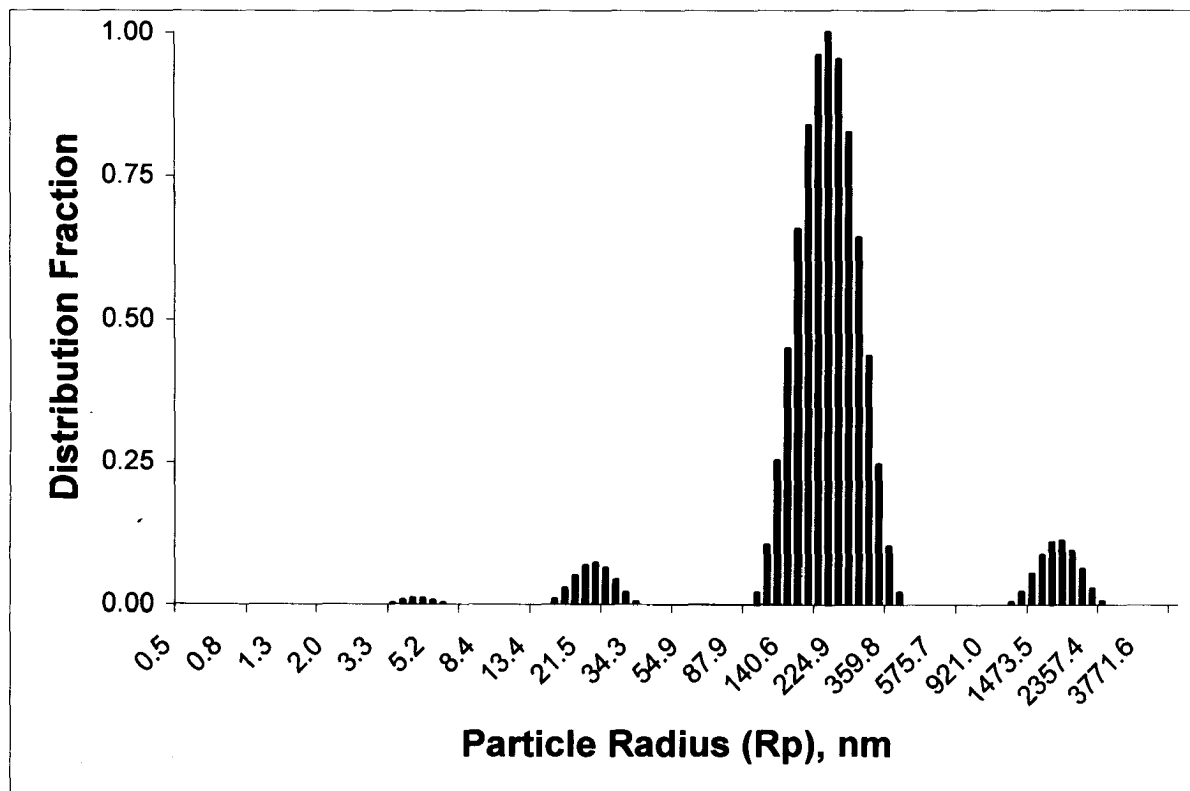
Figure 4-4: Effect of chitosan concentration on particle size distribution (Data are the average of three sets of measurement).

Chitosan concetration = 3 mg/ mL

Chitosan:TPP mass ratio = 5
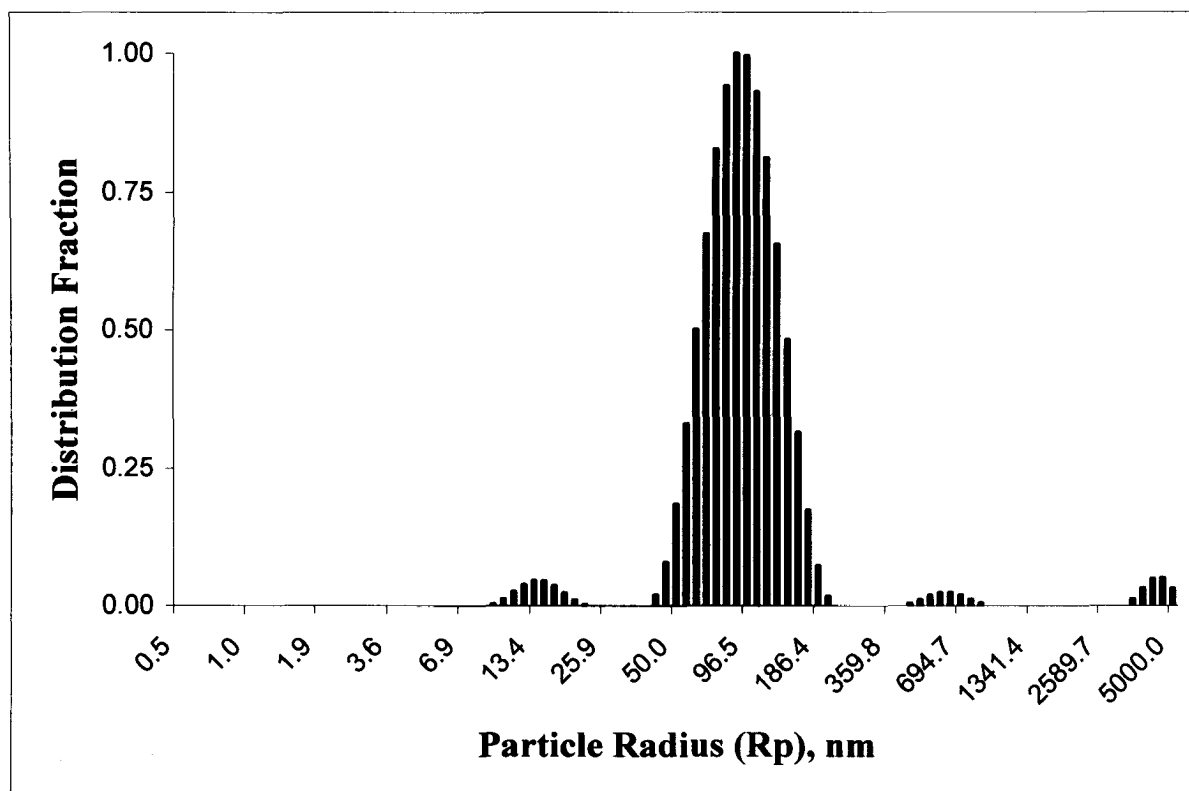
'Figure 4-5: Effect of chitosan concentration on particle size distribution (Data are

the average of three sets of measurement).

Chitosan concentration = 2 mg/ mL

Chitosan:TPP mass ratio = 5
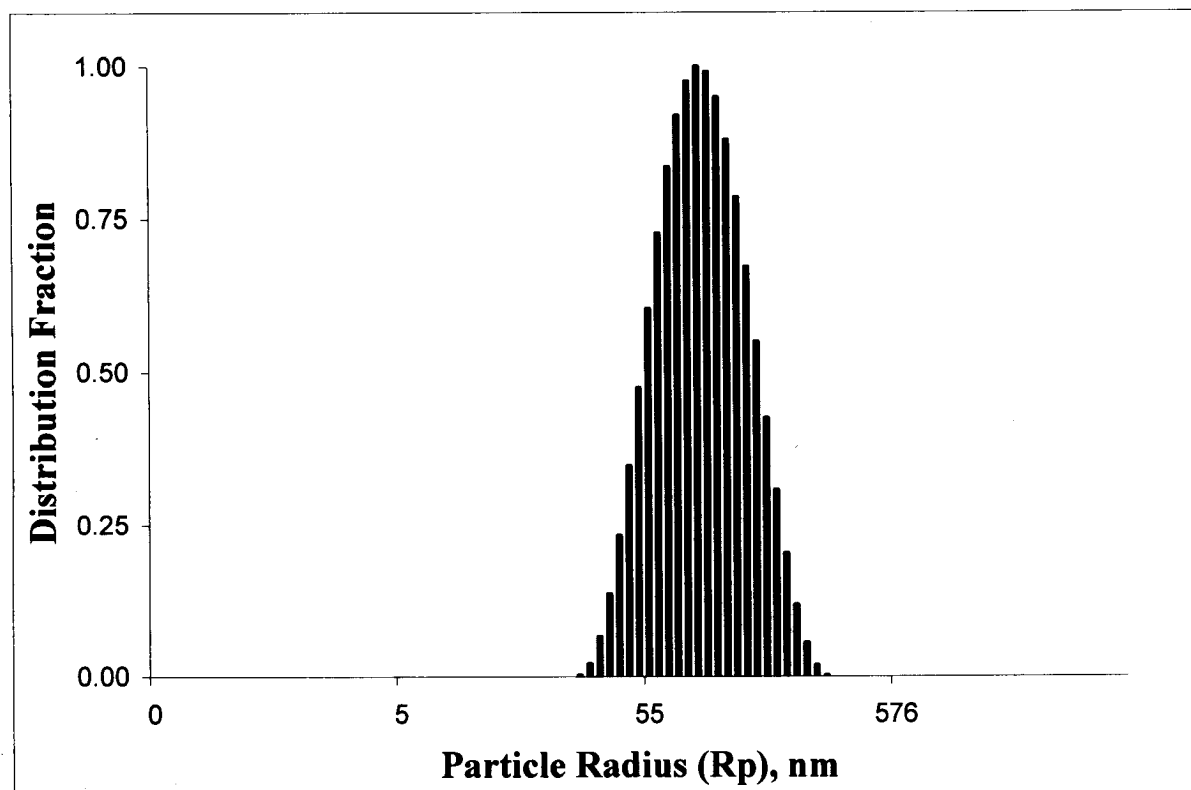
Figure 4-6: Effect of chitosan concentration on particle size distribution (Data are the average of three sets of measurement).

Chitosan concentration = 1 mg/ mL

Chitosan:TPP mass ratio = 5
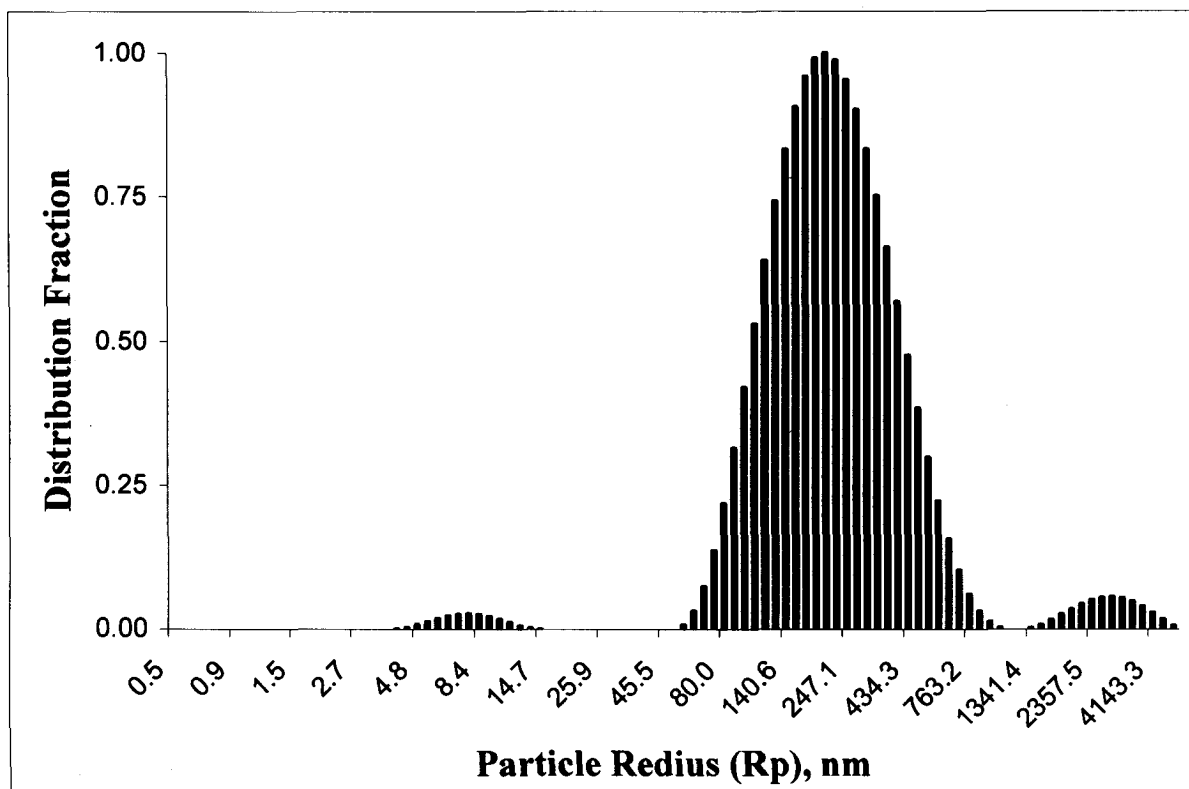
Figure 4-7: Effect of chitosan concentration on particle size distribution (Data are the average of three sets of measurement).

Chitosan concentration = 3 mg/ mL

Chitosan:TPP mass ratio = 4
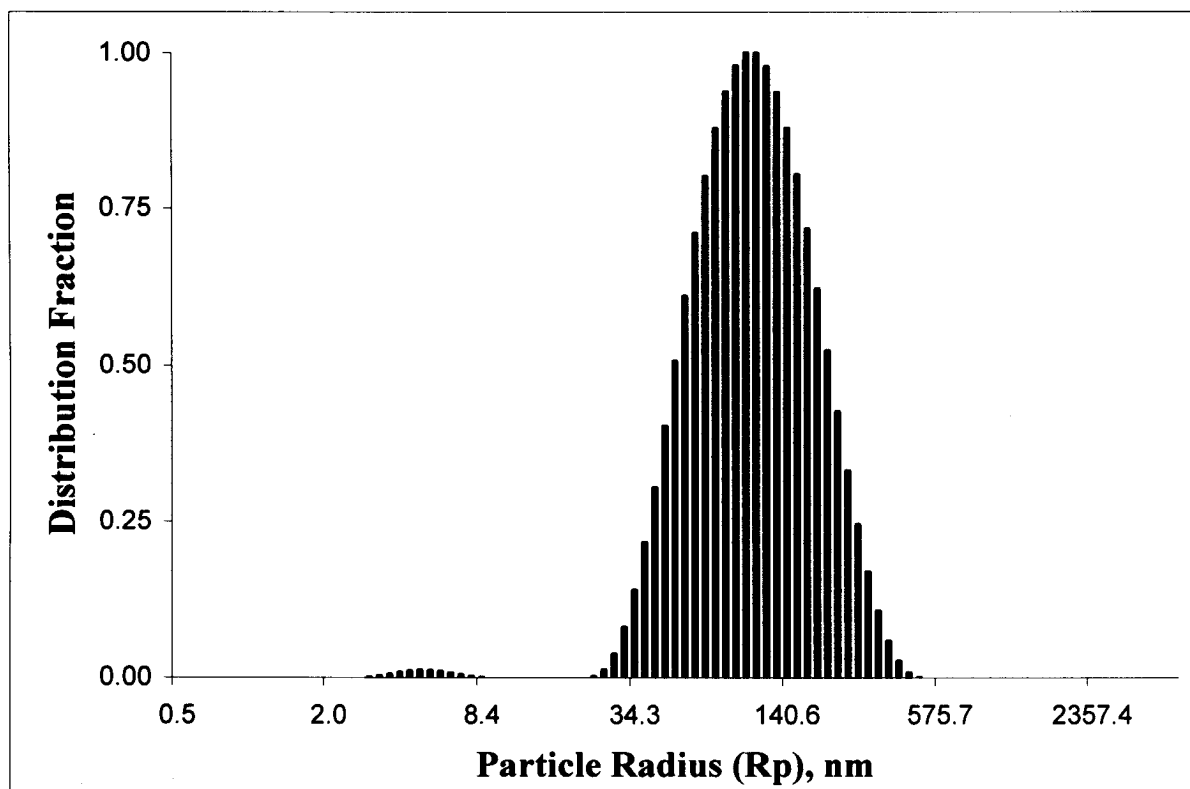
Figure 4-8: Effect of chitosan concentration on particle size distribution (Data are the average of three sets of measurement).

Chitosan concentration= 2 mg/ mL

Chitosan:TPP mass ratio = 4
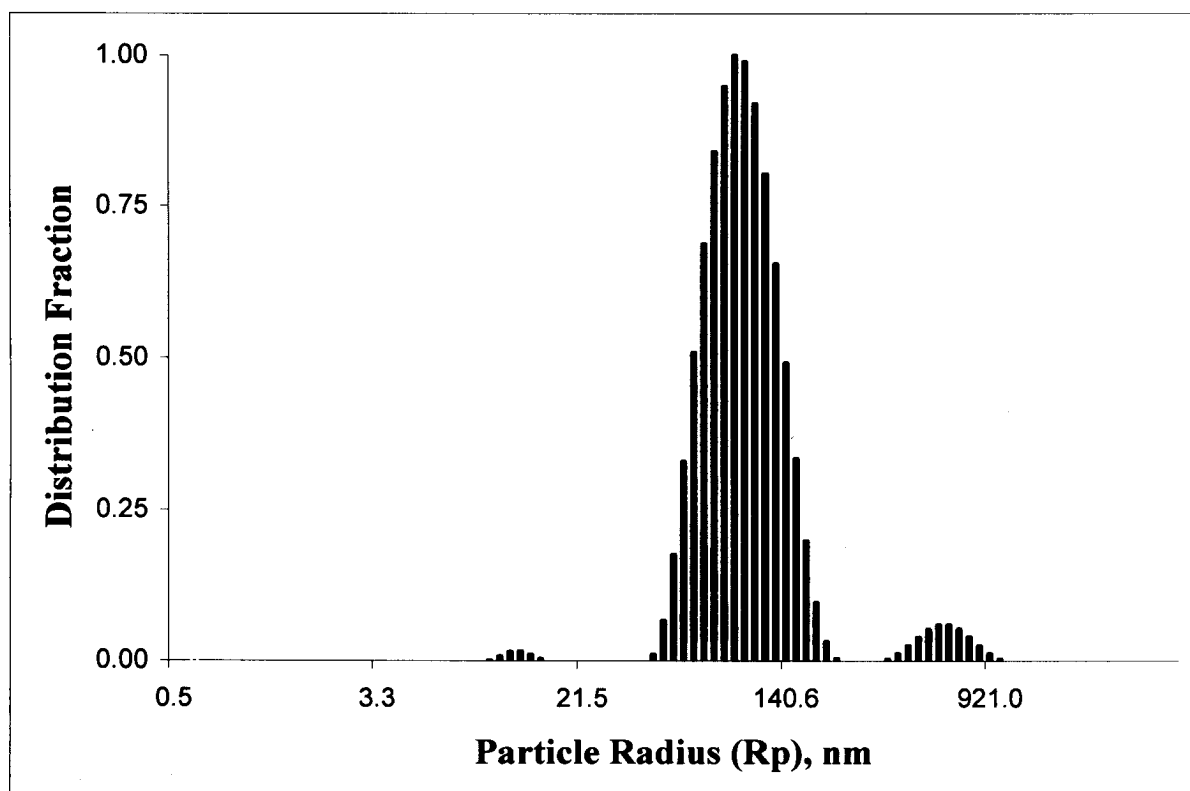
Figure 4-9: Effect of chitosan concentration on particle size distribution (Data are the average of three sets of measurement).

Chitosan concentration = 1 mg/ mL

Chitosan:TPP mass ratio = 4
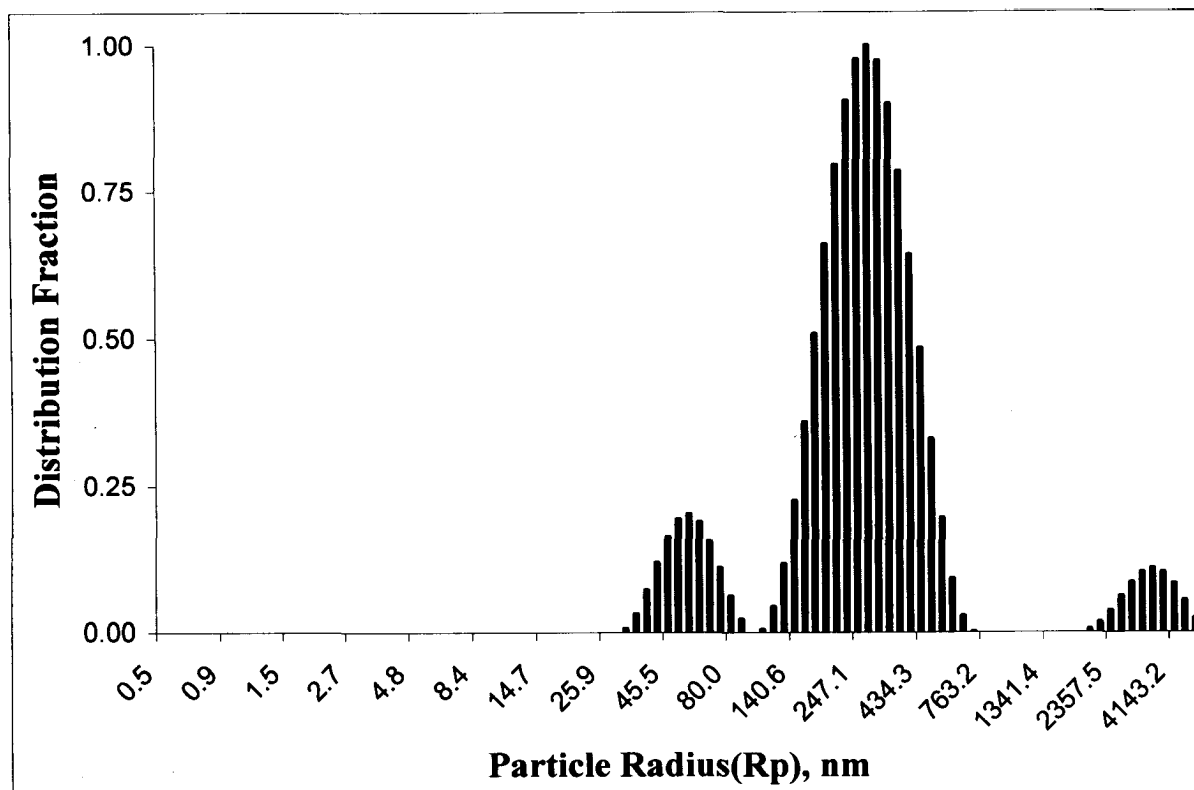
Figure 4-10: Effect of chitosan concentration on particle size distribution (Data are the average of three sets of measurement).

Chitosan concentration = 3 mg/mL

Chitosan:TPP mass ratio = 3
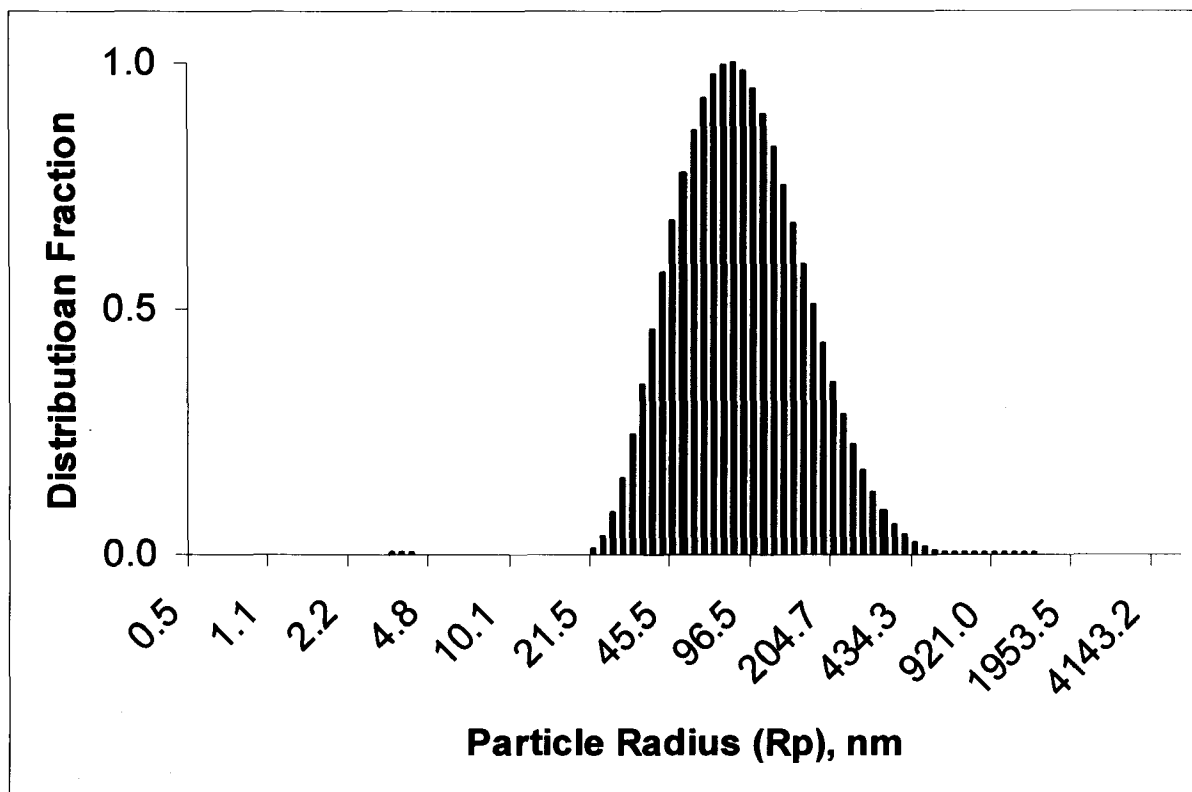
Figure 4-11: Effect of chitosan concentration on particle size distribution (Data are the average of three sets of measurement).

Chitosan concentration = 2 mg/ mL

Chitosan:TPP mass ratio = 3
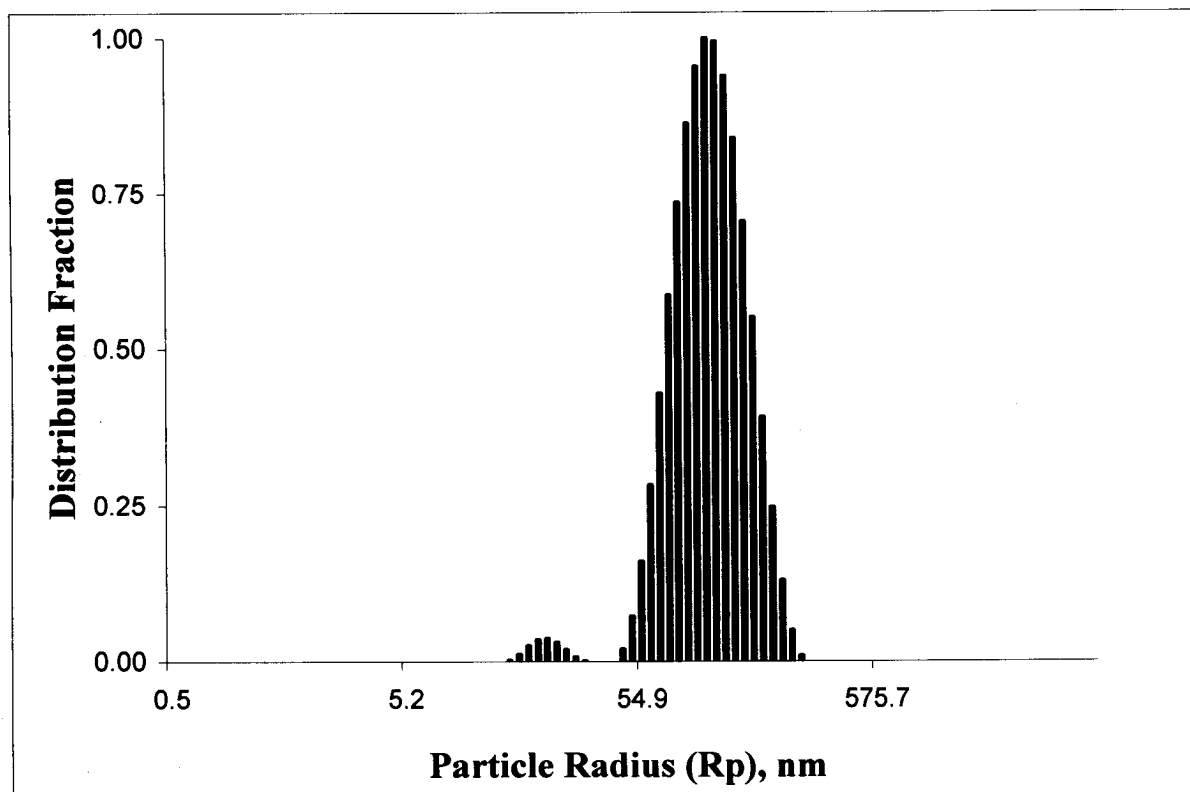
Figure 4-12: Effect of chitosan concentration on particle size distribution (Data are the average of three sets of measurement).

Chitosan concetration = 1 mg/ mL

Chitosan:TPP mass ratio = 3
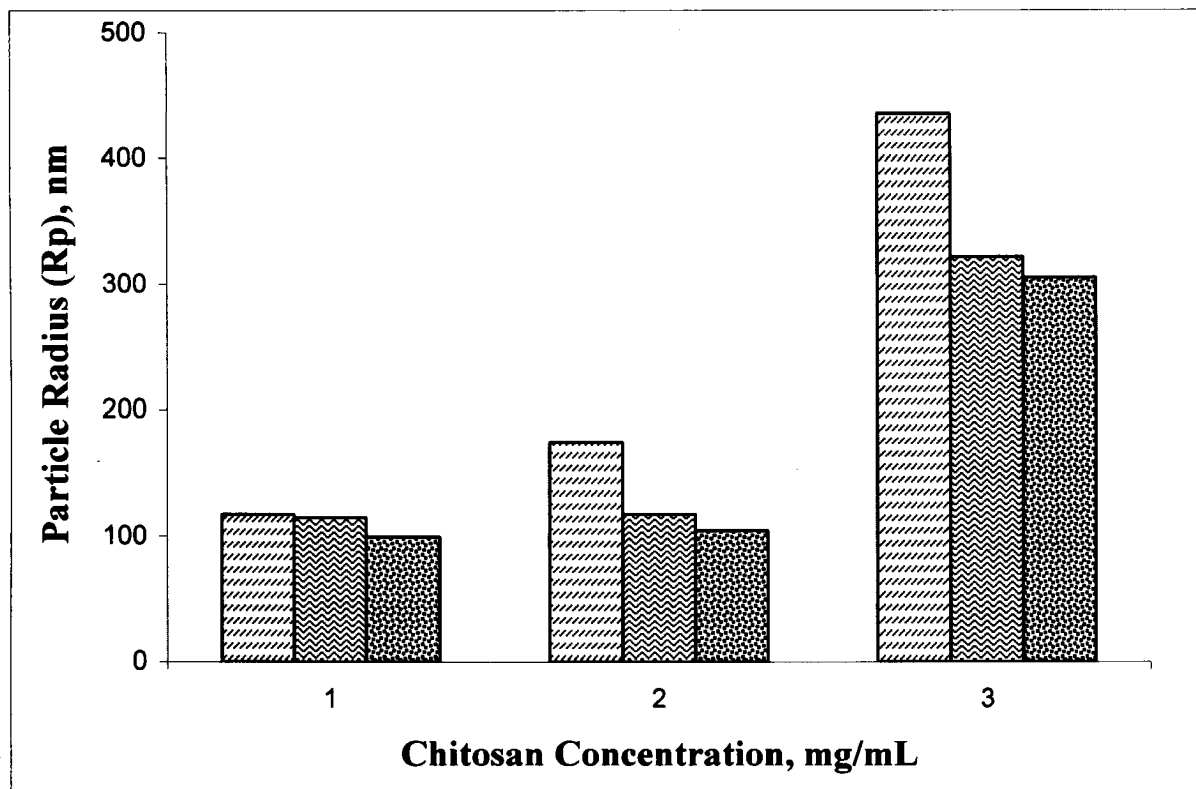
Figure 4-13: Effect of chitosan to TPP mass ratio at different chitosan concentrations (Data are the average of three set of experiments).

▨ Chitosan to TPP mass ratio = 3

▨ Chitosan to TPP mass ratio = 4

▨ Chitosan to TPP mass ratio = 5

In the next section the effect of TPP solution pH on particle size and particle size distribution was studied under the aforementioned optimum conditions (chitosan concentration = 1 mg/ml and chitosan to TPP mass ratio = 5).

4-2-2. Effect of TPP solution pH on particles size and particles size distribution

pH is an important factor in producing chitosan nanoparticles by ionotropic gelation. The basic principle of this encapsulation method is ionic interaction, therefore, it is required to adjust the working pH to an optimum level to protonise amine groups in the chitosan molecule.

It was found that, by increasing the pH of the TPP solution from 5 to 9, average chitosan particle size increased and the particle size distribution broadened. Results are shown in fig 4-14 to 4-17. When TPP solution with higher pH was mixed with chitosan solution, it may decrease the ionization of amine groups in chitosan molecule by increasing the pH of the solution, therefore the crosslinking density of particles which are formed at pH 9 is lower than that at pH 7 and it is lower than that at pH 5. This difference in cross linking cause the larger particles formed at higher pH.

4-2-3. Morphological characterization of chitosan nanoparticles

Chitosan nanoparticles were prepared at pH 5 and 9 of the TPP solution and they were photographed by transmission electron microscope (TEM). It was observed that chitosan particles prepared at pH 5 had a completely spherical shape and a smooth surface, while the particles prepared at pH 9 were not spherical, (Fig 4-18 and 4-19). Addition of TPP
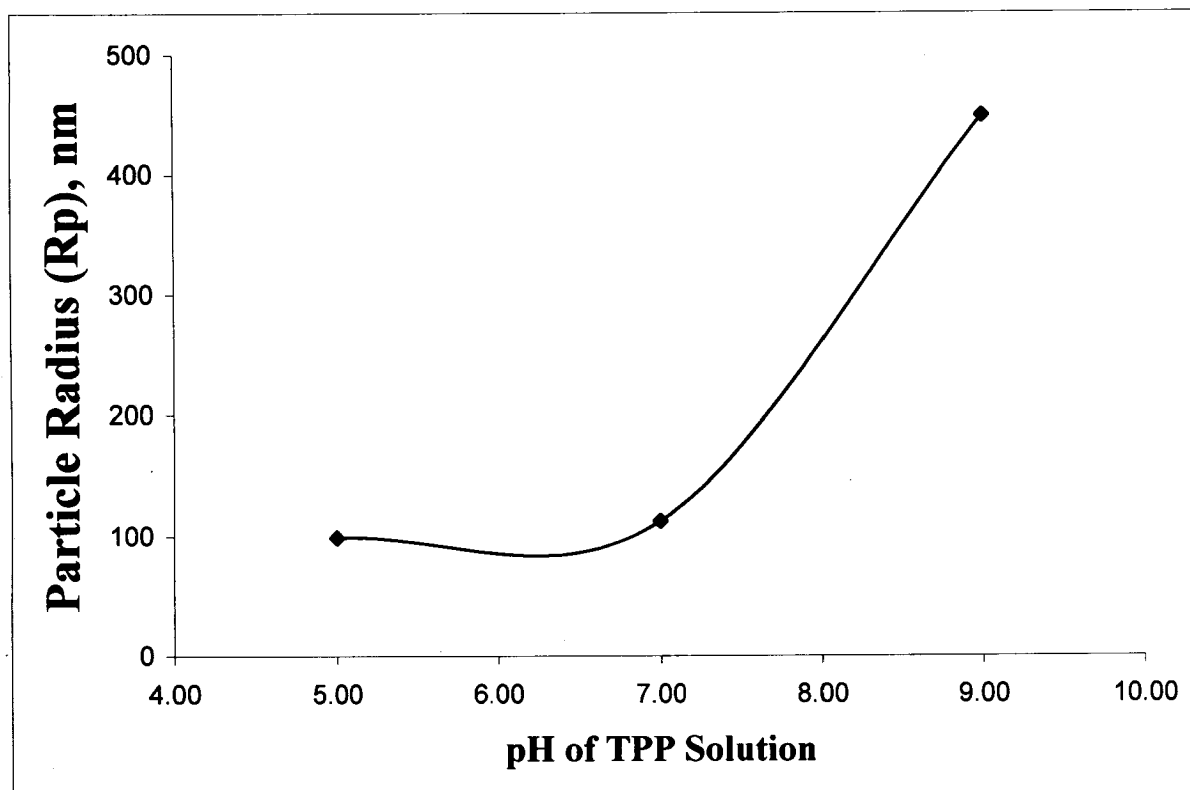
Figure 4-14: Effect of the pH of TPP solution on chitosan particles size (Data are the average of three sets of measurement).

Chitosan concentration = 1 mg/mL

Chitosan to TPP mass ratio = 5
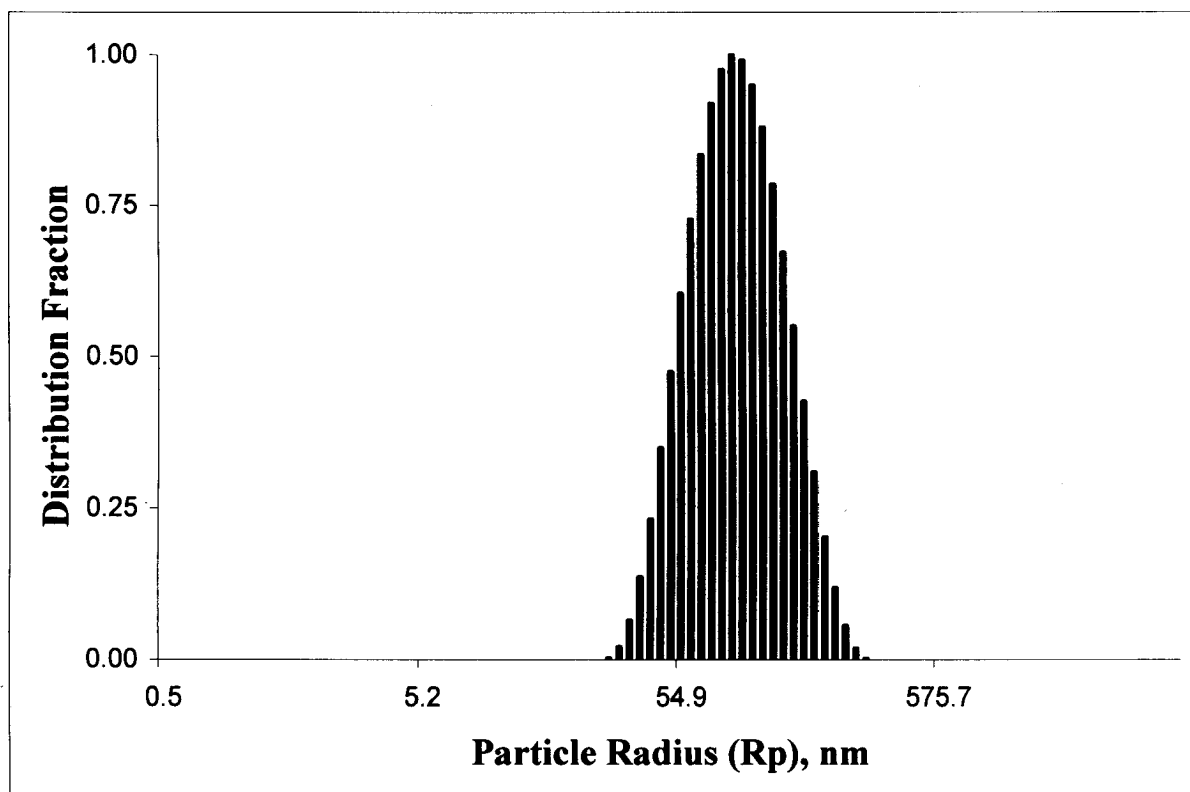
Figure 4-15: Effect of TPP solution pH on chitosan particles size distribution (Data are the average of three sets of measurement).

Chitosan concentration = 1 mg/ml

Chitosan solution pH = 5

Chitosan to TPP mass ratio = 5

TPP solution pH = 5
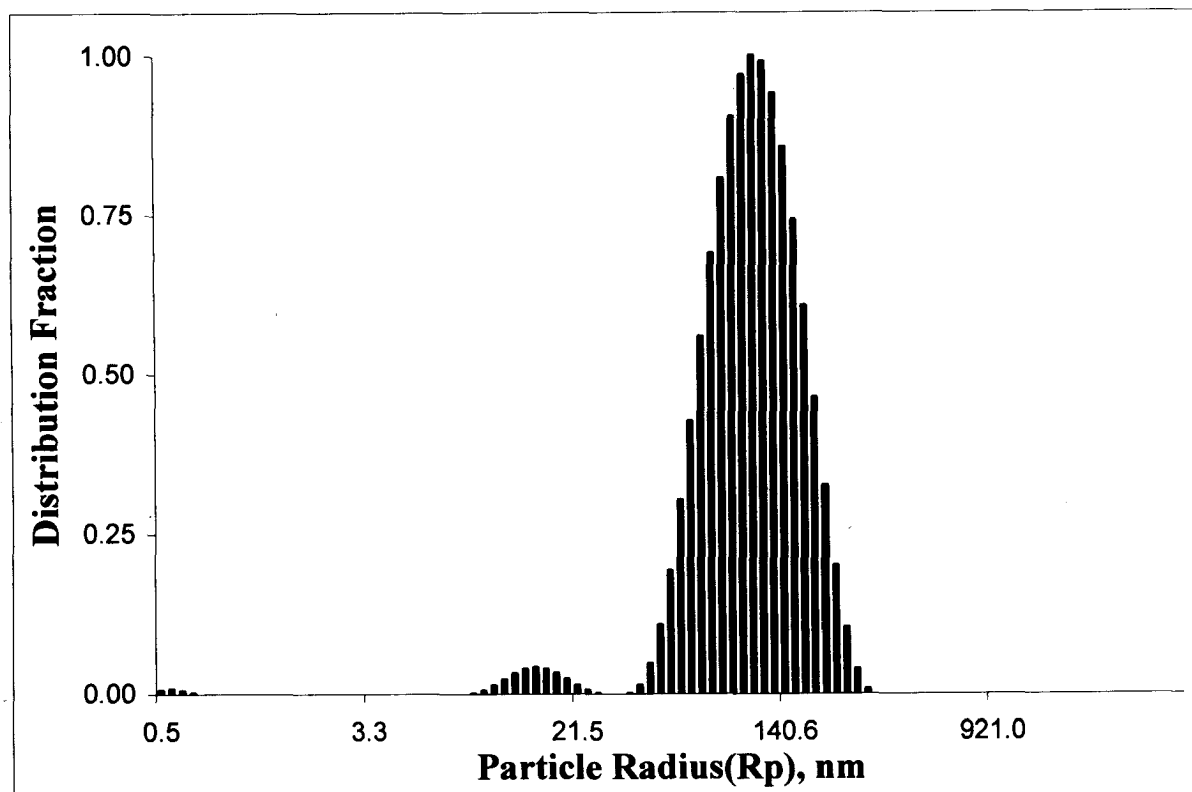
Figure 4-16: Effect of the pH of TPP solution on chitosan particles size distribution

(Data are the average of three sets of measurement).

Chitosan concentration = 1 mg/ml

Chitosan solution pH = 5

Chitosan to TPP mass ratio = 5

TPP solution pH = 7
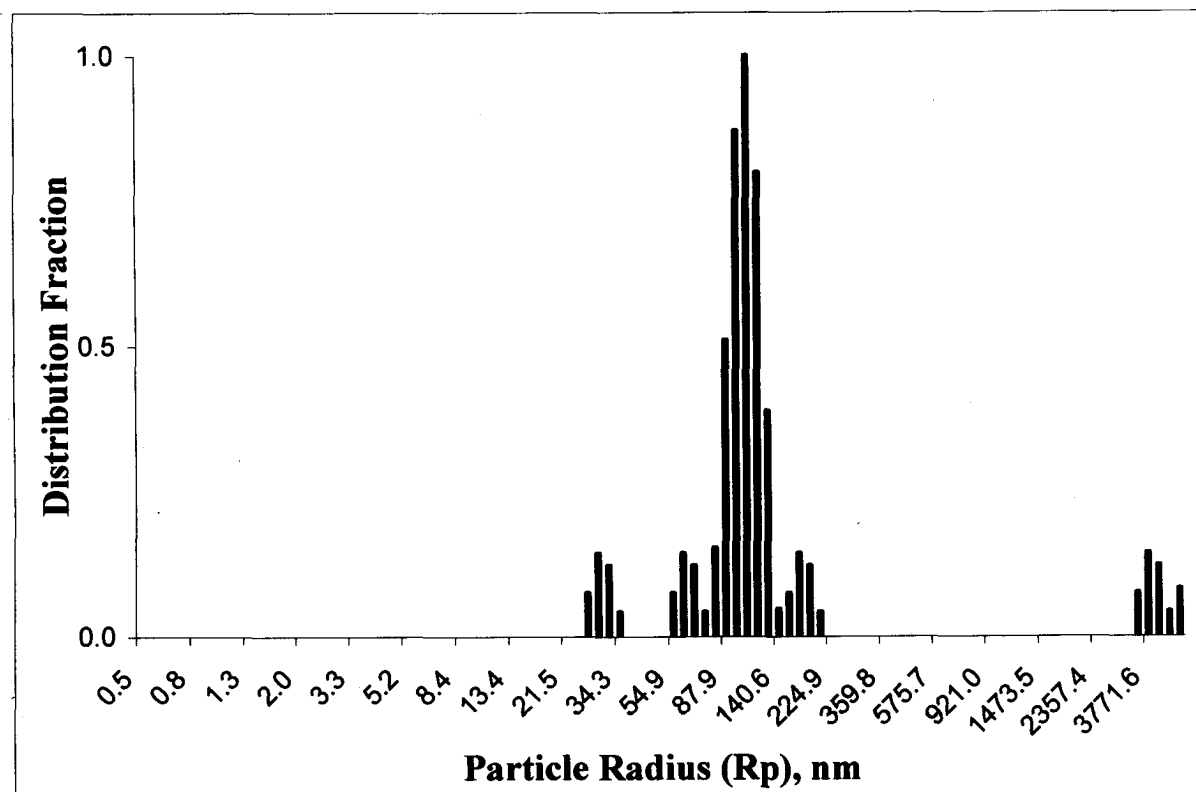
Figure 4-17: Effect of TPP solution pH on chitosan particles size distribution (Data are the average of three sets of measurement).

Chitosan concentration = 1 mg/ml

Chitosan solution pH = 5

Chitosan to TPP mass ratio = 5

TPP solution pH = 9
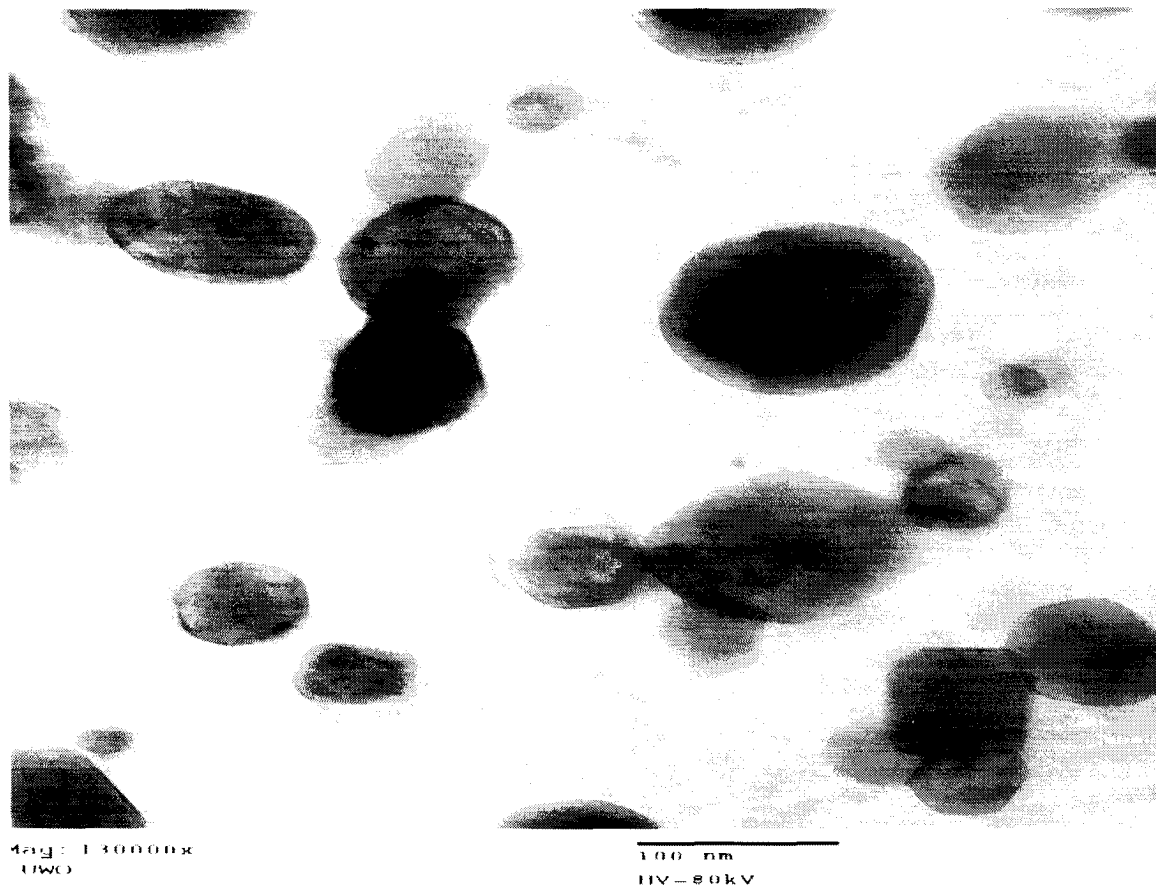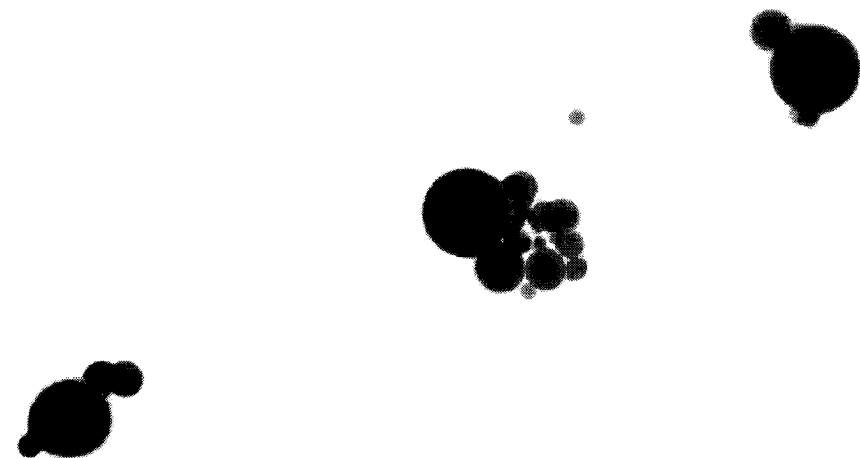
Figure 4-18: Transmission electron microscope image of chitosan nanoparticle

prepared by iontropic gelation method.

Chitosan solution = 1 mg/mL at pH 5

TPP solution 1 mg/mL at pH 9

Chitosan to TPP mass ratio = 5

Figure 4-19: Transmission electron microscope image of chitosan nanoparticle prepared by iontropic gelation method.

Chitosan solution = 1 mg/mL at pH 5

TPP solution 1 mg/mL at pH 5

Chitosan to TPP mass ratio = 5

solution at pH 9 to chitosan solution causes pH of the solution increases which will result in deportonation of the $NH_3^{\oplus}$ in the chitosan molecule, and affect the interaction between chitosan and TPP molecules. Consequently, it will affect the size and shape of the particles.

4-2-4. rh-EPO Encapsulatioon

Two hundred microliter (320µg/mL) rh-EPO was encapsulated in chitosan nanoparticles by ionotropic gelation method according to the method explained in section 3-6, supernatant was used for determination of drug loading efficiency and particles were collected for *in vitro* release study.

4-2-4. (a) Drug loading efficiency

rh-EPO concentration in supernatant was determined by fluorometric assay and drug loading efficiency was calculated according the method described in section 3-8.

$$rh - EPO \; Loading \; Efficiency = \frac{80\mu g - 52.42\mu g}{80\mu g} = 0.345$$

4-2-4.(b) In vitro release of rh-EPO

So far, the reported results in the literatures for release of rh-EPO from nano and microparticles showed an exponential drug release profile with an initial burst up to 40% in the first 48 hours and release of 80% of total loaded drug in 15 days (Pistel *et al.* 1999; Hahn *et al.* 2006).

Figure 4-20 shows the rh-EPO release profile form the chitosan nanoparticles *in vitro*. The study of rh-EPO release from the chitosan naoparticles (200 nm) into PBS solution showed a significant decrease in initial drug release form the particles in the first 24 hours. It was observed that only 22% of rh-EPO loaded in chitosan nanoparticles was released in first 24 hours, and the amount of rh-EPO released in first 48 hours is almost 30%. Then, after 48 hours , rh-EPO released from the particles for two weeks linearly and the total cumulative release was almost 60% in 15 days.

It is known that initial release of the drugs from nano and microparticles is due to adsorption of drugs to the surface of particles and diffusion of drugs which are dispersed inside the particles very close to the surface (Xu and Du, 2993). In the case of rh-EPO release, the significant decrease in initial release can be due to great affinity between chitosan molecule and sialic acids on rh-EPO molecule which prevent easy dissociation of protein from the particles in physiological buffer. The chitosan - sialic acid interaction can also be responsible for the retardation of rh-EPO release for the next 15 days. Moreover, adjusting TPP solution pH at 5 causes formation of denser particles and consequently the pores size will decrease which results in slower diffusion of rh-EPO through the particles pores. This was observed in BSA and felodipine release from chitosan-TPP nanoparticles as well when the pH of TPP solution was reduced from 7 to 5 (Xu and Du, 2003; Sinha *et al.,* 2004).

Drug release from the nanoparticles involves diffusion of rh-EPO and degradation of chitosan molecule. As it is shown in figure 4-20, rh-EPO release profile from chitosan
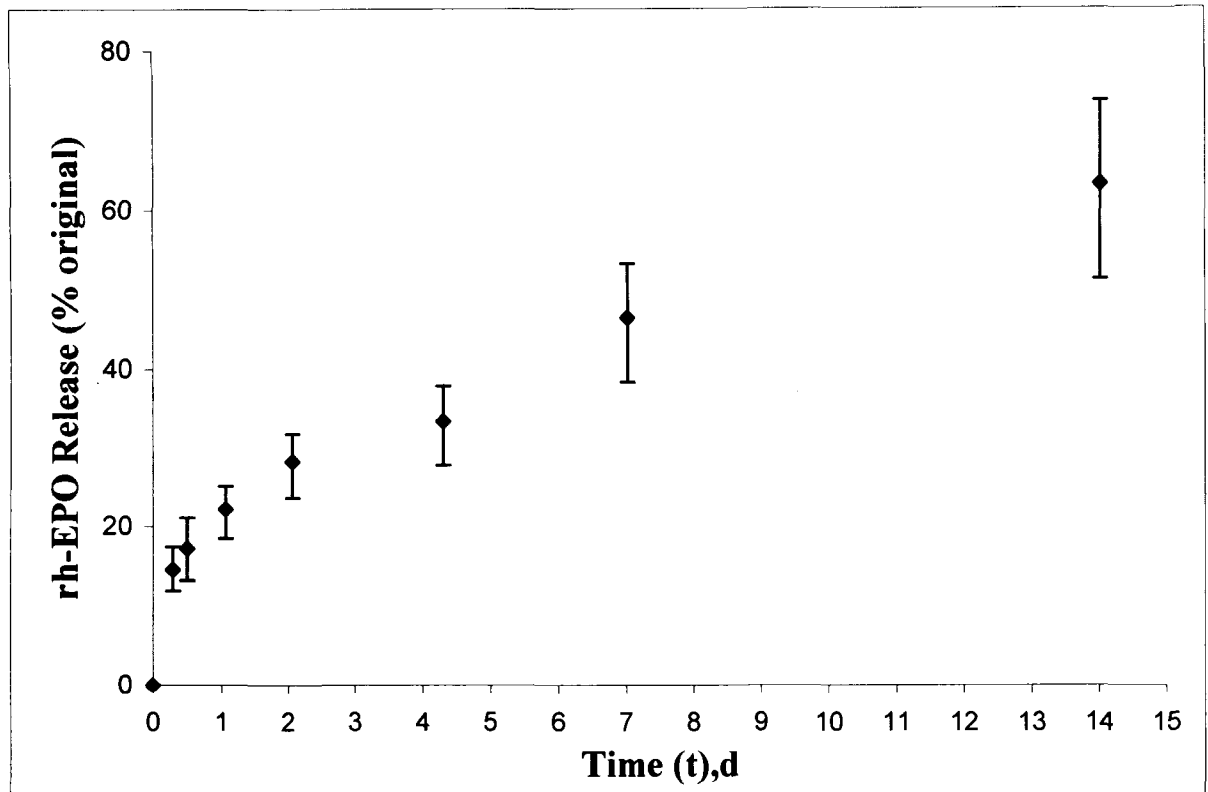
Figure 4-20: rh-EPO release profile from chitosan nanoparticles (200 nm) in PBS solution at 37°C. rh-EPO release study was repeated three times.

nanoparticles has an exponential phase at the beginning and a linear phase from day 2 to 15. Equations 2-8 and 2-16 show that drug release from an spherical particles is exponential when diffusion controls the drug release. Therefore, it can be concluded that diffusion is the dominant mechanism in rh-EPO drug release from chitosan naoparticles for the first 48. Then drug release becomes linear which was hypothesized to be due to polymer dissolution. Lee (1980) reported that in surface erosion drug release becomes zero order so cumulative release becomes linear. It is speculated here that in chitosan-TPP nanoparticles, the polymer starts disintegrating from the surface after 48 hours, and polymer dissolution controls the drug release.

4-2-5. Estimation of rh-EPO diffusivity in chitosan nanoparticles

rh-EPO diffusivity was calculated by immersing the loaded chitosan nanoparticles in 10 ml PBS solution and the drug release over time was measured.. rh-EPO is miscible in aqueous media and chitosan loaded nanoaprticles was prepared with a very small amount of rh-EPO, therefore, as it was discussed in section 2-2-1, it is more appropriate to use the mathematical model for immersing of spherical particles in infinite liquid volume. Under this circumstance, equation 4-1 can be used to estimate the diffusivity of rh-EPO in chitosan nanoparticles.

$$\frac{M_s^t}{M_s^0} = 1 - \frac{6}{\pi^2} \sum_{n=1}^{\infty} \frac{1}{n^2} \exp\left(-\frac{D_e n^2 \pi^2 t}{R^2}\right) \qquad (4\text{-}1)$$

The experimental results which were used to calculate the diffusion coefficient of rh-EPO in chitosan nanoparticles is shown in Appendix D, Table 2. According to the data in the table and equation 4-1, it was calculated that the rh-EPO diffusion coefficient

is 2.651 x 10^{-19} m^2/s. Comparing this value with diffusivity of bovine serum albumin in alginate bead which is 2.4 x 10^{-11} m^2/s (Millman, 1992), noticed that the rh-EPO has mush lower diffusion coefficient. This might be because of great affinity between chitosan and sialic acid and ionic interaction between chitosan and rh-EPO which slow down the movement of rh-EPO molecule through chitosan pores.

4-2-6. Developing rh-EPO assay method by HPLC

ELISA method is the most accurate and sensitive method which is used for measuring rh-EPO concentration so far. ELISA works based on antibody-antigen interaction between rh-EPO and EPO receptor. Although, it is very accurate method and widely used in clinical laboratories, its maximum level of detection is 800 ng/L. This low level of detection is only practical for *in vivo* studies. In addition, ELISA is an expensive and time consuming assay. Therefore, developing a method which can detect rh-EPO in higher concentration but with the same accuracy level as ELISA is very important. High-Performance Liquid Chromatography (HPLC) is a fast, accurate and less expensive analytical technique which can be considered as a good substituent.

rh-EPO assays by HPLC have already been reported by Morlock *et al.* (1997) and Hahn *et al.* (2006). They utilized size exclusion chromatography and reverse phase HPLC (RP-HPLC), respectively. Although they have reported rh-EPO has been detected with good resolution, the detection level was fairly high (100 µg/mL) and there is no report of minimum detectable levels.

To overcome this issue, a method for rh-EPO assay by RP-HPLC was developed which can quantitatively detect rh-EPO as low as 500 ng/mL. In this method, a C4 reverse phase column was utilized and rh-EPO was monitored in the eluent by fluorescence detection (Waters 474). Excitation wavelength was set at 280 nm and fluorescence emission was recorded at 340 nm.

The method was developed in two stages. In the first stage, the goal was finding the appropriate conditions for rh-EPO detection qualitatively. Therefore, acetonitrile which is the most common solvent for reverse phase HPLC (Sadek 1996), was used as solvent. Mobile phases A and B prepared by mixing 5% and 80% acetonitrile with double distilled water, respectively, and 0.1% triflouroacetic acid (TFA) was added to each phase as ion pairing agent. The gradient was starting from 0% mobile phase B to 100% mobile phase B over 10 min which was recommended condition in Phenomenex brochure of the purchased C4 column for detection of bovine serum albumin (BSA). First BSA was injected and column performance was tested for BSA (fig 4-21), and then 15 µL of 16000 ng/mL EPO was injected. As it is shown in Fig 4-22, rh-EPO peak appeared after 15 min with a symmetrical shape, but it has two small peaks attached to it. Small peaks can be due to spreading of rh-EPO band while it was moving through the column. To eliminate these peaks and improve the column efficiency, one approach is to change the strength of mobile phase. According to solvophobic theory, binding of solute to the stationary phase depends on the molecular structure of alkyl chains and the surface tension of eluent solvent. Therefore, increasing the concentration of organic solvent in mobile phase, will reduce the surface tension. As a result analyte can not form a strong
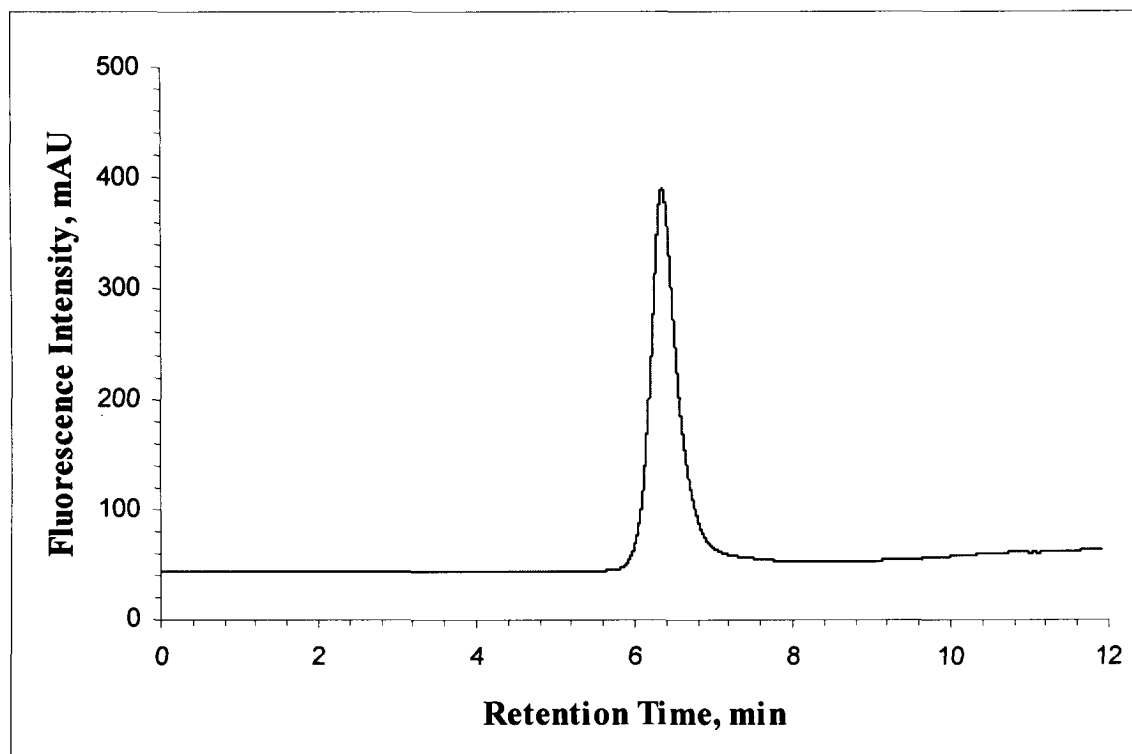
Figure 4-21: BSA chromatogram by RP-HPLC. Mobile phase A=5% acetonitrile, Mobile phase B= 80% acetonitrile, Gradient= 0% B to 100 % B over 15 min. Flow rate 0.5 mL/min. C4 column (150 X 4.6 mm, 300°A, 5μm), Excitation wavelength 280 nm and emission wavelength 340 nm.
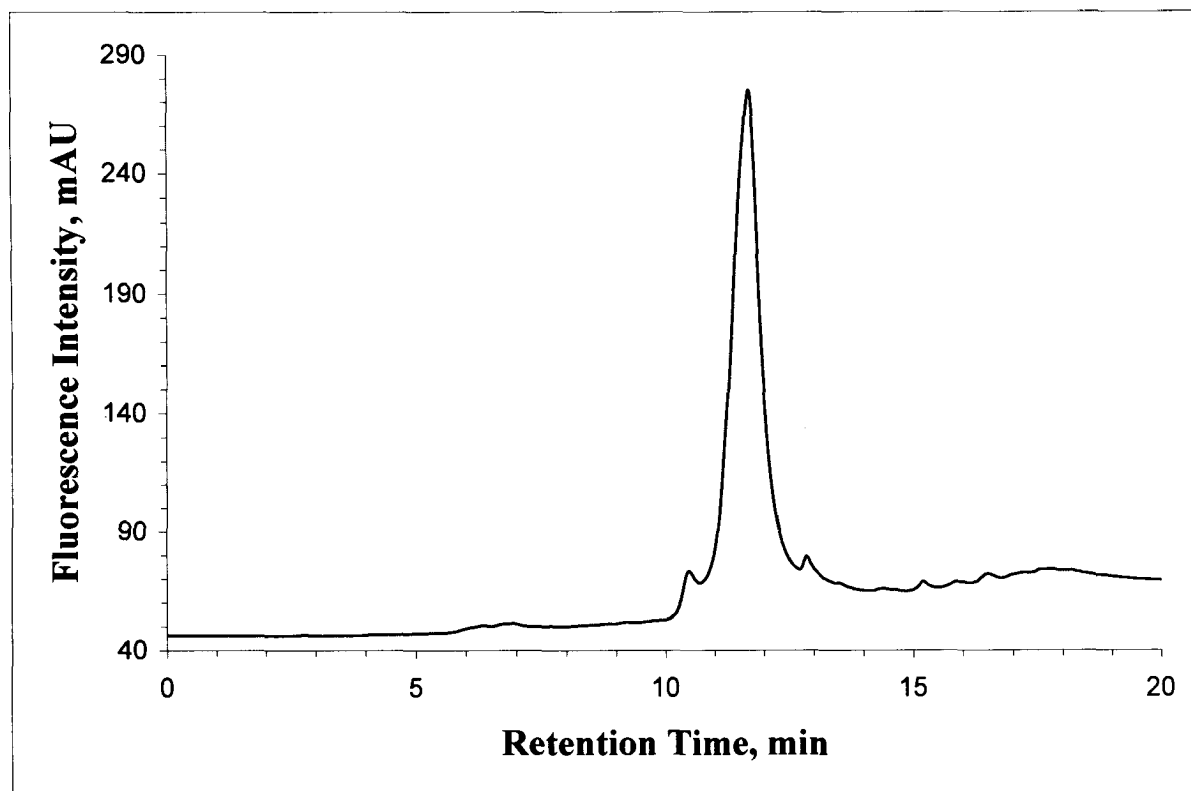
Figure 4-22: EPO chromatogram by RP-HPLC. EPO concentration =16 µg/mL; Injection volume 15 µl ; Mobile phase A=5% acetonitrile, Mobile phase B= 80% acetonitrile; Gradient= 0% B to 100 % B over 10 min; Flow rate 0.5 mL/min; C4 column (150 X 4.6 mm, 300°A, 5µm); Excitation wavelength 280 nm and emission wavelength 340 nm.

bound with the stationary phase and it will not spread throughout the column (Szepesi, 1992; Viseras *et al.*, 1987).

To investigate this effect, shallower gradients were used by increasing concentration of acetonitrile at time zero and decreasing its final concentration and gradient was run over 10 min. The best result was obtained when gradient was set at 50% mobile phase B at time zero to 85% mobile phase B at time 10. The results are shown in fig 4-23 and 4-24. For these analyses the rh-EPO samples which were used contained human serum albumin and benzyl alcohol. The first two peaks which are seen in chromatograms belong to these two compounds. Although, the method was not optimized for protein separation, it can be concluded from the graphs that the operating condition has the potential to be used for separation of rh-EPO from albumin or possibly different proteins with good selectivity.

Acetonitrile uses in protein chromatography by HPLC due to its low UV cut off which causes a very low background absorbance when low wavelength is used (Sadek 1996). If the resolution is not sacrificed, at higher wavelength (>235 nm) it is possible to use other solvents which are less expensive and have less health and safety hazards, such as, methanol (Sadek 1996). In case of rh-EPO assay by HPLC, the fluorescence detector is used and the excitation wavelength is 280 nm which is far beyond the methanol UV cut off of 205 nm. Therefore, in the next stage of method development, acetonitrile was replaced by methanol. Methanol is considered as a weaker solvent in reverse phase chromatography. So, the concentration of mobile phase and the starting point and end point in gradient was set higher to maintain almost the same resolution as acetonitrile.
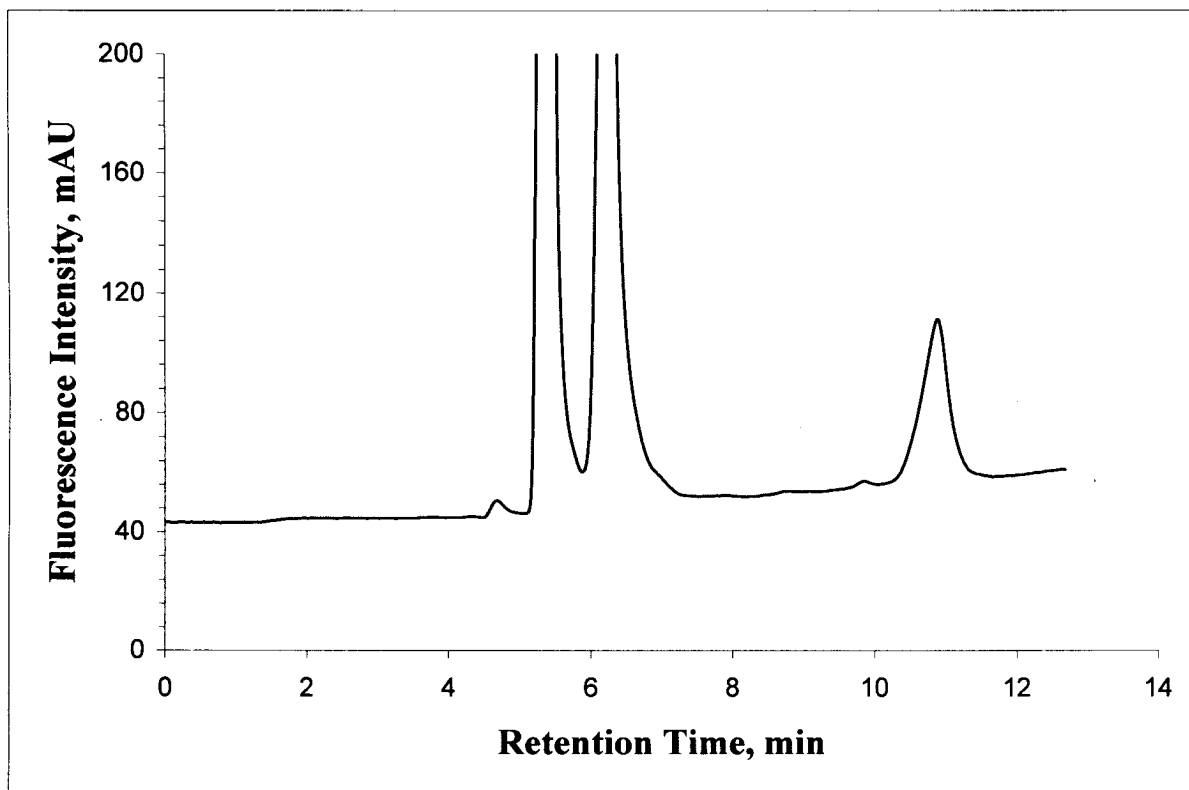
Figure 4-23: EPO chromatogram by RP-HPLC. EPO concentration = 16 μg/mL, (EPO sample contained HSA and benzyl alcohol); Injection volume= 5 μL; Mobile phase A=5% acetonitrile, Mobile phase B= 80% acetonitrile; Gradient= 45% B to 70 % B over 10 min; Flow rate 0.5 mL/min; C4 column (150 X 4.6 mm, 300°A, 5μm), Excitation wavelength 280 nm and emission wavelength 340 nm.
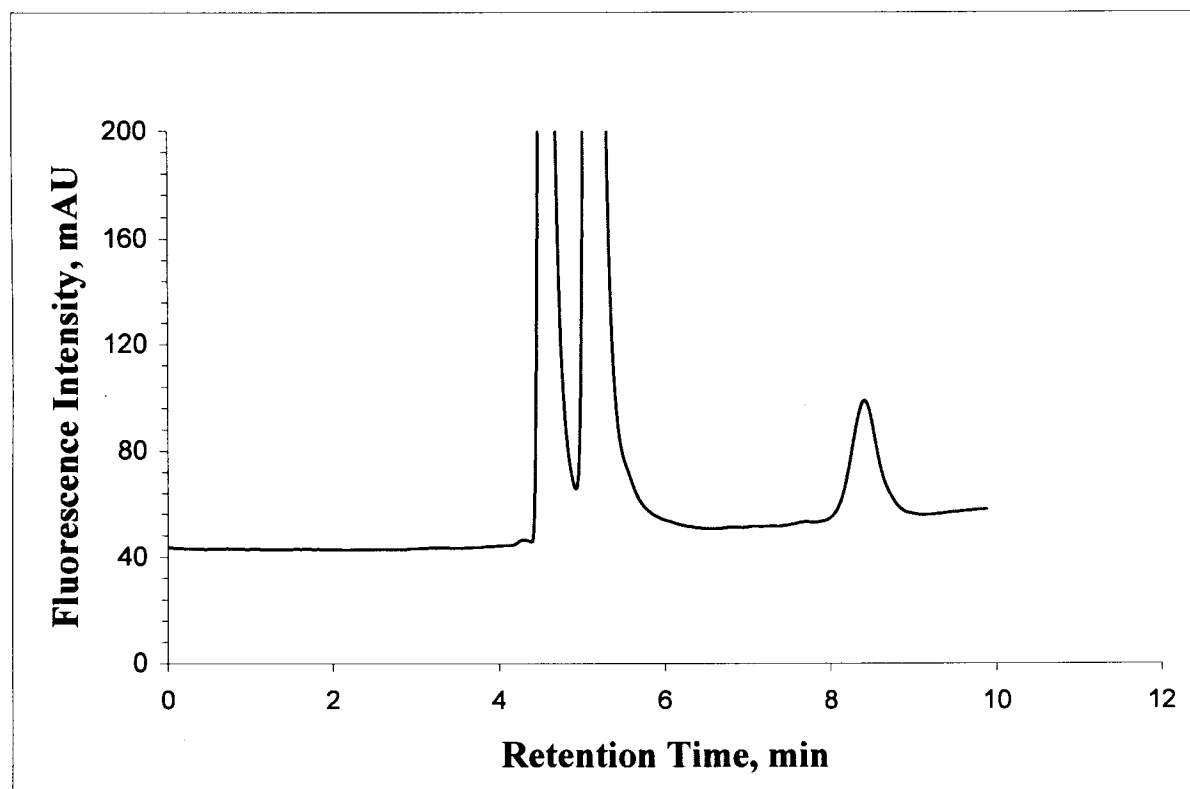
Figure 4-24: EPO chromatogram by RP-HPLC. EPO concentration = 16 µg/mL, (EPO sample contained HSA and benzyl alcohol); Injection volume= 5 µL; Mobile phase A=5% acetonitrile, Mobile phase B= 80% acetonitrile; Gradient= 50% B to 85 % B over 10 min; Flow rate 0.5 mL/min; C4 column (150 X 4.6 mm, 300°A, 5µm), Excitation wavelength 280 nm and emission wavelength 340 nm.

Mobile phase A was 60% methanol in double distilled water, and mobile phase B was 100% methanol. 0.1 % TFA was added to both mobile phases. rh-EPO was analyzed by running a gradient from 0% mobile phase B to 100% mobile phase B over 10 min, then keep the system running at 100% methanol for 3 min. EPO was detected at 10.2 min with a very good peak symmetry. To confirm the reproducibility of the method, samples was run several times and the results obtained where the same for all of them. Figure 4-25 shows the results which was obtained by three times injection of a 2 µg/mL rh-EPO sample. Four different concentration of rh-EPO were analyzed by HPLC using the aforementioned condition. Figure 4-26 shows that peak size varies by changing the rh-EPO concentration. Standard curve was generated by plotting rh-EPO concentration vs. area under the peak. As it is shown in figure 4-27, this correlation is linear with $R^2 = 0.989$.

4-2-7. PLGA Microparticle Production

Poly(lactic-co-glycolic acid) (PLGA) microparticles were prepared by emulsification – evaporation method and the effect of homogenization time and speed was investigated on particle size and particle size distribution (Fig 4-28 to Fig 4-39). Final size of the particles in this method depends greatly on the size of the droplets which are formed during the homogenization. By increasing the homogenization time and speed, shear stress increases and consequently finer droplets are formed (Zhao *et al.*, 2007; Lee *et al.*,2000). As it is shown in Fig 4-28 and Fig 4-34, it was observed that at constant homogenization speed particles size decrease by increasing the homogenization time up to a certain point then it starts increasing again as homogenization time increases. During the experiment, it was

72
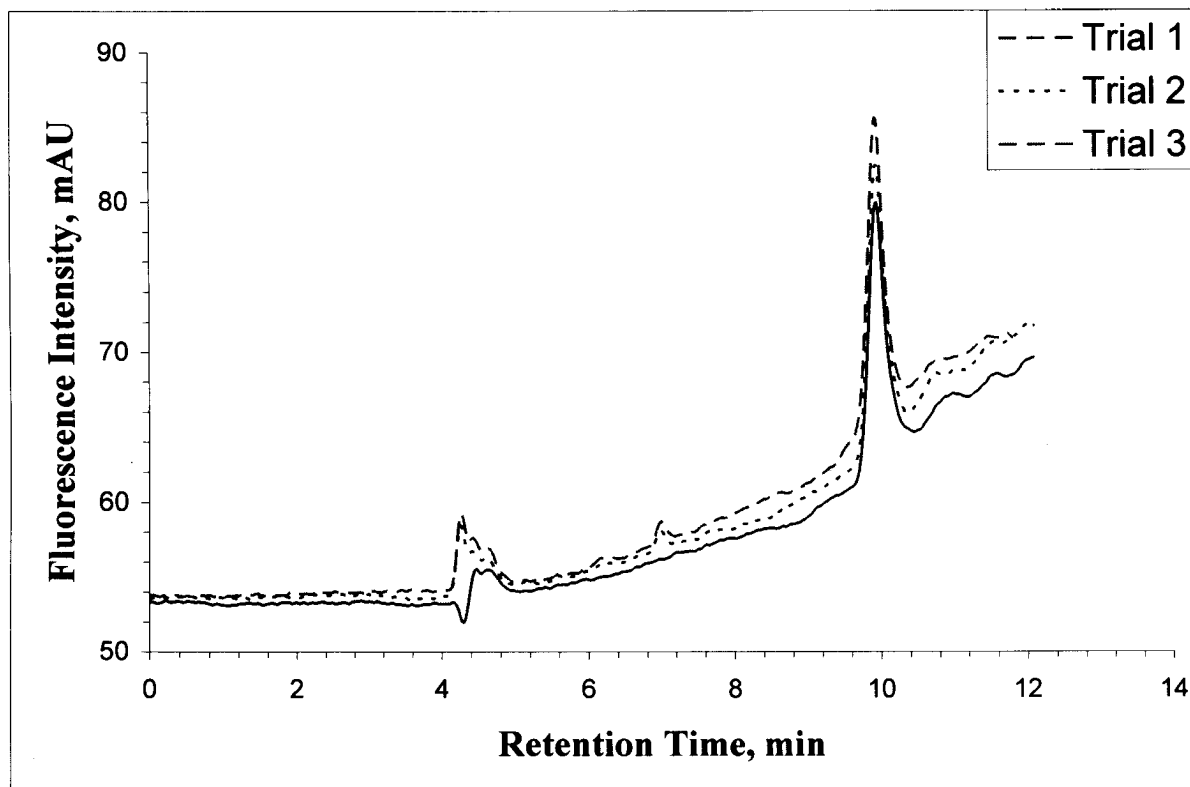
Figure 4-25: Chromatogram of 3 samples of EPO (2000 ng/mL) analyzed by RP-HPLC. EPO Concentration =2 µg/mL; Injection Volume = 15 µL; Mobile phase A=60% methanol, Mobile Phase B= 100% methanol; Gradient= 0% B to 100 % B over 10 min; Flow rate 0.5 mL/min; C4 Column (150 X 4.6 mm, 300°A, 5µm); excitation wavelength 280 nm and emission wavelength 340 nm.
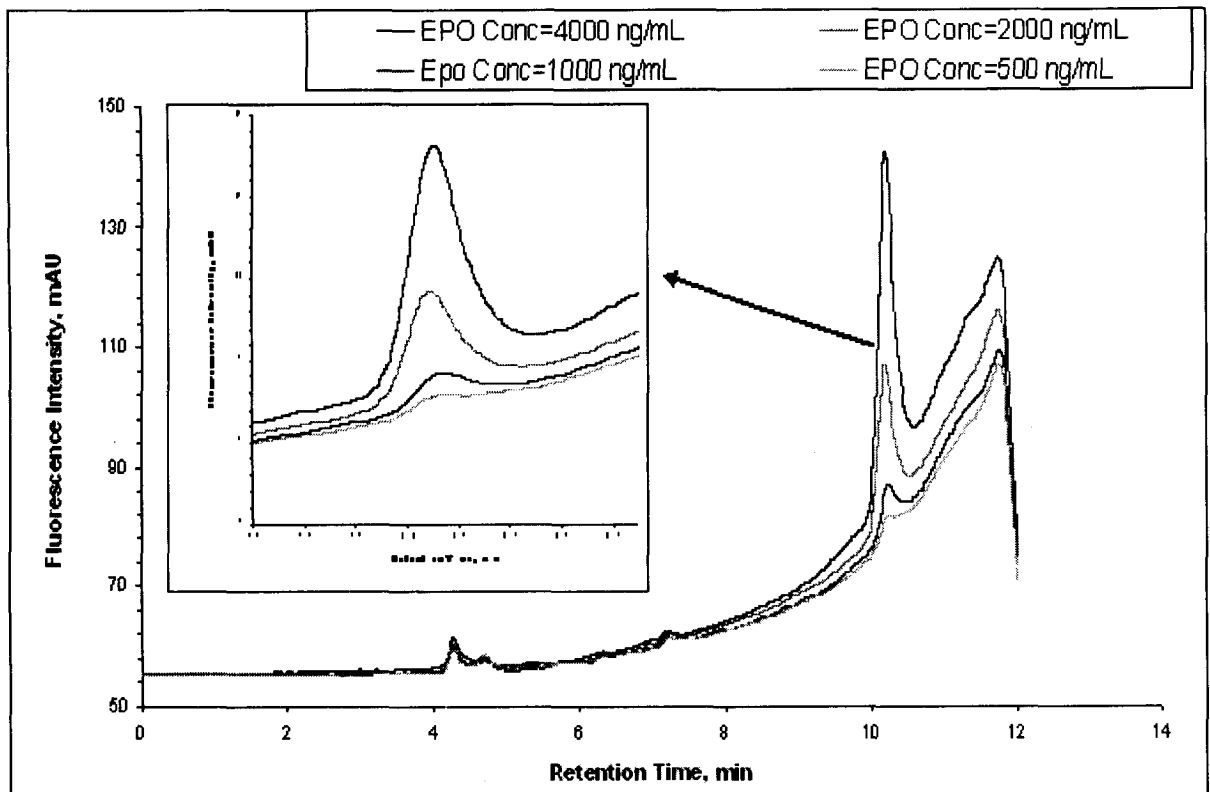
Figure 4-26: Chromatogram of standard rh-EPO samples. Area under the curve was used to generate standard curve. Injection volume= 15µl; Mobile phase A=60% methanol, Mobile phase B= 100% methanol; Gradient= 0% B to 100 % B over 10 min; Flow rate 0.5 mL/min; C4 column (150 X 4.6 mm, 300°A, 5µm); Excitation wavelength 280 nm and emission wavelength 340 nm.
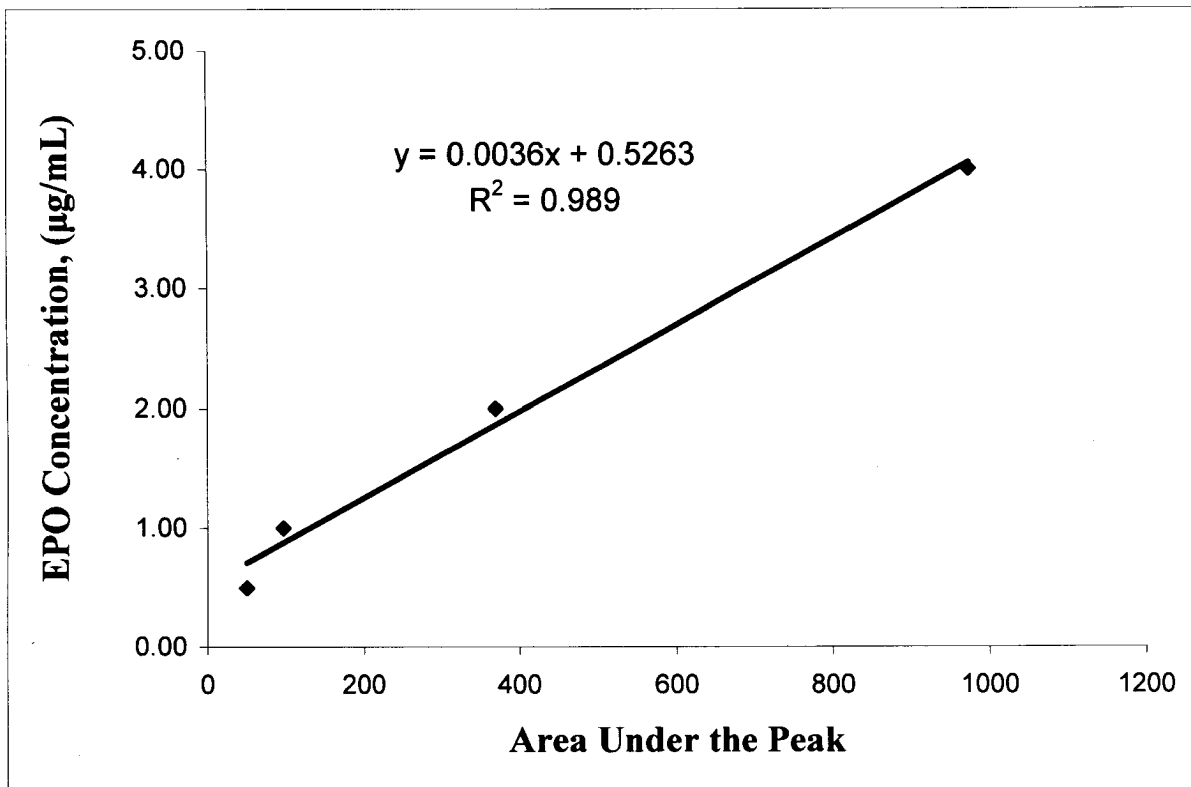
Figure 4-27: Standard curve for rh-EPO assay by RP-HPLC.
Injection volume = 15 µg/mL; Mobile phase A=60% methanol, Mobile phase B= 100% methanol; Gradient= 0% B to 100 % B over 10 min; Flow rate 0.5 mL/min; C4 column (150 X 4.6 mm, 300°A, 5µm); Excitation wavelength 280 nm and emission wavelength 340 nm.

observed that when the homogenization time increases, volume of foam which is formed on top of the liquid phase increases and at longer homogenization time almost whole of the liquid change to the foam due to dispersion of air into the liquid. It was hypothesized that, this phase changes cause the shear stress reduces and therefore, fine droplets aggregate and form larger ones which influence the final particle size. This effect can be seen well in figure 4-40 at time 6 and 8, size of the particles which are formed at 24000 rpm are significantly larger than the ones which are formed at 13500 rpm. Although, the homogenization speed is higher but the shear stress reduces due to formation of foam.
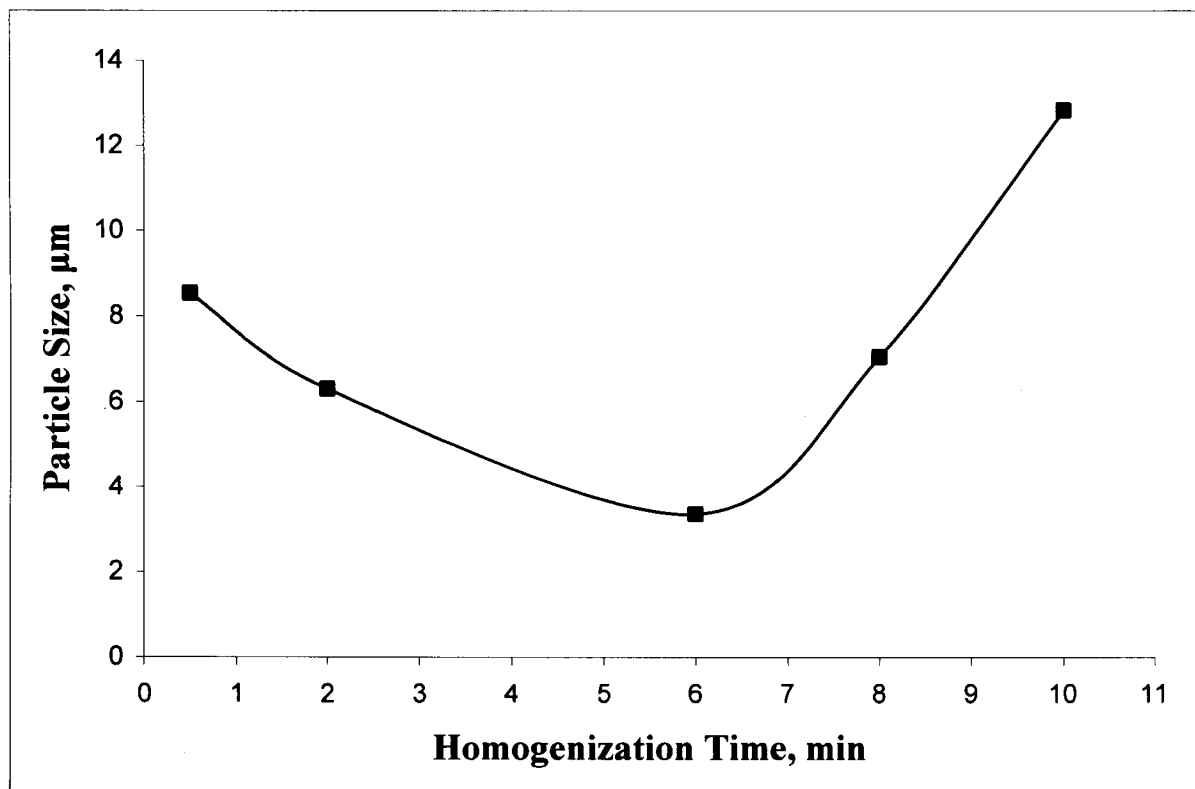
Figure 4-28: Effect of homogenization time on PLGA average particle size (Data are the average of three sets of measurement).

Homogenizer speed =13500 rpm
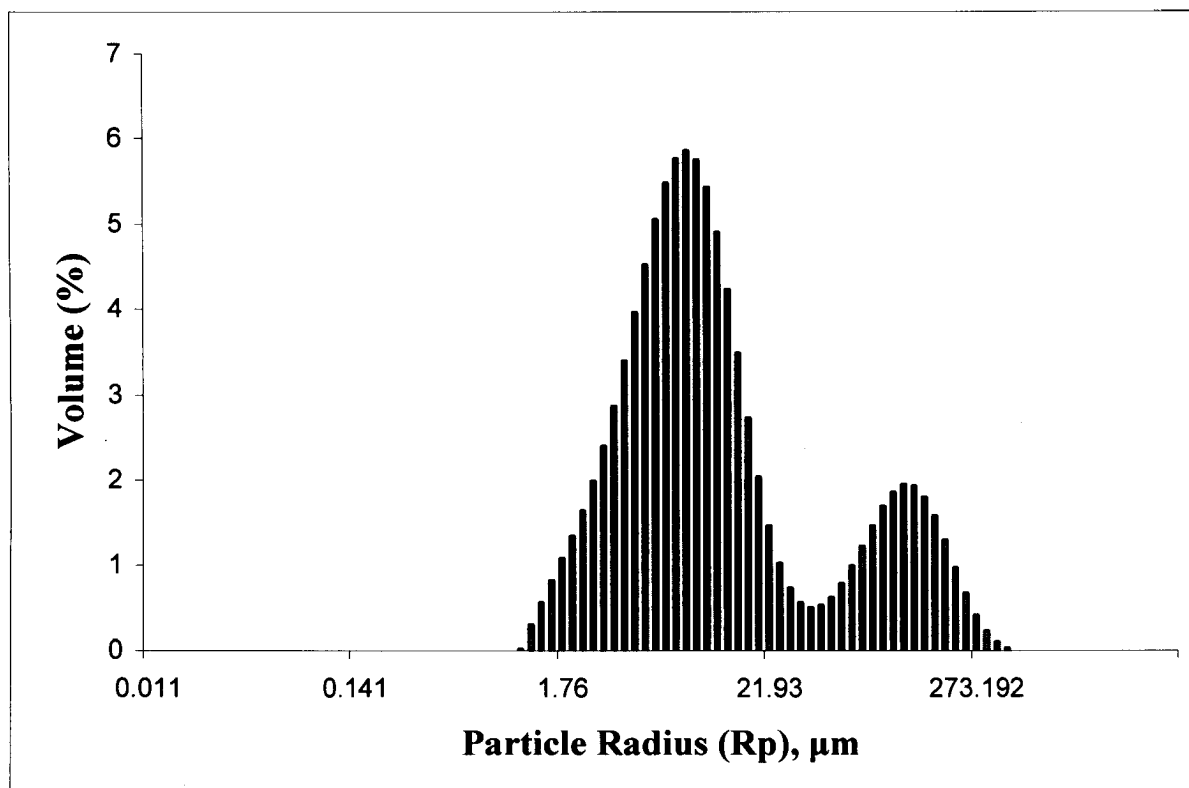
Figure 4-29: PLGA particle size distribution produced by emulsification-evaporation method (Data are the average of three sets of measurement).

Homogenization speed = 13500 rpm

Homogenization Time = 30 s
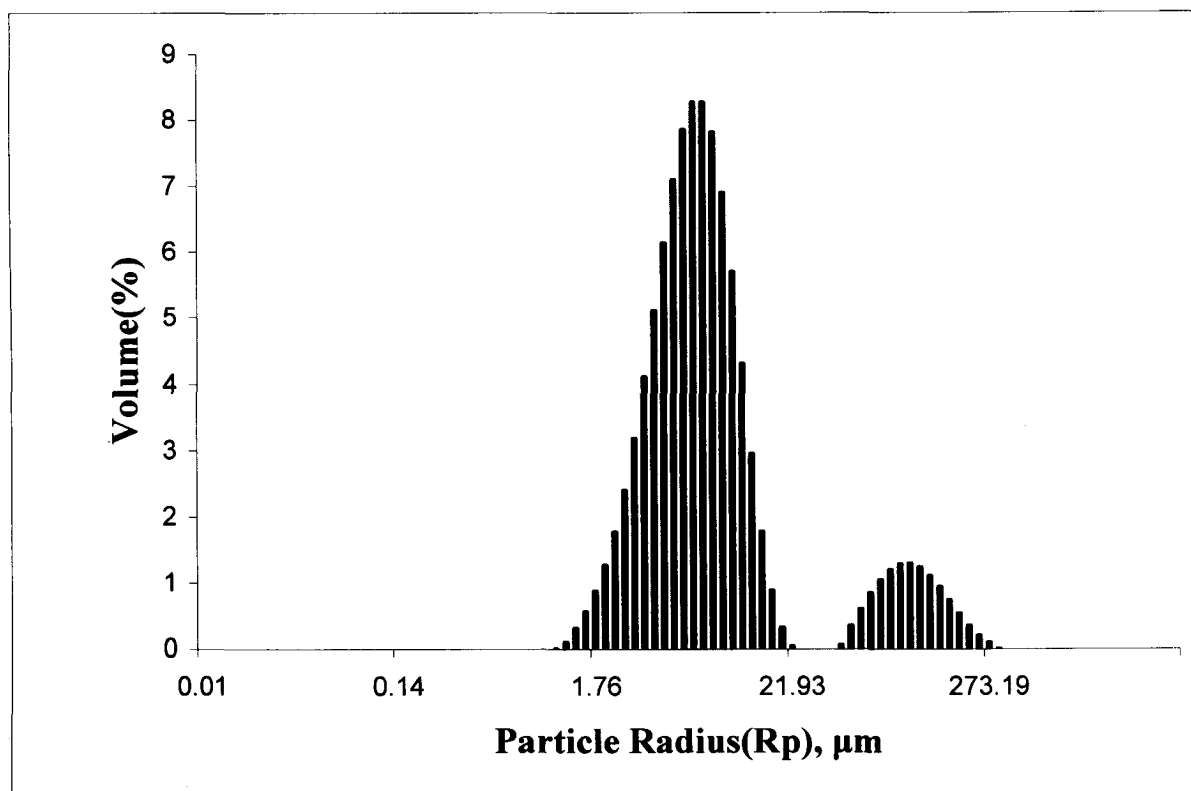
Figure 4.30: PLGA particle size distribution produced by emulsification-evaporation method (Data are the average of three sets of measurement).

Homogenization speed = 13500 rpm

Homogenization Time = 2 min
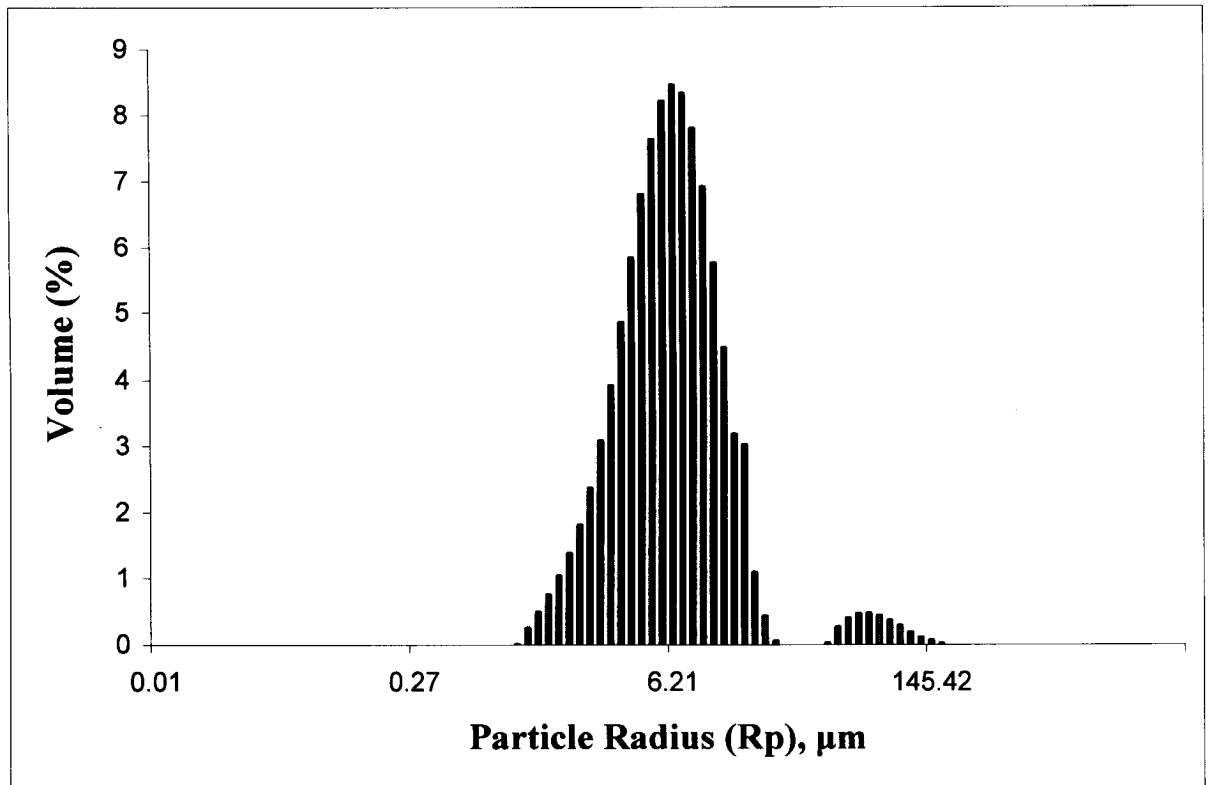
Figure 4.31: PLGA particle size distribution produced by emulsification-evaporation method (Data are the average of three sets of measurement).

Homogenization speed = 13500 rpm

Homogenization Time = 6 min
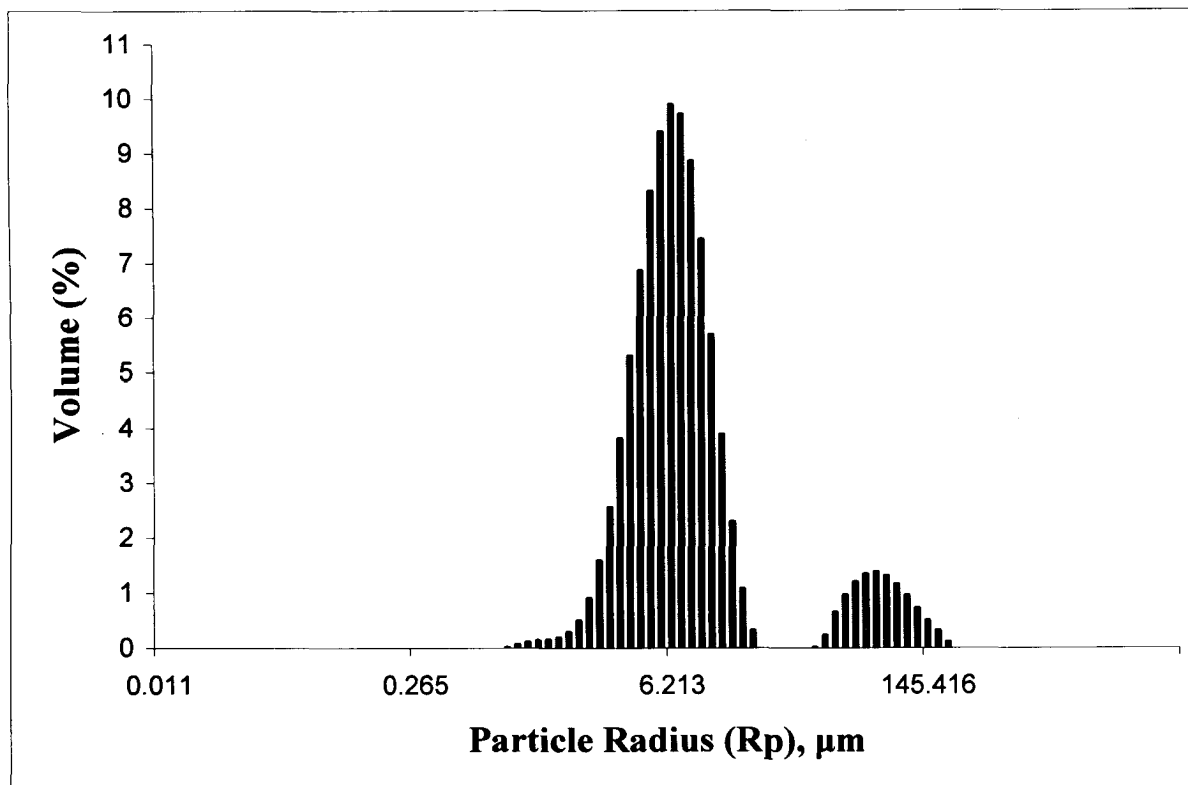
Figure 4.32: PLGA particle size distribution produced by emulsification-evaporation method (Data are the average of three sets of measurement).

Homogenization speed = 13500 rpm

Homogenization Time = 8 min
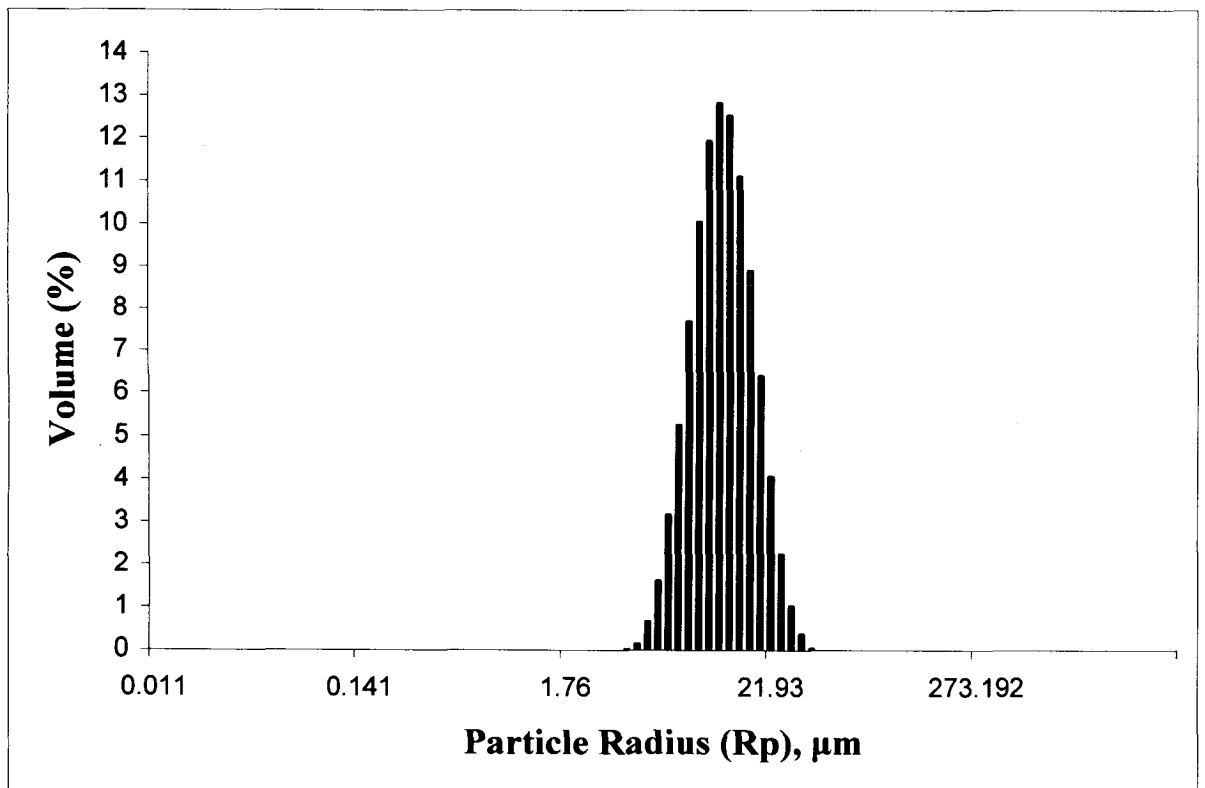
Figure 4.33: PLGA particle size distribution produced by emulsification-evaporation method (Data are the average of three sets of measurement).

Homogenization speed = 13500 rpm

Homogenization Time = 10 min
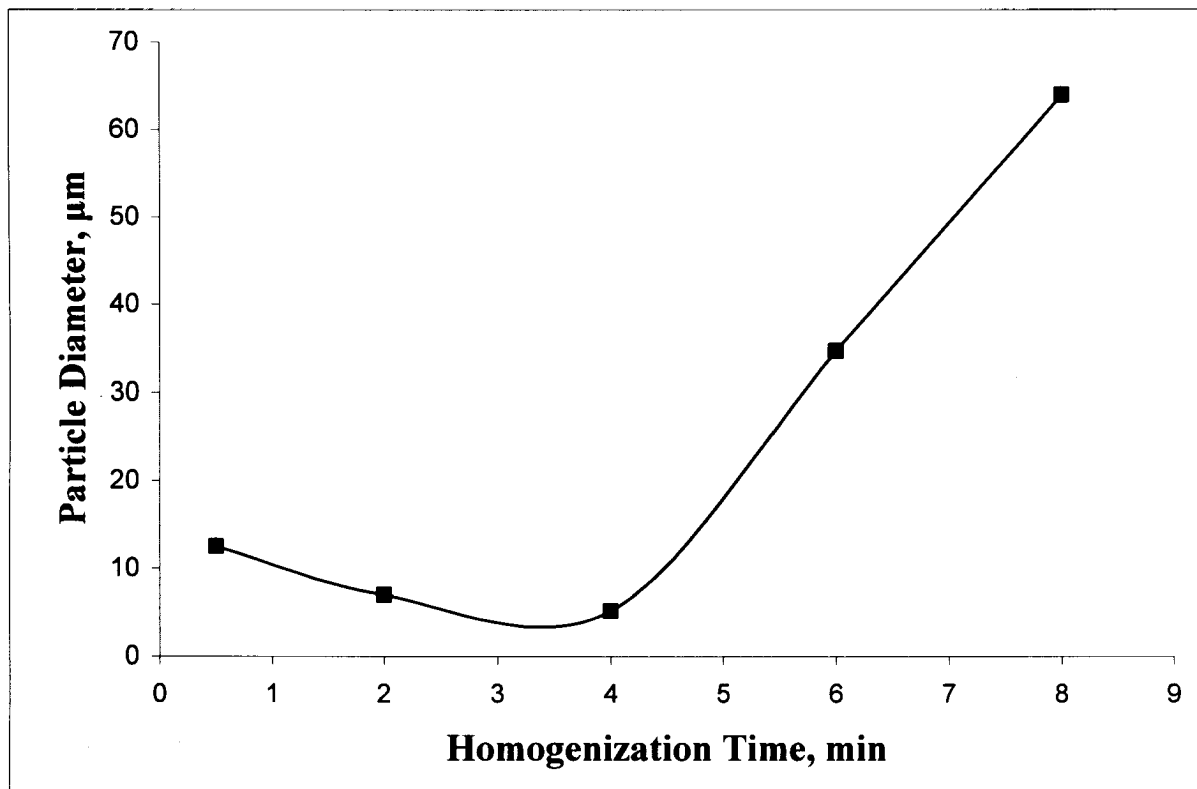
Figure 4-34: Effect of Homogenization time on PLGA average particle size (Data are the average of three sets of measurement).

Homogenization speed = 24000 rpm
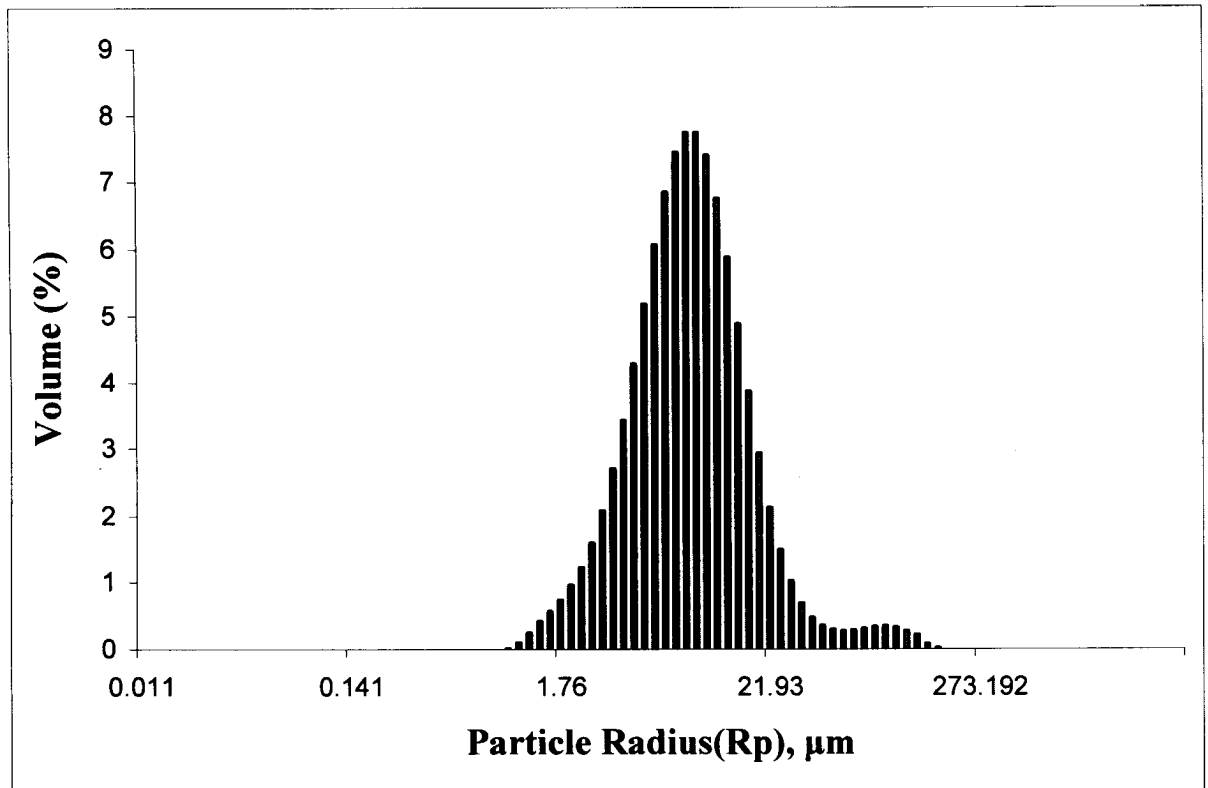
Figure 4.35: PLGA particle size distribution produced by emulsification-evaporation method (Data are the average of three sets of measurement).

Homogenization speed = 24000 rpm

Homogenization Time = 0.5 min
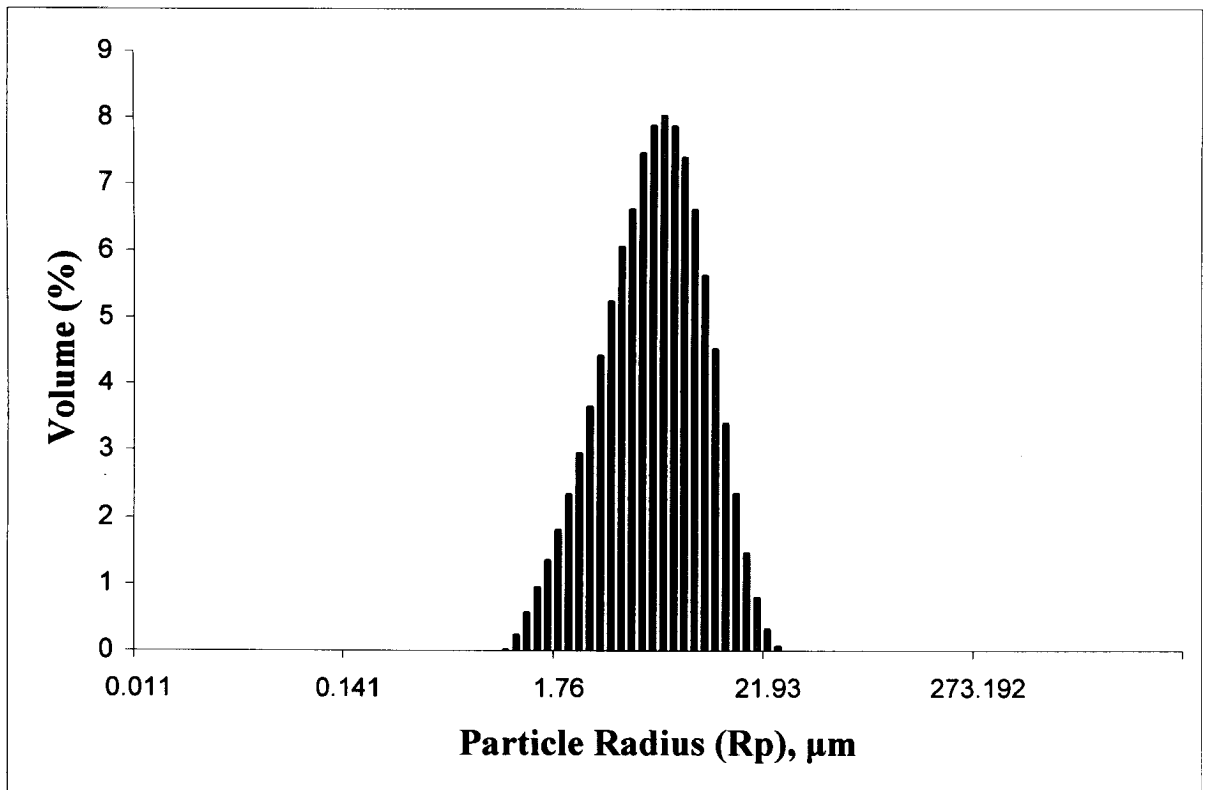
Figure 4.36: PLGA particle size distribution produced by emulsification-evaporation method (Data are the average of three sets of measurement).

Homogenization speed = 24000 rpm

Homogenization Time = 2 min
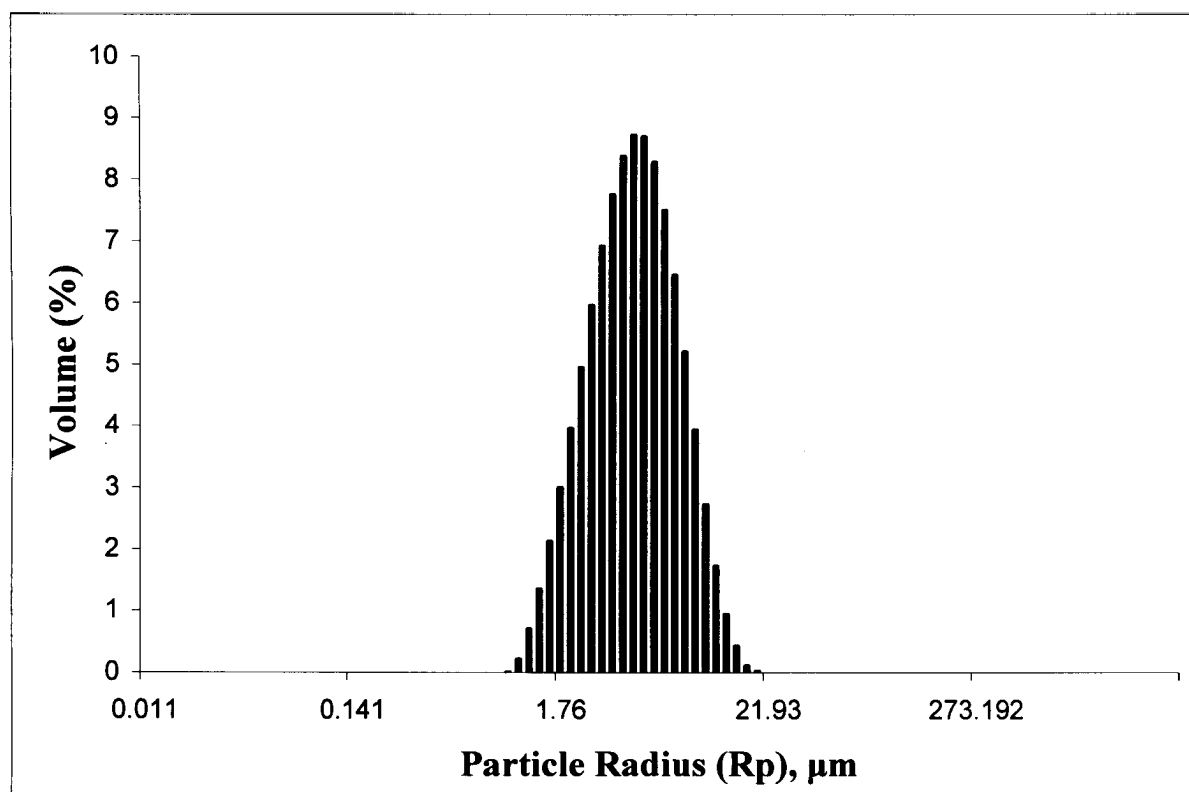
Figure 4.37: **PLGA particle size distribution produced by emulsification-evaporation method (Data are the average of three sets of measurement).**

Homogenization speed = 24000 rpm

Homogenization Time = 4 min
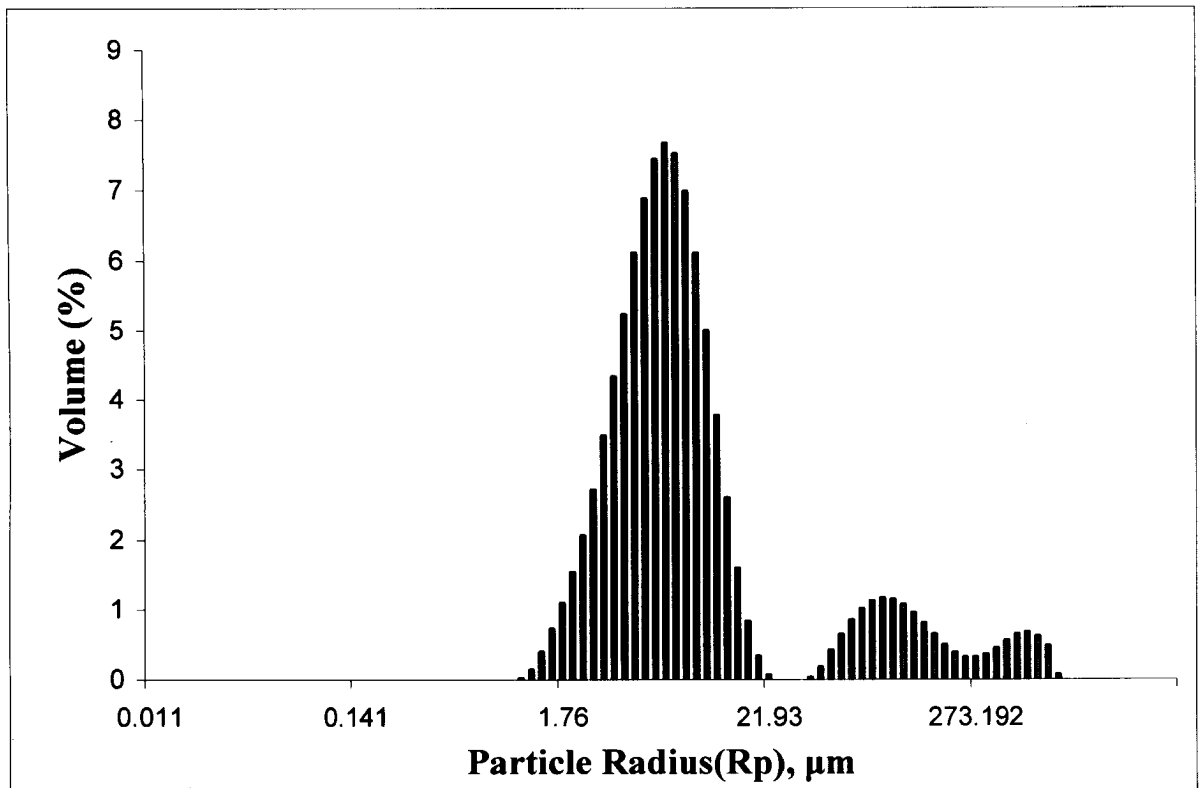
Figure 4.38: PLGA particle size distribution produced by emulsification-evaporation method (Data are the average of three sets of measurement).

Homogenization speed = 24000 rpm

Homogenization Time = 6 min
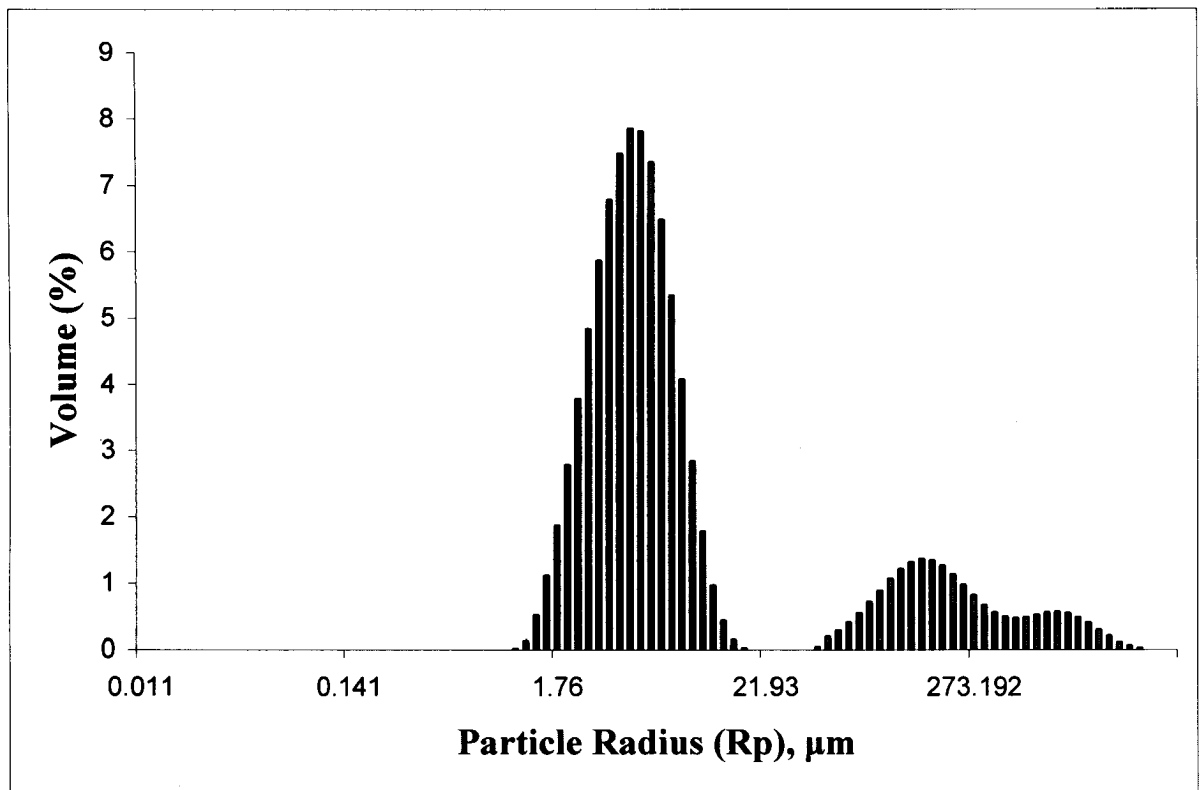
Figure 4.39: PLGA particle size distribution produced by emulsification-evaporation method (Data are the average of three sets of measurement).

Homogenization speed = 24000 rpm

Homogenization Time = 8 min
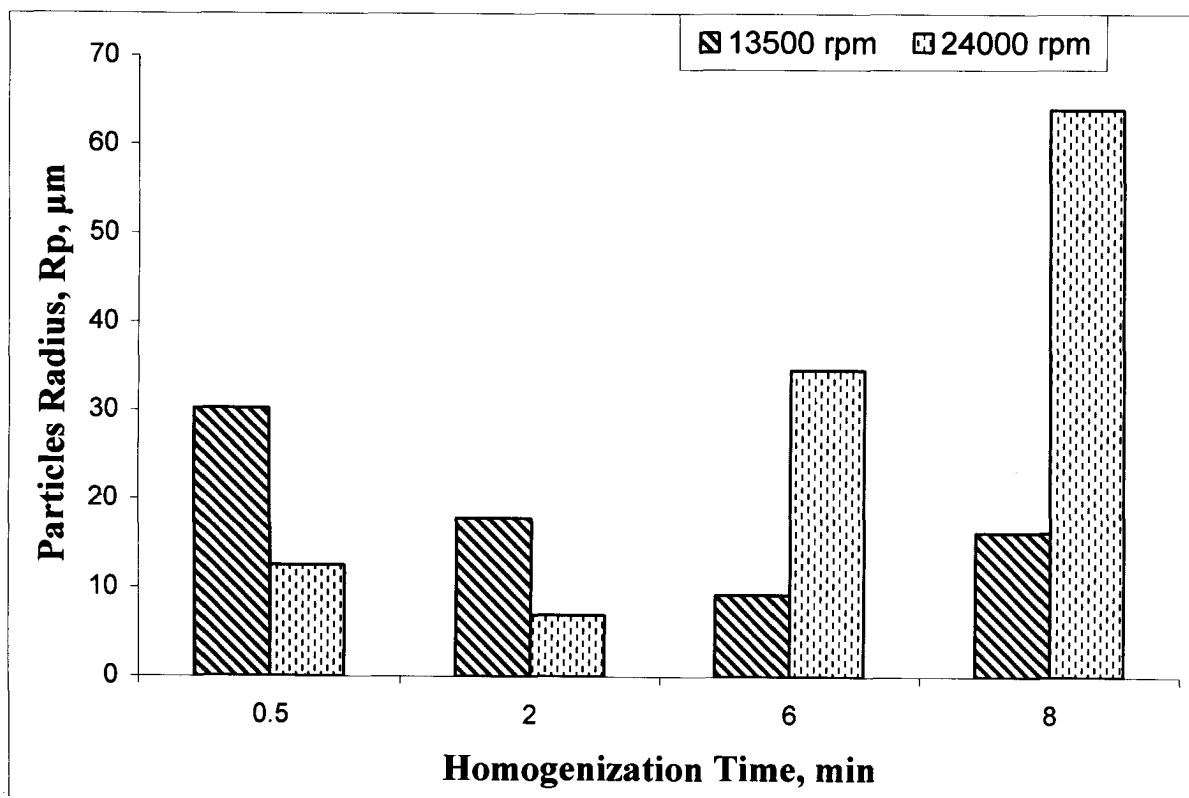
Figure 4-40; Effect of homogenization speed on particles size at different homogenization time

CHAPTER 5

CONCLUSIONS AND RECOMMENDATIONS

5-1) Conclusions

i) Different sizes of spherical shape chitosan nanoparticles were prepared by ionotropic gelation method. It was observed that chitosan particle size is affected by chitosan concentration, chitosan to TPP mass ratio and TPP solution concentration. The 200 nm spherical chitosan particles with smooth surface was prepared by reducing TPP solution pH to 5, chitosan concentration to 1 mg/ mL and increasing chitosan to TPP mass ratio to 5.

ii) rh-EPO was encapsulated in chitosan-TPP nanoparticles with rh-EPO loading efficiency equal to 34.5%. Drug release was studied in PBS solution at pH 7.4 and 37°C. It was observed that for the first 48 hours the rh-EPO release from chitosan nanoparticles is almost 30%, then after that the drug was released linearly for 13 %. The total drug release for 15 days was 63%. Comparing the results with literature, showed that encapsulation of rh-EPO in chitosan-TPP nanoparticles could reduce the initial drug release from more than 40% to below 30% for first 48 hours. Moreover, total drug release reduced from 80% to 63% in 15 days. Therefore, it is concluded that chitosan-TPP nanoparticles can be considered as a promising carrier for delivery of rh-EPO to the body.

iii) An assay method for rh-EPO was developed by HPLC. With the developed method, the minimum level of rh-EPO concentration which was detected quantitatively in PBS was 500 ng/mL. The method is fast and sensitive enough and it can be used for kinetic study with acceptable level of sensitivity.

iv) Effect of homogenization speed and time on the size of PLGA micropartciles produced by emulsification-evaporation method (double emulsion) was investigated. It was observed that particle size varied significantly by changing the homogenization time and speed. It can concluded from the data that at each homogenization speed there is only one time at which the particle size are minimum and the particle size distribution is more uniform.

5-2) Recommendations

i) Effect of different operational parameters on chitosan-TPP nanoparticles production was investigated. It was observed that in addition to the pH, chitosan concentration and chitosan to TPP mass ratio, stirrer speed has significant influence on particles uniformity. Therefore, it would be necessary to investigate the effect of magnetic stirrer speed and geometry of the vessel on the particle size distribution, systematically.

ii) Encapsulation of rh-EPO in chitosan was done successfully. The data can be used to improve the encapsulation efficiency of chitosan particles and the drug release profile of rh-EPO from chitosan-TPP nanoparticles to eliminate very slow drug release period

which was occurred from day 2 to day 4. This can be done by conjugating a cross linker to chitosan or using another polyanion such as alginate or a combination of both.

iii) Furthermore, it was shown that, HPLC can be used to quantify the rh-EPO *in vitro* with a good level of sensitivity. This method can still be improved more to increase the resolution and sensitivity of the system. It can be done by decreasing the column size which prevent the rh-EPO from spreading throughout the column or by derivatization. Since there are four cysteine molecules on EPO, it is possible to attach a fluorescence compound such as maleimido-butyryl-biocytin (MBB) to the rh-EPO molecule to intensify the fluorescent property of the molecule; therefore, lower amount of rh-EPO becomes detectable.

iv) PLGA is biocompatible and nontoxic synthetic polymer. Drug release from the polymer can be controlled by varying the copolymer ratio, but, it is a hydrophobic polymer and it is necessary to use organic solvent for micropartilces production. PLGA is a hydrophobic polymer requires administration of organic solvent for mciroparticles production which is not suitable for hydrophilic drugs such as rh-EPO. The data obtained can be used to encapsulate rh-EPO in chitosan-TPP nanopartciles and cover the particles by PLGA to control the drug release from the particles. Immobilization of rh-EPO in chitosan particles may prevent rh-EPO aggregation upon mixing it with PLGA in an organic solvent.

Appendix A: Dynamic light scattering data for chitosan particles size and particles size distribution measurement. Effect of chitosan solution concentration and chitosan to TPP mass ratio

Table A-1: Chitosan particles size distribution. Chitosan Concentration= 3 mg/ mL, CS:TPP =3

Radius (nm)	Distribution Fraction				Radius (nm)	Distribution Fraction			
	Trial 1	Trial 2	Trial 3	Average		Trial 1	Trial 2	Trial 3	Average
3.953	0.0000	0.0000	0.0000	0.0000	204.7	0.8	0.8	0.8	0.8
4.343	0.0000	0.0000	0.0000	0.0000	224.9	0.9	0.9	0.9	0.9
4.771	0.0000	0.0000	0.0000	0.0000	247.1	1.0	0.9	1.0	1.0
5.241	0.0000	0.0000	0.0000	0.0000	271.4	1.0200	0.9720	1.0080	1.0000
5.757	0.0000	0.0000	0.0000	0.0000	298.2	0.9932	0.9465	0.9816	0.9738
6.324	0.0000	0.0000	0.0000	0.0000	327.6	0.9175	0.8743	0.9067	0.8995
6.948	0.0000	0.0000	0.0000	0.0000	359.8	0.8003	0.7626	0.7908	0.7846
7.632	0.0000	0.0000	0.0000	0.0000	395.3	0.6537	0.6230	0.6460	0.6409
8.384	0.0000	0.0000	0.0000	0.0000	434.3	0.4933	0.4701	0.4875	0.4837
9.210	0.0000	0.0000	0.0000	0.0000	477.1	0.3361	0.3203	0.3322	0.3295
10.12	0.0000	0.0000	0.0000	0.0000	524.1	0.1984	0.1891	0.1961	0.1945
11.12	0.0000	0.0000	0.0000	0.0000	575.7	0.0933	0.0889	0.0922	0.0914
12.21	0.0000	0.0000	0.0000	0.0000	632.4	0.0279	0.0266	0.0275	0.0273
13.41	0.0000	0.0000	0.0000	0.0000	694.8	0.0009	0.0008	0.0009	0.0008
14.74	0.0000	0.0000	0.0000	0.0000	763.2	0.0000	0.0000	0.0000	0.0000
16.19	0.0000	0.0000	0.0000	0.0000	838.4	0.0000	0.0000	0.0000	0.0000
17.78	0.0000	0.0000	0.0000	0.0000	921	0.0000	0.0000	0.0000	0.0000
19.53	0.0000	0.0000	0.0000	0.0000	1012	0.0000	0.0000	0.0000	0.0000
21.46	0.0000	0.0000	0.0000	0.0000	1112	0.0000	0.0000	0.0000	0.0000
23.57	0.0000	0.0000	0.0000	0.0000	1221	0.0000	0.0000	0.0000	0.0000
25.90	0.0000	0.0000	0.0000	0.0000	1341	0.0000	0.0000	0.0000	0.0000
28.45	0.0000	0.0000	0.0000	0.0000	1474	0.0000	0.0000	0.0000	0.0000
31.25	0.0069	0.0066	0.0068	0.0068	1619	0.0000	0.0000	0.0000	0.0000
34.33	0.0319	0.0304	0.0316	0.0313	1778	0.0000	0.0000	0.0000	0.0000
37.72	0.0732	0.0698	0.0724	0.0718	1953	0.0036	0.0035	0.0036	0.0036
41.43	0.1219	0.1161	0.1204	0.1195	2146	0.0159	0.0152	0.0157	0.0156
45.52	0.1664	0.1586	0.1645	0.1631	2357	0.0365	0.0348	0.0361	0.0358
50.00	0.1967	0.1874	0.1944	0.1928	2590	0.0617	0.0588	0.0610	0.0605
54.93	0.2060	0.1963	0.2035	0.2019	2845	0.0860	0.0819	0.0850	0.0843
60.34	0.1923	0.1833	0.1901	0.1885	3125	0.1038	0.0989	0.1025	0.1017
66.29	0.1587	0.1512	0.1568	0.1556	3433	0.1105	0.1053	0.1092	0.1083
72.82	0.1122	0.1070	0.1109	0.1100	3772	0.1038	0.0989	0.1026	0.1018
79.99	0.0630	0.0600	0.0622	0.0617	4143	0.0840	0.0800	0.0830	0.0823
87.88	0.0221	0.0210	0.0218	0.0216	4552	0.0547	0.0521	0.0540	0.0536
96.54	0.0000	0.0000	0.0000	0.0000	5000	0.0231	0.0220	0.0228	0.0226
106.1	0.0048	0.0045	0.0047	0.0047					
116.5	0.0437	0.0416	0.0432	0.0428					
128.0	0.1193	0.1137	0.1179	0.1170					
140.6	0.2291	0.2183	0.2264	0.2246					
154.4	0.3657	0.3484	0.3614	0.3585					
169.7	0.5177	0.4933	0.5116	0.5075					
186.4	0.6712	0.6396	0.6633	0.6581					

Table A-2: Chitosan particles size distribution. Chitosan Concentration= 3 mg/ mL, CS:TPP =4

Radius (nm)	Distribution Fraction				Radius (nm)	Distribution Fraction			
	Trial 1	Trial 2	Trial 3	Average		Trial 1	Trial 2	Trial 3	Average
3.953	0.0009	0.0009	0.0009	0.0009	204.8	0.9530	1.0250	1.0220	1.0000
4.343	0.0033	0.0036	0.0036	0.0035	224.9	0.9407	1.0117	1.0088	0.9871
4.771	0.0073	0.0078	0.0078	0.0076	247.1	0.9084	0.9771	0.9742	0.9532
5.241	0.0122	0.0131	0.0131	0.0128	271.4	0.8584	0.9233	0.9205	0.9007
5.757	0.0173	0.0186	0.0185	0.0181	298.2	0.7934	0.8533	0.8508	0.8325
6.324	0.0217	0.0233	0.0232	0.0227	327.6	0.7167	0.7708	0.7686	0.7520
6.948	0.0246	0.0265	0.0264	0.0258	359.9	0.6320	0.6797	0.6777	0.6631
7.632	0.0255	0.0275	0.0274	0.0268	395.3	0.5429	0.5839	0.5822	0.5697
8.384	0.0243	0.0262	0.0261	0.0256	434.3	0.4531	0.4874	0.4860	0.4755
9.210	0.0212	0.0228	0.0227	0.0222	477.1	0.3661	0.3938	0.3926	0.3842
10.12	0.0166	0.0178	0.0178	0.0174	524.1	0.2849	0.3064	0.3055	0.2989
11.12	0.0113	0.0121	0.0121	0.0119	575.7	0.2119	0.2279	0.2273	0.2224
12.21	0.0063	0.0068	0.0068	0.0066	632.4	0.1491	0.1604	0.1599	0.1565
13.41	0.0025	0.0027	0.0027	0.0027	694.8	0.0977	0.1050	0.1047	0.1025
14.74	0.0005	0.0005	0.0005	0.0005	763.2	0.0580	0.0624	0.0622	0.0609
16.19	0.0000	0.0000	0.0000	0.0000	838.4	0.0299	0.0321	0.0320	0.0313
17.78	0.0000	0.0000	0.0000	0.0000	921.0	0.0121	0.0130	0.0130	0.0127
19.54	0.0000	0.0000	0.0000	0.0000	1012	0.0030	0.0032	0.0032	0.0032
21.46	0.0000	0.0000	0.0000	0.0000	1112	0.0000	0.0000	0.0000	0.0000
23.58	0.0000	0.0000	0.0000	0.0000	1221	0.0000	0.0000	0.0000	0.0000
25.90	0.0000	0.0000	0.0000	0.0000	1341	0.0028	0.0030	0.0030	0.0029
28.45	0.0000	0.0000	0.0000	0.0000	1474	0.0081	0.0087	0.0087	0.0085
31.25	0.0000	0.0000	0.0000	0.0000	1619	0.0155	0.0167	0.0166	0.0163
34.33	0.0000	0.0000	0.0000	0.0000	1778	0.0241	0.0260	0.0259	0.0253
37.72	0.0000	0.0000	0.0000	0.0000	1953	0.0331	0.0356	0.0355	0.0347
41.43	0.0000	0.0000	0.0000	0.0000	2146	0.0414	0.0445	0.0443	0.0434
45.52	0.0000	0.0000	0.0000	0.0000	2357	0.0480	0.0516	0.0515	0.0504
50.00	0.0000	0.0000	0.0000	0.0000	2590	0.0522	0.0562	0.0560	0.0548
54.93	0.0075	0.0081	0.0080	0.0079	2845	0.0534	0.0575	0.0573	0.0561
60.34	0.0296	0.0319	0.0318	0.0311	3125	0.0513	0.0552	0.0550	0.0538
66.29	0.0702	0.0755	0.0753	0.0737	3433	0.0459	0.0494	0.0492	0.0482
72.82	0.1300	0.1398	0.1394	0.1364	3772	0.0376	0.0404	0.0403	0.0394
79.99	0.2075	0.2231	0.2225	0.2177	4143	0.0273	0.0293	0.0292	0.0286
87.88	0.2992	0.3218	0.3208	0.3139	4552	0.0162	0.0175	0.0174	0.0170
96.54	0.4005	0.4307	0.4295	0.4202	5000	0.0064	0.0069	0.0068	0.0067
106.0	0.5060	0.5442	0.5426	0.5310					
116.5	0.6101	0.6562	0.6543	0.6402					
128.0	0.7073	0.7608	0.7586	0.7422					
140.6	0.7929	0.8528	0.8503	0.8320					
154.4	0.8627	0.9279	0.9252	0.9053					
169.7	0.9138	0.9828	0.9799	0.9588					
186.4	0.9441	1.0155	1.0125	0.9907					

Table A-3: Chitosan particles size distribution. Chitosan Concentration= 3 mg/ mL, CS:TPP =5

Radius (nm)	Distribution Fraction				Radius (nm)	Distribution Fraction			
	Trial 1	Trial 2	Trial 3	Average		Trial 1	Trial 2	Trial 3	Average
2.249	0.0000	0.0000	0.0000	0.0000	116.5	0.0971	0.0993	0.1129	0.1031
2.471	0.0000	0.0000	0.0000	0.0000	128.0	0.2377	0.2430	0.2763	0.2523
2.714	0.0000	0.0000	0.0000	0.0000	140.6	0.4220	0.4314	0.4906	0.4480
2.982	0.0000	0.0000	0.0000	0.0000	154.4	0.6177	0.6315	0.7181	0.6558
3.276	0.0000	0.0000	0.0000	0.0000	169.7	0.7888	0.8064	0.9169	0.8374
3.598	0.0022	0.0022	0.0025	0.0023	186.4	0.9038	0.9240	1.0506	0.9595
3.953	0.0067	0.0069	0.0078	0.0071	204.7	0.9420	0.9630	1.0950	1.0000
4.343	0.0102	0.0104	0.0119	0.0108	224.9	0.8968	0.9168	1.0425	0.9520
4.770	0.0101	0.0103	0.0117	0.0107	247.1	0.7769	0.7942	0.9031	0.8248
5.241	0.0066	0.0067	0.0076	0.0070	271.4	0.6045	0.6179	0.7026	0.6417
5.757	0.0022	0.0023	0.0026	0.0024	298.2	0.4109	0.4201	0.4777	0.4362
6.324	0.0000	0.0000	0.0000	0.0000	327.6	0.2311	0.2362	0.2686	0.2453
6.948	0.0000	0.0000	0.0000	0.0000	359.8	0.0950	0.0971	0.1104	0.1008
7.632	0.0000	0.0000	0.0000	0.0000	395.3	0.0197	0.0201	0.0229	0.0209
8.384	0.0000	0.0000	0.0000	0.0000	434.3	0.0000	0.0000	0.0000	0.0000
9.210	0.0000	0.0000	0.0000	0.0000	477.0	0.0000	0.0000	0.0000	0.0000
10.12	0.0000	0.0000	0.0000	0.0000	524.1	0.0000	0.0000	0.0000	0.0000
11.12	0.0000	0.0000	0.0000	0.0000	575.7	0.0000	0.0000	0.0000	0.0000
12.21	0.0000	0.0000	0.0000	0.0000	632.4	0.0000	0.0000	0.0000	0.0000
13.41	0.0000	0.0000	0.0000	0.0000	694.8	0.0000	0.0000	0.0000	0.0000
14.74	0.0000	0.0000	0.0000	0.0000	763.2	0.0000	0.0000	0.0000	0.0000
16.19	0.0085	0.0087	0.0099	0.0091	838.4	0.0000	0.0000	0.0000	0.0000
17.78	0.0262	0.0268	0.0305	0.0278	921.0	0.0000	0.0000	0.0000	0.0000
19.53	0.0471	0.0482	0.0548	0.0500	1012	0.0000	0.0000	0.0000	0.0000
21.46	0.0632	0.0646	0.0735	0.0671	1112	0.0029	0.0030	0.0034	0.0031
23.57	0.0681	0.0696	0.0791	0.0722	1221	0.0207	0.0212	0.0241	0.0220
25.90	0.0595	0.0609	0.0692	0.0632	1341	0.0504	0.0515	0.0586	0.0535
28.45	0.0408	0.0418	0.0475	0.0434	1474	0.0813	0.0831	0.0945	0.0863
31.25	0.0195	0.0199	0.0227	0.0207	1619	0.1018	0.1041	0.1183	0.1080
34.33	0.0043	0.0044	0.0050	0.0046	1778	0.1042	0.1065	0.1211	0.1106
37.72	0.0000	0.0000	0.0000	0.0000	1953	0.0873	0.0892	0.1015	0.0927
41.43	0.0000	0.0000	0.0000	0.0000	2146	0.0574	0.0587	0.0667	0.0609
45.52	0.0000	0.0000	0.0000	0.0000	2357	0.0259	0.0265	0.0302	0.0275
50.00	0.0000	0.0000	0.0000	0.0000	2590	0.0050	0.0051	0.0058	0.0053
54.93	0.0000	0.0000	0.0000	0.0000	2845	0.0000	0.0000	0.0000	0.0000
60.34	0.0000	0.0000	0.0000	0.0000	3125	0.0000	0.0000	0.0000	0.0000
66.29	0.0000	0.0000	0.0000	0.0000	3433	0.0000	0.0000	0.0000	0.0000
72.82	0.0000	0.0000	0.0000	0.0000	3772	0.0000	0.0000	0.0000	0.0000
79.99	0.0000	0.0000	0.0000	0.0000	4143	0.0000	0.0000	0.0000	0.0000
87.88	0.0000	0.0000	0.0000	0.0000	4552	0.0000	0.0000	0.0000	0.0000
96.54	0.0000	0.0000	0.0000	0.0000	5000	0.0000	0.0000	0.0000	0.0000
106.0	0.0194	0.0198	0.0226	0.0206					

Table A-4: Chitosan particles size distribution. Chitosan Concentration= 2 mg/ mL, CS:TPP =3

Radius (nm)	Distribution Fraction				Radius (nm)	Distribution Fraction			
	Trial 1	Trial 2	Trial 3	Average		Trial 1	Trial 2	Trial 3	Average
2.047	0.0000	0.0000	0.0000	0.0000	106.0	0.8256	0.9773	0.8747	0.8925
2.249	0.0000	0.0000	0.0000	0.0000	116.5	0.7653	0.9059	0.8108	0.8273
2.471	0.0000	0.0000	0.0000	0.0000	128.0	0.6964	0.8244	0.7379	0.7529
2.714	0.0007	0.0008	0.0007	0.0007	140.6	0.6222	0.7365	0.6592	0.6726
2.982	0.0018	0.0021	0.0019	0.0019	154.4	0.5455	0.6458	0.5779	0.5897
3.276	0.0028	0.0033	0.0029	0.0030	169.7	0.4691	0.5554	0.4970	0.5072
3.598	0.0031	0.0037	0.0033	0.0034	186.4	0.3954	0.4681	0.4189	0.4275
3.953	0.0027	0.0031	0.0028	0.0029	204.7	0.3263	0.3862	0.3457	0.3527
4.343	0.0016	0.0019	0.0017	0.0018	224.9	0.2631	0.3115	0.2788	0.2844
4.770	0.0006	0.0007	0.0006	0.0006	247.1	0.2070	0.2450	0.2193	0.2237
5.241	0.0000	0.0000	0.0000	0.0000	271.4	0.1584	0.1875	0.1678	0.1712
5.757	0.0000	0.0000	0.0000	0.0000	298.2	0.1175	0.1391	0.1245	0.1270
6.324	0.0000	0.0000	0.0000	0.0000	327.6	0.0841	0.0996	0.0891	0.0909
6.947	0.0000	0.0000	0.0000	0.0000	359.8	0.0578	0.0684	0.0613	0.0625
7.632	0.0000	0.0000	0.0000	0.0000	395.3	0.0379	0.0449	0.0401	0.0410
8.384	0.0000	0.0000	0.0000	0.0000	434.3	0.0235	0.0279	0.0249	0.0254
9.210	0.0000	0.0000	0.0000	0.0000	477.0	0.0138	0.0164	0.0146	0.0149
10.12	0.0000	0.0000	0.0000	0.0000	524.1	0.0078	0.0093	0.0083	0.0085
11.11	0.0000	0.0000	0.0000	0.0000	575.7	0.0046	0.0055	0.0049	0.0050
12.21	0.0000	0.0000	0.0000	0.0000	632.4	0.0034	0.0040	0.0036	0.0037
13.41	0.0000	0.0000	0.0000	0.0000	694.7	0.0034	0.0040	0.0036	0.0036
14.74	0.0000	0.0000	0.0000	0.0000	763.2	0.0039	0.0046	0.0041	0.0042
16.19	0.0000	0.0000	0.0000	0.0000	838.4	0.0045	0.0053	0.0048	0.0049
17.78	0.0000	0.0000	0.0000	0.0000	921.0	0.0049	0.0058	0.0052	0.0053
19.53	0.0000	0.0000	0.0000	0.0000	1012	0.0048	0.0057	0.0051	0.0052
21.46	0.0095	0.0112	0.0101	0.0103	1111	0.0044	0.0052	0.0046	0.0047
23.57	0.0352	0.0417	0.0374	0.0381	1221	0.0035	0.0041	0.0037	0.0038
25.90	0.0804	0.0952	0.0852	0.0869	1341	0.0025	0.0029	0.0026	0.0027
28.45	0.1449	0.1715	0.1535	0.1567	1474	0.0014	0.0017	0.0015	0.0015
31.25	0.2265	0.2681	0.2399	0.2448	1619	0.0006	0.0007	0.0006	0.0006
34.33	0.3209	0.3799	0.3400	0.3469	1778	0.0001	0.0002	0.0001	0.0001
37.72	0.4230	0.5008	0.4482	0.4573	1953	0.0000	0.0000	0.0000	0.0000
41.43	0.5271	0.6240	0.5585	0.5699	2146	0.0000	0.0000	0.0000	0.0000
45.51	0.6275	0.7429	0.6649	0.6784	2357	0.0000	0.0000	0.0000	0.0000
50.00	0.7190	0.8511	0.7617	0.7773	2590	0.0000	0.0000	0.0000	0.0000
54.93	0.7971	0.9436	0.8445	0.8617	2845	0.0000	0.0000	0.0000	0.0000
60.34	0.8584	1.0161	0.9094	0.9280	3125	0.0000	0.0000	0.0000	0.0000
66.29	0.9007	1.0662	0.9542	0.9737	3433	0.0000	0.0000	0.0000	0.0000
72.82	0.9229	1.0925	0.9777	0.9977	3772	0.0000	0.0000	0.0000	0.0000
79.99	0.9250	1.0950	0.9800	1.0000	4143	0.0000	0.0000	0.0000	0.0000
87.88	0.9081	1.0750	0.9621	0.9818	4551	0.0000	0.0000	0.0000	0.0000
96.53	0.8742	1.0348	0.9261	0.9450	5000	0.0000	0.0000	0.0000	0.0000

Table A-5: Chitosan particles size distribution. Chitosan Concentration= 2 mg/ mL, CS:TPP =4

Radius (nm)	Distribution Fraction				Radius (nm)	Distribution Fraction			
	Trial 1	Trial 2	Trial 3	Average		Trial 1	Trial 2	Trial 3	Average
2.249	0.0000	0.0000	0.0000	0.0000	116.5	0.9506	0.9633	1.0200	0.9779
2.471	0.0000	0.0000	0.0000	0.0000	128.0	0.9103	0.9225	0.9768	0.9365
2.714	0.0000	0.0000	0.0000	0.0000	140.6	0.8527	0.8641	0.9149	0.8772
2.982	0.0008	0.0008	0.0009	0.0009	154.4	0.7803	0.7908	0.8373	0.8028
3.276	0.0028	0.0028	0.0030	0.0029	169.7	0.6965	0.7058	0.7474	0.7166
3.598	0.0055	0.0056	0.0059	0.0056	186.4	0.6049	0.6130	0.6491	0.6223
3.953	0.0083	0.0084	0.0089	0.0086	204.7	0.5094	0.5162	0.5466	0.5241
4.343	0.0106	0.0107	0.0114	0.0109	224.9	0.4139	0.4195	0.4442	0.4258
4.770	0.0117	0.0119	0.0126	0.0121	247.1	0.3224	0.3267	0.3459	0.3317
5.241	0.0115	0.0117	0.0124	0.0119	271.4	0.2383	0.2415	0.2557	0.2452
5.757	0.0100	0.0101	0.0107	0.0102	298.2	0.1648	0.1670	0.1768	0.1695
6.324	0.0075	0.0076	0.0080	0.0077	327.6	0.1041	0.1055	0.1117	0.1071
6.947	0.0046	0.0047	0.0050	0.0047	359.8	0.0578	0.0585	0.0620	0.0594
7.632	0.0021	0.0021	0.0023	0.0022	395.3	0.0260	0.0263	0.0279	0.0267
8.384	0.0005	0.0005	0.0006	0.0005	434.3	0.0077	0.0078	0.0083	0.0080
9.210	0.0000	0.0000	0.0000	0.0000	477.0	0.0005	0.0005	0.0005	0.0005
10.12	0.0000	0.0000	0.0000	0.0000	524.1	0.0000	0.0000	0.0000	0.0000
11.11	0.0000	0.0000	0.0000	0.0000	575.7	0.0000	0.0000	0.0000	0.0000
12.21	0.0000	0.0000	0.0000	0.0000	632.4	0.0000	0.0000	0.0000	0.0000
13.41	0.0000	0.0000	0.0000	0.0000	694.7	0.0000	0.0000	0.0000	0.0000
14.74	0.0000	0.0000	0.0000	0.0000	763.2	0.0000	0.0000	0.0000	0.0000
16.19	0.0000	0.0000	0.0000	0.0000	838.4	0.0000	0.0000	0.0000	0.0000
17.78	0.0000	0.0000	0.0000	0.0000	921.0	0.0000	0.0000	0.0000	0.0000
19.53	0.0000	0.0000	0.0000	0.0000	1012	0.0000	0.0000	0.0000	0.0000
21.46	0.0000	0.0000	0.0000	0.0000	1111	0.0000	0.0000	0.0000	0.0000
23.57	0.0018	0.0018	0.0019	0.0018	1221	0.0000	0.0000	0.0000	0.0000
25.90	0.0126	0.0128	0.0135	0.0130	1341	0.0000	0.0000	0.0000	0.0000
28.45	0.0373	0.0378	0.0401	0.0384	1474	0.0000	0.0000	0.0000	0.0000
31.25	0.0784	0.0795	0.0841	0.0807	1619	0.0000	0.0000	0.0000	0.0000
34.33	0.1363	0.1382	0.1463	0.1403	1778	0.0000	0.0000	0.0000	0.0000
37.72	0.2098	0.2126	0.2251	0.2159	1953	0.0000	0.0000	0.0000	0.0000
41.43	0.2962	0.3002	0.3179	0.3047	2146	0.0000	0.0000	0.0000	0.0000
45.51	0.3919	0.3971	0.4205	0.4032	2357	0.0000	0.0000	0.0000	0.0000
50.00	0.4925	0.4991	0.5285	0.5067	2590	0.0000	0.0000	0.0000	0.0000
54.93	0.5934	0.6013	0.6368	0.6105	2845	0.0000	0.0000	0.0000	0.0000
60.34	0.6899	0.6991	0.7403	0.7098	3125	0.0000	0.0000	0.0000	0.0000
66.29	0.7776	0.7880	0.8344	0.8000	3433	0.0000	0.0000	0.0000	0.0000
72.82	0.8525	0.8639	0.9148	0.8771	3772	0.0000	0.0000	0.0000	0.0000
79.99	0.9114	0.9236	0.9779	0.9376	4143	0.0000	0.0000	0.0000	0.0000
87.88	0.9517	0.9645	1.0213	0.9791	4551	0.0000	0.0000	0.0000	0.0000
96.53	0.9720	0.9850	1.0430	1.0000	5000	0.0000	0.0000	0.0000	0.0000
106.0	0.9715	0.9845	1.0425	0.9995					

Table A-6: Chitosan particles size distribution. Chitosan Concentration= 2 mg/ mL, CS:TPP =5

Radius (nm)	Distribution Fraction				Radius (nm)	Distribution Fraction			
	Trial 1	Trial 2	Trial 3	Average		Trial 1	Trial 2	Trial 3	Average
4.343	0.0000	0.0000	0.0000	0.0000	224.9	0.0000	0.0000	0.0000	0.0000
4.770	0.0000	0.0000	0.0000	0.0000	247.1	0.0000	0.0000	0.0000	0.0000
5.241	0.0000	0.0000	0.0000	0.0000	271.4	0.0000	0.0000	0.0000	0.0000
5.757	0.0000	0.0000	0.0000	0.0000	298.2	0.0000	0.0000	0.0000	0.0000
6.324	0.0000	0.0000	0.0000	0.0000	327.6	0.0000	0.0000	0.0000	0.0000
6.947	0.0000	0.0000	0.0000	0.0000	359.8	0.0000	0.0000	0.0000	0.0000
7.632	0.0000	0.0000	0.0000	0.0000	395.3	0.0000	0.0000	0.0000	0.0000
8.384	0.0000	0.0000	0.0000	0.0000	434.3	0.0035	0.0036	0.0029	0.0033
9.210	0.0029	0.0029	0.0023	0.0027	477.0	0.0108	0.0109	0.0087	0.0101
10.12	0.0127	0.0128	0.0103	0.0119	524.1	0.0189	0.0191	0.0153	0.0178
11.12	0.0272	0.0275	0.0220	0.0255	575.7	0.0243	0.0246	0.0197	0.0229
12.21	0.0411	0.0414	0.0332	0.0386	632.4	0.0247	0.0249	0.0199	0.0232
13.41	0.0491	0.0496	0.0397	0.0461	694.7	0.0198	0.0200	0.0160	0.0186
14.74	0.0484	0.0489	0.0391	0.0455	763.2	0.0117	0.0118	0.0095	0.0110
16.19	0.0393	0.0396	0.0317	0.0369	838.4	0.0041	0.0041	0.0033	0.0038
17.78	0.0250	0.0252	0.0202	0.0235	921.0	0.0000	0.0000	0.0000	0.0000
19.53	0.0109	0.0110	0.0088	0.0102	1012	0.0000	0.0000	0.0000	0.0000
21.46	0.0020	0.0020	0.0016	0.0019	1112	0.0000	0.0000	0.0000	0.0000
23.57	0.0000	0.0000	0.0000	0.0000	1221	0.0000	0.0000	0.0000	0.0000
25.90	0.0000	0.0000	0.0000	0.0000	1341	0.0000	0.0000	0.0000	0.0000
28.45	0.0000	0.0000	0.0000	0.0000	1474	0.0000	0.0000	0.0000	0.0000
31.25	0.0000	0.0000	0.0000	0.0000	1619	0.0000	0.0000	0.0000	0.0000
34.33	0.0000	0.0000	0.0000	0.0000	1778	0.0000	0.0000	0.0000	0.0000
37.72	0.0000	0.0000	0.0000	0.0000	1953	0.0000	0.0000	0.0000	0.0000
41.43	0.0204	0.0206	0.0165	0.0192	2146	0.0000	0.0000	0.0000	0.0000
45.51	0.0838	0.0846	0.0677	0.0787	2357	0.0000	0.0000	0.0000	0.0000
50.00	0.1966	0.1985	0.1588	0.1846	2590	0.0000	0.0000	0.0000	0.0000
54.93	0.3519	0.3552	0.2842	0.3304	2845	0.0000	0.0000	0.0000	0.0000
60.34	0.5330	0.5380	0.4304	0.5005	3125	0.0000	0.0000	0.0000	0.0000
66.29	0.7173	0.7241	0.5793	0.6736	3433	0.0116	0.0117	0.0094	0.0109
72.82	0.8810	0.8893	0.7114	0.8272	3772	0.0328	0.0331	0.0265	0.0308
79.99	1.0022	1.0117	0.8093	0.9411	4143	0.0514	0.0519	0.0415	0.0483
87.88	1.0650	1.0750	0.8600	1.0000	4551	0.0533	0.0538	0.0430	0.0500
96.54	1.0610	1.0709	0.8567	0.9962	5000	0.0320	0.0323	0.0258	0.0300
106.0	0.9908	1.0001	0.8001	0.9303					
116.5	0.8640	0.8721	0.6977	0.8113					
128.0	0.6976	0.7042	0.5633	0.6550					
140.6	0.5135	0.5184	0.4147	0.4822					
154.4	0.3354	0.3386	0.2709	0.3150					
169.7	0.1848	0.1866	0.1493	0.1736					
186.4	0.0772	0.0779	0.0624	0.0725					
204.7	0.0181	0.0183	0.0146	0.0170					

Table A-7: Chitosan particles size distribution. Chitosan Concentration= 1 mg/ mL, CS:TPP =3

Radius (nm)	Distribution Fraction				Radius (nm)	Distribution Fraction			
	Trial 1	Trial 2	Trial 3	Average		Trial 1	Trial 2	Trial 3	Average
3.953	0.0000	0.0000	0.0000	0.0000	204.7	0.2437	0.2583	0.2395	0.2471
4.343	0.0000	0.0000	0.0000	0.0000	224.9	0.1281	0.1358	0.1259	0.1299
4.770	0.0000	0.0000	0.0000	0.0000	247.1	0.0493	0.0522	0.0484	0.0500
5.241	0.0000	0.0000	0.0000	0.0000	271.4	0.0093	0.0099	0.0092	0.0094
5.757	0.0000	0.0000	0.0000	0.0000	298.2	0.0000	0.0000	0.0000	0.0000
6.324	0.0000	0.0000	0.0000	0.0000	327.6	0.0000	0.0000	0.0000	0.0000
6.947	0.0000	0.0000	0.0000	0.0000	359.8	0.0000	0.0000	0.0000	0.0000
7.632	0.0000	0.0000	0.0000	0.0000	395.3	0.0000	0.0000	0.0000	0.0000
8.384	0.0000	0.0000	0.0000	0.0000	434.3	0.0000	0.0000	0.0000	0.0000
9.210	0.0000	0.0000	0.0000	0.0000	477.0	0.0000	0.0000	0.0000	0.0000
10.12	0.0000	0.0000	0.0000	0.0000	524.1	0.0000	0.0000	0.0000	0.0000
11.12	0.0000	0.0000	0.0000	0.0000	575.7	0.0000	0.0000	0.0000	0.0000
12.21	0.0000	0.0000	0.0000	0.0000	632.4	0.0000	0.0000	0.0000	0.0000
13.41	0.0000	0.0000	0.0000	0.0000	694.7	0.0000	0.0000	0.0000	0.0000
14.74	0.0021	0.0022	0.0021	0.0021	763.2	0.0000	0.0000	0.0000	0.0000
16.19	0.0119	0.0126	0.0117	0.0120	838.4	0.0000	0.0000	0.0000	0.0000
17.78	0.0249	0.0263	0.0244	0.0252	921.0	0.0000	0.0000	0.0000	0.0000
19.53	0.0345	0.0366	0.0339	0.0350	1012	0.0000	0.0000	0.0000	0.0000
21.46	0.0364	0.0386	0.0358	0.0369	1111	0.0000	0.0000	0.0000	0.0000
23.57	0.0302	0.0320	0.0296	0.0306	1221	0.0000	0.0000	0.0000	0.0000
25.90	0.0189	0.0200	0.0186	0.0192	1341	0.0000	0.0000	0.0000	0.0000
28.45	0.0077	0.0082	0.0076	0.0078	1474	0.0000	0.0000	0.0000	0.0000
31.25	0.0010	0.0011	0.0010	0.0010	1619	0.0000	0.0000	0.0000	0.0000
34.33	0.0000	0.0000	0.0000	0.0000	1778	0.0000	0.0000	0.0000	0.0000
37.72	0.0000	0.0000	0.0000	0.0000	1953	0.0000	0.0000	0.0000	0.0000
41.43	0.0000	0.0000	0.0000	0.0000	2146	0.0000	0.0000	0.0000	0.0000
45.51	0.0190	0.0201	0.0187	0.0193	2357	0.0000	0.0000	0.0000	0.0000
50.00	0.0703	0.0745	0.0691	0.0713	2590	0.0000	0.0000	0.0000	0.0000
54.93	0.1582	0.1677	0.1555	0.1605	2845	0.0000	0.0000	0.0000	0.0000
60.34	0.2792	0.2959	0.2744	0.2832	3125	0.0000	0.0000	0.0000	0.0000
66.29	0.4235	0.4489	0.4162	0.4295	3433	0.0000	0.0000	0.0000	0.0000
72.82	0.5774	0.6119	0.5674	0.5855	3772	0.0000	0.0000	0.0000	0.0000
79.99	0.7249	0.7683	0.7124	0.7352	4143	0.0000	0.0000	0.0000	0.0000
87.88	0.8505	0.9014	0.8359	0.8626	4551	0.0000	0.0000	0.0000	0.0000
96.53	0.9408	0.9971	0.9246	0.9542	5000	0.0000	0.0000	0.0000	0.0000
106.0	0.9860	1.0450	0.9690	1.0000					
116.5	0.9810	1.0397	0.9641	0.9950					
128.0	0.9262	0.9817	0.9103	0.9394					
140.6	0.8273	0.8768	0.8130	0.8390					
154.4	0.6946	0.7361	0.6826	0.7044					
169.7	0.5422	0.5747	0.5329	0.5499					
186.4	0.3865	0.4096	0.3798	0.3920					

Table A-8: Chitosan particles size distribution. Chitosan Concentration= 1 mg/ mL, CS:TPP =4

Radius (nm)	Distribution Fraction				Radius (nm)	Distribution Fraction			
	Trial 1	Trial 2	Trial 3	Average		Trial 1	Trial 2	Trial 3	Average
3.953	0.0000	0.0000	0.0000	0.0000	204.7	0.0315	0.0313	0.0348	0.0325
4.343	0.0000	0.0000	0.0000	0.0000	224.9	0.0040	0.0040	0.0045	0.0042
4.771	0.0000	0.0000	0.0000	0.0000	247.1	0.0000	0.0000	0.0000	0.0000
5.241	0.0000	0.0000	0.0000	0.0000	271.4	0.0000	0.0000	0.0000	0.0000
5.757	0.0000	0.0000	0.0000	0.0000	298.2	0.0000	0.0000	0.0000	0.0000
6.324	0.0000	0.0000	0.0000	0.0000	327.6	0.0000	0.0000	0.0000	0.0000
6.948	0.0000	0.0000	0.0000	0.0000	359.8	0.0032	0.0032	0.0035	0.0033
7.632	0.0000	0.0000	0.0000	0.0000	395.3	0.0117	0.0116	0.0129	0.0121
8.384	0.0000	0.0000	0.0000	0.0000	434.3	0.0244	0.0243	0.0270	0.0252
9.210	0.0009	0.0009	0.0010	0.0010	477.1	0.0385	0.0383	0.0425	0.0398
10.12	0.0078	0.0078	0.0086	0.0081	524.1	0.0504	0.0501	0.0557	0.0521
11.12	0.0147	0.0146	0.0162	0.0152	575.7	0.0573	0.0569	0.0633	0.0592
12.21	0.0158	0.0157	0.0175	0.0163	632.4	0.0574	0.0570	0.0634	0.0593
13.41	0.0106	0.0105	0.0117	0.0109	694.8	0.0507	0.0503	0.0560	0.0523
14.74	0.0035	0.0034	0.0038	0.0036	763.2	0.0387	0.0385	0.0428	0.0400
16.19	0.0000	0.0000	0.0000	0.0000	838.4	0.0245	0.0244	0.0271	0.0253
17.78	0.0000	0.0000	0.0000	0.0000	921.0	0.0116	0.0115	0.0128	0.0120
19.53	0.0000	0.0000	0.0000	0.0000	1012	0.0031	0.0030	0.0034	0.0032
21.46	0.0000	0.0000	0.0000	0.0000	1112	0.0000	0.0000	0.0000	0.0000
23.57	0.0000	0.0000	0.0000	0.0000	1221	0.0000	0.0000	0.0000	0.0000
25.90	0.0000	0.0000	0.0000	0.0000	1341	0.0000	0.0000	0.0000	0.0000
28.45	0.0000	0.0000	0.0000	0.0000	1474	0.0000	0.0000	0.0000	0.0000
31.25	0.0000	0.0000	0.0000	0.0000	1619	0.0000	0.0000	0.0000	0.0000
34.33	0.0000	0.0000	0.0000	0.0000	1778	0.0000	0.0000	0.0000	0.0000
37.72	0.0000	0.0000	0.0000	0.0000	1953	0.0000	0.0000	0.0000	0.0000
41.43	0.0106	0.0105	0.0117	0.0110	2146	0.0000	0.0000	0.0000	0.0000
45.52	0.0646	0.0642	0.0715	0.0668	2357	0.0000	0.0000	0.0000	0.0000
50.00	0.1706	0.1696	0.1886	0.1763	2590	0.0000	0.0000	0.0000	0.0000
54.93	0.3197	0.3177	0.3534	0.3303	2845	0.0000	0.0000	0.0000	0.0000
60.34	0.4924	0.4894	0.5443	0.5087	3125	0.0000	0.0000	0.0000	0.0000
66.29	0.6648	0.6607	0.7348	0.6868	3433	0.0000	0.0000	0.0000	0.0000
72.82	0.8132	0.8081	0.8989	0.8401	3772	0.0000	0.0000	0.0000	0.0000
79.99	0.9184	0.9127	1.0152	0.9487	4143	0.0000	0.0000	0.0000	0.0000
87.88	0.9680	0.9620	1.0700	1.0000	4552	0.0000	0.0000	0.0000	0.0000
96.54	0.9576	0.9516	1.0585	0.9892	5000	0.0000	0.0000	0.0000	0.0000
106.0	0.8906	0.8851	0.9844	0.9200					
116.5	0.7773	0.7725	0.8592	0.8030					
128.0	0.6330	0.6291	0.6997	0.6540					
140.6	0.4758	0.4728	0.5259	0.4915					
154.4	0.3236	0.3216	0.3577	0.3343					
169.7	0.1924	0.1912	0.2127	0.1988					
186.4	0.0934	0.0928	0.1032	0.0965					

Table A-9: Chitosan particles size distribution. Chitosan Concentration= 1 mg/ mL, CS:TPP =5

Radius (nm)	Distribution Fraction				Radius (nm)	Distribution Fraction			
	Trial 1	Trial 2	Trial 3	Average		Trial 1	Trial 2	Trial 3	Average
3.953	0.0000	0.0000	0.0000	0.0000	204.7	0.2012	0.2110	0.1994	0.2038
4.343	0.0000	0.0000	0.0000	0.0000	224.9	0.1172	0.1229	0.1162	0.1188
4.770	0.0000	0.0000	0.0000	0.0000	247.1	0.0561	0.0588	0.0556	0.0568
5.241	0.0000	0.0000	0.0000	0.0000	271.4	0.0186	0.0196	0.0185	0.0189
5.757	0.0000	0.0000	0.0000	0.0000	298.2	0.0023	0.0024	0.0022	0.0023
6.324	0.0000	0.0000	0.0000	0.0000	327.6	0.0000	0.0000	0.0000	0.0000
6.947	0.0000	0.0000	0.0000	0.0000	359.8	0.0000	0.0000	0.0000	0.0000
7.632	0.0000	0.0000	0.0000	0.0000	395.3	0.0000	0.0000	0.0000	0.0000
8.384	0.0000	0.0000	0.0000	0.0000	434.3	0.0000	0.0000	0.0000	0.0000
9.210	0.0000	0.0000	0.0000	0.0000	477.0	0.0000	0.0000	0.0000	0.0000
10.12	0.0000	0.0000	0.0000	0.0000	524.1	0.0000	0.0000	0.0000	0.0000
11.11	0.0000	0.0000	0.0000	0.0000	575.7	0.0000	0.0000	0.0000	0.0000
12.21	0.0000	0.0000	0.0000	0.0000	632.4	0.0000	0.0000	0.0000	0.0000
13.41	0.0000	0.0000	0.0000	0.0000	694.7	0.0000	0.0000	0.0000	0.0000
14.74	0.0000	0.0000	0.0000	0.0000	763.2	0.0000	0.0000	0.0000	0.0000
16.19	0.0000	0.0000	0.0000	0.0000	838.4	0.0000	0.0000	0.0000	0.0000
17.78	0.0000	0.0000	0.0000	0.0000	921.0	0.0000	0.0000	0.0000	0.0000
19.53	0.0000	0.0000	0.0000	0.0000	1012	0.0000	0.0000	0.0000	0.0000
21.46	0.0000	0.0000	0.0000	0.0000	1111	0.0000	0.0000	0.0000	0.0000
23.57	0.0000	0.0000	0.0000	0.0000	1221	0.0000	0.0000	0.0000	0.0000
25.90	0.0000	0.0000	0.0000	0.0000	1341	0.0000	0.0000	0.0000	0.0000
28.45	0.0024	0.0025	0.0023	0.0024	1474	0.0000	0.0000	0.0000	0.0000
31.25	0.0214	0.0225	0.0212	0.0217	1619	0.0000	0.0000	0.0000	0.0000
34.33	0.0650	0.0681	0.0644	0.0658	1778	0.0000	0.0000	0.0000	0.0000
37.72	0.1352	0.1418	0.1340	0.1370	1953	0.0000	0.0000	0.0000	0.0000
41.43	0.2299	0.2411	0.2278	0.2329	2146	0.0000	0.0000	0.0000	0.0000
45.51	0.3437	0.3604	0.3405	0.3482	2357	0.0000	0.0000	0.0000	0.0000
50.00	0.4688	0.4916	0.4645	0.4750	2590	0.0000	0.0000	0.0000	0.0000
54.93	0.5965	0.6255	0.5910	0.6043	2845	0.0000	0.0000	0.0000	0.0000
60.34	0.7176	0.7525	0.7110	0.7270	3125	0.0000	0.0000	0.0000	0.0000
66.28	0.8236	0.8637	0.8161	0.8345	3433	0.0000	0.0000	0.0000	0.0000
72.82	0.9073	0.9514	0.8990	0.9192	3772	0.0000	0.0000	0.0000	0.0000
79.99	0.9629	1.0097	0.9541	0.9756	4143	0.0000	0.0000	0.0000	0.0000
87.87	0.9870	1.0350	0.9780	1.0000	4551	0.0000	0.0000	0.0000	0.0000
96.53	0.9782	1.0258	0.9693	0.9911	5000	0.0000	0.0000	0.0000	0.0000
106.0	0.9376	0.9832	0.9290	0.9499					
116.5	0.8681	0.9103	0.8602	0.8795					
128.0	0.7747	0.8124	0.7676	0.7849					
140.6	0.6639	0.6962	0.6579	0.6727					
154.4	0.5432	0.5697	0.5383	0.5504					
169.7	0.4207	0.4412	0.4169	0.4263					
186.4	0.3043	0.3191	0.3015	0.3083					

Appendix B: Dynamic light scattering data for chitosan particles size and particles size distribution measurement. Effect of TPP solution pH

Table B-1:Chitosan particles size distribution. Chitosan Concentration= 1 mg/ mL, CS:TPP =5, TPP solution pH=5

Radius (nm)	Distribution Fraction				Radius (nm)	Distribution Fraction			
	Trial 1	Trial 2	Trial 3	Average		Trial 1	Trial 2	Trial 3	Average
3.953	0.0000	0.0000	0.0000	0.0000	204.7	0.2000	0.2098	0.2018	0.2038
4.343	0.0000	0.0000	0.0000	0.0000	224.9	0.1165	0.1222	0.1176	0.1188
4.770	0.0000	0.0000	0.0000	0.0000	247.1	0.0557	0.0585	0.0563	0.0568
5.241	0.0000	0.0000	0.0000	0.0000	271.4	0.0185	0.0194	0.0187	0.0189
5.757	0.0000	0.0000	0.0000	0.0000	298.2	0.0022	0.0024	0.0023	0.0023
6.324	0.0000	0.0000	0.0000	0.0000	327.6	0.0000	0.0000	0.0000	0.0000
6.947	0.0000	0.0000	0.0000	0.0000	359.8	0.0000	0.0000	0.0000	0.0000
7.632	0.0000	0.0000	0.0000	0.0000	395.3	0.0000	0.0000	0.0000	0.0000
8.384	0.0000	0.0000	0.0000	0.0000	434.3	0.0000	0.0000	0.0000	0.0000
9.210	0.0000	0.0000	0.0000	0.0000	477.0	0.0000	0.0000	0.0000	0.0000
10.12	0.0000	0.0000	0.0000	0.0000	524.1	0.0000	0.0000	0.0000	0.0000
11.11	0.0000	0.0000	0.0000	0.0000	575.7	0.0000	0.0000	0.0000	0.0000
12.21	0.0000	0.0000	0.0000	0.0000	632.4	0.0000	0.0000	0.0000	0.0000
13.41	0.0000	0.0000	0.0000	0.0000	694.7	0.0000	0.0000	0.0000	0.0000
14.74	0.0000	0.0000	0.0000	0.0000	763.2	0.0000	0.0000	0.0000	0.0000
16.19	0.0000	0.0000	0.0000	0.0000	838.4	0.0000	0.0000	0.0000	0.0000
17.78	0.0000	0.0000	0.0000	0.0000	921.0	0.0000	0.0000	0.0000	0.0000
19.53	0.0000	0.0000	0.0000	0.0000	1012	0.0000	0.0000	0.0000	0.0000
21.46	0.0000	0.0000	0.0000	0.0000	1111	0.0000	0.0000	0.0000	0.0000
23.57	0.0000	0.0000	0.0000	0.0000	1221	0.0000	0.0000	0.0000	0.0000
25.90	0.0000	0.0000	0.0000	0.0000	1341	0.0000	0.0000	0.0000	0.0000
28.45	0.0023	0.0025	0.0024	0.0024	1474	0.0000	0.0000	0.0000	0.0000
31.25	0.0213	0.0223	0.0215	0.0217	1619	0.0000	0.0000	0.0000	0.0000
34.33	0.0646	0.0677	0.0652	0.0658	1778	0.0000	0.0000	0.0000	0.0000
37.72	0.1344	0.1409	0.1356	0.1370	1953	0.0000	0.0000	0.0000	0.0000
41.43	0.2285	0.2397	0.2306	0.2329	2146	0.0000	0.0000	0.0000	0.0000
45.51	0.3416	0.3583	0.3447	0.3482	2357	0.0000	0.0000	0.0000	0.0000
50.00	0.4660	0.4888	0.4702	0.4750	2590	0.0000	0.0000	0.0000	0.0000
54.93	0.5928	0.6219	0.5983	0.6043	2845	0.0000	0.0000	0.0000	0.0000
60.34	0.7132	0.7481	0.7198	0.7270	3125	0.0000	0.0000	0.0000	0.0000
66.28	0.8186	0.8587	0.8261	0.8345	3433	0.0000	0.0000	0.0000	0.0000
72.82	0.9017	0.9459	0.9100	0.9192	3772	0.0000	0.0000	0.0000	0.0000
79.99	0.9570	1.0039	0.9658	0.9756	4143	0.0000	0.0000	0.0000	0.0000
87.87	0.9810	1.0290	0.9900	1.0000	4551	0.0000	0.0000	0.0000	0.0000
96.53	0.9723	1.0199	0.9812	0.9911	5000	0.0000	0.0000	0.0000	0.0000
106.0	0.9319	0.9775	0.9404	0.9499					
116.5	0.8628	0.9050	0.8707	0.8795					
128.0	0.7700	0.8077	0.7771	0.7849					
140.6	0.6599	0.6922	0.6659	0.6727					
154.4	0.5399	0.5664	0.5449	0.5504					
169.7	0.4182	0.4386	0.4220	0.4263					
186.4	0.3024	0.3172	0.3052	0.3083					

Table B-2:Chitosan particles size distribution. Chitosan Concentration= 1 mg/ mL, CS:TPP =5, TPP solution pH=7

Radius (nm)	Distribution Fraction				Radius (nm)	Distribution Fraction			
	Trial 1	Trial 2	Trial 3	Average		Trial 1	Trial 2	Trial 3	Average
3.953	0.0000	0.0000	0.0000	0.0000	204.7	0.3131	0.3413	0.3170	0.3238
4.343	0.0000	0.0000	0.0000	0.0000	224.9	0.1939	0.2113	0.1963	0.2005
4.771	0.0000	0.0000	0.0000	0.0000	247.1	0.1000	0.1090	0.1012	0.1034
5.241	0.0000	0.0000	0.0000	0.0000	271.4	0.0374	0.0408	0.0379	0.0387
5.757	0.0000	0.0000	0.0000	0.0000	298.2	0.0066	0.0072	0.0067	0.0068
6.324	0.0000	0.0000	0.0000	0.0000	327.6	0.0000	0.0000	0.0000	0.0000
6.948	0.0000	0.0000	0.0000	0.0000	359.8	0.0000	0.0000	0.0000	0.0000
7.632	0.0000	0.0000	0.0000	0.0000	395.3	0.0000	0.0000	0.0000	0.0000
8.384	0.0007	0.0008	0.0007	0.0007	434.3	0.0000	0.0000	0.0000	0.0000
9.210	0.0048	0.0053	0.0049	0.0050	477.1	0.0000	0.0000	0.0000	0.0000
10.12	0.0124	0.0136	0.0126	0.0129	524.1	0.0000	0.0000	0.0000	0.0000
11.12	0.0220	0.0239	0.0222	0.0227	575.7	0.0000	0.0000	0.0000	0.0000
12.21	0.0311	0.0339	0.0315	0.0322	632.4	0.0000	0.0000	0.0000	0.0000
13.41	0.0376	0.0410	0.0381	0.0389	694.8	0.0000	0.0000	0.0000	0.0000
14.74	0.0401	0.0437	0.0406	0.0414	763.2	0.0000	0.0000	0.0000	0.0000
16.19	0.0378	0.0413	0.0383	0.0391	838.4	0.0000	0.0000	0.0000	0.0000
17.78	0.0315	0.0344	0.0319	0.0326	921.0	0.0000	0.0000	0.0000	0.0000
19.53	0.0226	0.0247	0.0229	0.0234	1012	0.0000	0.0000	0.0000	0.0000
21.46	0.0133	0.0145	0.0135	0.0137	1112	0.0000	0.0000	0.0000	0.0000
23.57	0.0056	0.0061	0.0057	0.0058	1221	0.0000	0.0000	0.0000	0.0000
25.90	0.0012	0.0013	0.0012	0.0012	1341	0.0000	0.0000	0.0000	0.0000
28.45	0.0000	0.0000	0.0000	0.0000	1474	0.0000	0.0000	0.0000	0.0000
31.25	0.0000	0.0000	0.0000	0.0000	1619	0.0000	0.0000	0.0000	0.0000
34.33	0.0004	0.0004	0.0004	0.0004	1778	0.0000	0.0000	0.0000	0.0000
37.72	0.0130	0.0142	0.0132	0.0135	1953	0.0000	0.0000	0.0000	0.0000
41.43	0.0460	0.0502	0.0466	0.0476	2146	0.0000	0.0000	0.0000	0.0000
45.52	0.1037	0.1130	0.1050	0.1072	2357	0.0000	0.0000	0.0000	0.0000
50.00	0.1863	0.2031	0.1886	0.1927	2590	0.0000	0.0000	0.0000	0.0000
54.93	0.2909	0.3170	0.2945	0.3008	2845	0.0000	0.0000	0.0000	0.0000
60.34	0.4113	0.4483	0.4164	0.4254	3125	0.0000	0.0000	0.0000	0.0000
66.29	0.5395	0.5881	0.5462	0.5580	3433	0.0000	0.0000	0.0000	0.0000
72.82	0.6659	0.7258	0.6742	0.6886	3772	0.0000	0.0000	0.0000	0.0000
79.99	0.7805	0.8507	0.7902	0.8072	4143	0.0000	0.0000	0.0000	0.0000
87.88	0.8739	0.9525	0.8848	0.9037	4552	0.0000	0.0000	0.0000	0.0000
96.54	0.9380	1.0224	0.9497	0.9700	5000	0.0000	0.0000	0.0000	0.0000
106.0	0.9670	1.0540	0.9790	1.0000					
116.5	0.9577	1.0439	0.9696	0.9904					
128.0	0.9102	0.9921	0.9215	0.9412					
140.6	0.8277	0.9022	0.8380	0.8559					
154.4	0.7167	0.7812	0.7256	0.7412					
169.7	0.5864	0.6391	0.5937	0.6064					
186.4	0.4478	0.4881	0.4534	0.4631					

Table B-3:Chitosan particles size distribution. Chitosan Concentration= 1 mg/ mL, CS:TPP =5, TPP solution pH=9

Radius (nm)	Distribution Fraction				Radius (nm)	Distribution Fraction			
	Trial 1	Trial 2	Trial 3	Average		Trial 1	Trial 2	Trial 3	Average
3.953	0.0000	0.0000	0.0000	0.0000	204.7	0.0403	0.0454	0.0422	0.0427
4.343	0.0000	0.0000	0.0000	0.0000	224.9	0.0000	0.0000	0.0000	0.0000
4.770	0.0000	0.0000	0.0000	0.0000	247.1	0.0000	0.0000	0.0000	0.0000
5.241	0.0000	0.0000	0.0000	0.0000	271.4	0.0000	0.0000	0.0000	0.0000
5.757	0.0000	0.0000	0.0000	0.0000	298.2	0.0000	0.0000	0.0000	0.0000
6.324	0.0000	0.0000	0.0000	0.0000	327.6	0.0000	0.0000	0.0000	0.0000
6.947	0.0000	0.0000	0.0000	0.0000	359.8	0.0000	0.0000	0.0000	0.0000
7.632	0.0000	0.0000	0.0000	0.0000	395.3	0.0000	0.0000	0.0000	0.0000
8.384	0.0000	0.0000	0.0000	0.0000	434.3	0.0000	0.0000	0.0000	0.0000
9.210	0.0000	0.0000	0.0000	0.0000	477.0	0.0000	0.0000	0.0000	0.0000
10.12	0.0000	0.0000	0.0000	0.0000	524.1	0.0000	0.0000	0.0000	0.0000
11.12	0.0000	0.0000	0.0000	0.0000	575.7	0.0000	0.0000	0.0000	0.0000
12.21	0.0000	0.0000	0.0000	0.0000	632.4	0.0000	0.0000	0.0000	0.0000
13.41	0.0000	0.0000	0.0000	0.0000	694.7	0.0000	0.0000	0.0000	0.0000
14.74	0.0000	0.0000	0.0000	0.0000	763.2	0.0000	0.0000	0.0000	0.0000
16.19	0.0000	0.0000	0.0000	0.0000	838.4	0.0000	0.0000	0.0000	0.0000
17.78	0.0000	0.0000	0.0000	0.0000	921.0	0.0000	0.0000	0.0000	0.0000
19.53	0.0000	0.0000	0.0000	0.0000	1012	0.0000	0.0000	0.0000	0.0000
21.46	0.0000	0.0000	0.0000	0.0000	1112	0.0000	0.0000	0.0000	0.0000
23.57	0.0000	0.0000	0.0000	0.0000	1221	0.0000	0.0000	0.0000	0.0000
25.90	0.0711	0.0802	0.0745	0.0753	1341	0.0000	0.0000	0.0000	0.0000
28.45	0.1363	0.1537	0.1428	0.1443	1474	0.0000	0.0000	0.0000	0.0000
31.25	0.1164	0.1312	0.1220	0.1232	1619	0.0000	0.0000	0.0000	0.0000
34.33	0.0403	0.0454	0.0422	0.0427	1778	0.0000	0.0000	0.0000	0.0000
37.72	0.0000	0.0000	0.0000	0.0000	1953	0.0000	0.0000	0.0000	0.0000
41.43	0.0000	0.0000	0.0000	0.0000	2146	0.0000	0.0000	0.0000	0.0000
45.52	0.0000	0.0000	0.0000	0.0000	2357	0.0000	0.0000	0.0000	0.0000
50.00	0.0000	0.0000	0.0000	0.0000	2590	0.0000	0.0000	0.0000	0.0000
54.93	0.0711	0.0802	0.0745	0.0753	2845	0.0000	0.0000	0.0000	0.0000
60.34	0.1363	0.1537	0.1428	0.1443	3125	0.0000	0.0000	0.0000	0.0000
66.29	0.1164	0.1312	0.1220	0.1232	3433	0.0711	0.0802	0.0745	0.0753
72.82	0.0403	0.0454	0.0422	0.0427	3772	0.1364	0.1537	0.1428	0.1443
79.99	0.1446	0.1630	0.1515	0.1531	4143	0.1164	0.1312	0.1220	0.1232
87.88	0.4829	0.5442	0.5059	0.5110	4552	0.0403	0.0454	0.0422	0.0427
96.54	0.8236	0.9282	0.8628	0.8716	5000	0.0779	0.0878	0.0816	0.0824
106.0	0.9450	1.0650	0.9900	1.0000					
116.5	0.7554	0.8514	0.7914	0.7994					
128.0	0.3671	0.4137	0.3846	0.3885					
140.6	0.0451	0.0508	0.0472	0.0477					
154.4	0.0711	0.0802	0.0745	0.0753					
169.7	0.1363	0.1537	0.1428	0.1443					
186.4	0.1164	0.1312	0.1220	0.1232					

Appendix C: Experimental results for rh-EPO release from chitosan nanoparticles in PBS solution. rh-EPO concentration measured by fluorometric assay.

Table C-1: Experimental results for rh-EPO release (trial 1)

Initial rh-EPO mass			8000 IU		
Mass of rh-EPO in supernatant			330.76 IU		
Mass of total loaded rh-EPO=			2707.86 IU		
Sample	Time(h)	Intensity	Concentration (IU/ml)	Total release	Released percent
	0.00	0.00	0.00	0.00	0.00
S1	7.00	4254.00	96.35	385.41	14.23
S2	12.05	914.00	20.70	468.22	17.29
S3	25.58	1696.00	38.41	621.88	22.97
S4	49.58	1914.00	43.35	795.29	29.37
S5	103.28	1519.00	34.41	932.91	34.45
S6	168.58	3938.00	89.20	1289.69	47.63
S7	336.58	5063.00	114.68	1748.40	64.57

Table C-2: Experimental results for rh-EPO release (trial 2)

Initial rh-EPO mass			8000 IU		
Mass of rh-EPO in supernatant			302.16 IU		
Mass of total loaded rh-EPO=			3165.36 IU		
Sample	Time(h)	Intensity	Concentration (IU/ml)	Total release	Released percent
	0.00	0.00	0.00	0.00	0.00
S1	7.00	4173.93	94.54	378.16	11.95
S2	12.05	437.67	9.91	417.81	13.20
S3	25.58	1834.31	41.55	584.00	18.45
S4	49.58	1816.32	41.14	748.56	23.65
S5	103.28	1448.38	32.81	879.78	27.79
S6	168.58	3672.48	83.18	1212.51	38.31
S7	336.58	4499.19	101.91	1620.14	51.18

Table C-3: Experimental results for rh-EPO release (trial 3)

Initial rh-EPO mass			8000 IU		
Mass of rh-EPO in supernatant			349.82 IU		
Mass of total loaded rh-EPO=			2402.86 IU		
Sample	Time(h)	Intensity	Concentration (IU/ml)	Total release	Released percent
	0.00	0.00	0.00	0.00	0.00
S1	7.00	4614.31	104.51	418.06	17.40
S2	12.05	976.68	22.12	506.54	21.08
S3	25.58	1078.94	24.44	604.30	25.15
S4	49.58	1762.06	39.91	763.94	31.79
S5	103.28	1616.10	36.60	910.36	37.89
S6	168.58	4065.45	92.08	1278.69	53.22
S7	336.58	5438.87	123.19	1771.45	73.72

Appendix D: Experimental results for rh-EPO diffusivity study and sample calculation for estimation of rh-EPO diffusivity

Table D-1: Experimental Results from ELISA for rh-EPO standard Curve preparation

EPO Concentration (mU/mL)	Absorbance at 450 nm		Average	– Blank
100	2.0270	1.8510	1.9390	1.8567
50	1.3080	1.2140	1.2608	1.1786
25	0.6760	0.5300	0.6030	0.5208
12.50	0.3900	0.3830	0.3860	0.3038
6.25	0.2190	0.2240	0.2215	0.1392
3.12	0.1470	0.1470	0.1471	0.0649
1.560	0.1010	0.1110	0.1058	0.0236
0.000	0.0780	0.0860	0.0822	0.0000

Table D-2: Experimental data for rh-EPO diffusivity study

Parameter	Value	
Initial mass of rh-EPO loaded in chitsan nanoparticles (M_s^0)	72.302	μg
Mass of rh-EPO remained in the particles after time t (M_s^t)	71.906	μg
Diffusion time (t)	1200	Min
Particles size (R)	200	nm

Effective Diffusivity Calculation of Encapsulation rh-Erythropoietin in chitosan-tripolyphosphate nanoparticles

Initial mass of rh-EPO used for encapsulation= 96 µg

Diffusivity is calculated from the equation 2-16:

$$\frac{M_s^t}{M_s^0} = 1 - \frac{6}{\pi^2} \sum_{n=1}^{\infty} \frac{1}{n^2} \exp\left(-\frac{D_e n^2 \pi^2 t}{R^2}\right) \qquad \text{(D-1)}$$

Equation D-1 is solved to find D_e, using the boundary conditions for infinite liquid phase, where rh-EPO diffused out form the nanoparticles.

'n' assumed to be equal to 1

Total mass of rh-EPO encapsulated:

Absorbance of 1:2000 diluted supernatant sample at 450 nm= 2.722

Concentration of EPO in diluted sample from standard curve (Fig 4-1) = 1094.29 ng/L

EPO Concentration in supernatant = 2188.576 ng /mL = 2.188576 µg / mL

Volume of supernatant = 9.5 mL

Mass of rh-EPO in Supernatant = 9.5 x 2.188576 = 20.7915 µg

Total mass of EPO encapsulated = Initial mass of -EPO – Mass of EPO in Supernatant

$$= 96 \text{ µg} - 20.7915 \text{ µg} = \underline{75.2085 \text{ µg}}$$

Mass of EPO released due to initial burst (first 2 hours)

Absorbance of 1:2000 diluted sample at 450 nm = 0.4805

Concentration of EPO in diluted sample from standard curve (Fig 4-1) = 193.17 ng/L

Concentration of EPO in initial sample = 0.386336 µg/mL

Volume of the sample = 7.5 mL ➜ Mass of EPO released in first 2 hours = 2.898 µg

Total mass of EPO remained in Chitosan-TPP particles(M_s^0) = 75.2085 – 2.898 ➜

$$M_s^0 = 72.3105 \ \mu g$$

Mass of EPO released after 20 hours in PBS solution

Absorbance of 1:2000 diluted sample at 450 nm = 0.066

Concentration of EPO in diluted sample from standard curve (Fig 4-1) = 26.53 ng/L

Concentration of EPO in initial sample = 53.0656 ng/mL

Volume of sample: 7.5 mL ➜ Mass of EPO released after 20 hours = 0.398 µg

Mass of EPO remained in Chitosan-TPP particles M_s^t = 72.3105-0.398 ➜

$$M_s^t = 71.9125 \ \mu g$$

Average radius of particles determined by dynamic Light Scattering = 200 nm

Substituting the values into equation D-1 and solving for D_e :

$$D_e = 2.651 \times 10^{-19} \ m^2 / s$$

REFERENCES

Abdekhodaie M.J, Cheng Y.L, (1997), *"Diffusional release of Dispersed Solute from Planar and Spherical Matrices into Finite External Volume"*, J. Controlled Release, 43, 175-182.

Aoyagi Y., Nakajima M., Ochiai A., Oda T., Ohkohchi N., Satake M., Sugiura S., (2005) *"Size Control of Calcium Alginate Beads Containing living Cells Using micro-nozzle array"*, Biomaterials, 26 (1), 3327-3331.

Arcasoy M.O., (2008), *"The non-hematopoietic biological effects of erythropoietin"*, British Journal of Haematology, 141 (1), 14-31.

Alexabdridou S., Kiparissides C., (1994), *"Production of Oil-Containing Polytereohthaamide Microcapsules by Interfacial Polymerization, An Experimental Investigation of the Effect of Process Variables on the Microcapsule Size Distribution"*, J. Microencapsulation, 11 (6), 603-614.

Allemann E., Gurny R., doelker E.,(1993), *"Drug-Loaded Nanoparticles – Preparation Methods and Drug Targeting Issues"*, European Journal of Pharmaceutics and Biopharmaceutics, 39 (5), 173-191.

Bakan J.A, Anderson J.L, (1976) *" Microencapsulation"* in Lachman L., Alieberman A.H., Kanig L.J., *"Theory and Practice of Industrial Pharmacy"*, 2nd edition, Lea& Febiger.

Bao D.C., Liu X.D., Ma X.J., Xiong Y., Xue W.M., Yu W.T., Yuan Q., (2002), *"Preparation of Uniform Calcium Alginate Gel Beads by Membrane Emulsification Coupled with Internal gelation"*, J. Applied polymer Science, 87 (5), 848-852.

Baruch L., and Machluf M., (2006), *"Alginate-Chitosan complex Coacervation for cell Encapsulation: Effect on Mechanical Properties and on Long-term Viability"*, biopolymers, 82, 570-579.

Benita A., Fickat R., Benoit J.P., Bonnemain B., Samaille J.P., Madoules P., (1984), *"Biodegradable Cross-Linked Albumin microcapsules for embolization"*, J. Microencapsulation, 1 (4), 317-327.

Benoit J.P., Marchais H., (1996), *"Biodegradable Microspheres: Advances in Production Technology"*, in Benita S., *"Microencapsulation: Methods and Industrial Applications"*, Marcel Dekker , USA

Blandino A., Macias M., Cantero D., (1999), "Formation of Calcium Alginate gel Capsules: Influence of Sodium Alginate and $CaCl_2$ Concentration on Gelation Kinetics", J. Bioscience and Bioengineering, 88 (6), 686-689.

Bodmeier R., McGinity W.J., (1987), *"Polylactic acid Microspheres Containing quinidine Base and Quinindin Sulphate Prepared by the Solvent Evaporation Technique. II. Some Process Parameters Influencing the Preparation and Properties of Microspheres"*, J. Microencapsulation, 4 (4), 289-297.

Boogaerts M., (2006), *"Pleiotropic effects of erythropoietin in neuronal and vascular systems"*, Current Medical Research Opinions, 22 (4), 15-22.

Borchard G., (2001), *"Chitosans for Gene Delivery"*, Advanced Drug Delivery Reviews, 52, 145-150.

Briens L.A., Briens C.L., Margaritis A., Hay J., (1997), *"Minimum Liquid Fluidization Velocity in Gas-Liquid-Solid Fluidized Beds Flow Density particles"*, Chemical Engineering Science, 52, 4231-4238.

Broudy V. C., Tait J. F., Powell J. S., (1988), *"Recombinant human erythropoietin: Purification and analysis of carbohydrate linkage"*, Archives of .Biochemistry and .Biophysics, 265 (2), 329-336.

Calvo P., Remunan-Lopez C., Vila-Jato J.L., Alonso M.J., (1997), *"Novel Hydrophilic Chitosan-Polyethylen Oxide Nanoparticles as protein Carriers"*, J. Applied Polymer Science, 63, 125-132.

Capan Y., Woo H. B., Gebrekidan S., Ahmed S., DeLuca P.P., (1999), *"Influence of Formulation Parameters on the Characteristics of Poly(D,L-Lactide-co-Glycolide) Microspheres Containing Poly(L-Lysine) Complexed Plasmid DNA"*, J. Controlled Release, 60, 279-286.

Chai Y., Mei L.H., Wu G.L., Lin D.Q., Yao S.J., (2004), *"Gelation Conditions and transport Properties of Hollow Calcium Alginate Capsules"*, Biotechnology and Bioengineering, 87 (2), 228-233.

Cohen S., Yoshioka T., lucarlli M., Hwang L.H., Langer R.,(1991), *"Controlled Delivery Systems for Proteins Based on Poly(Lactic/Glycolic Acid) Microspheres"*, Pharmaceutical Research, 8 (6), 713-720.

Cooney D.O., (1972), *"Effect of Geometry on the Dissolution of Pharmaceutical Tablets and Other Solids: Surface Detachment kinetics Controlling"*, ALChE J., 18, 446-449.

Crank J., (1975), *"The Mathematics of Diffusion"*, Oxford University Press, UK.

De Kruif G.C., Wienbreck F., de Vries R.,(2004), *"Complex coacervation of proteins and anionic polysaccharides"*, Current opinion in Colloid & Interface Science, 9, 340-349.

114

Desai K. G. H., Park H. J., (2005), *"Recent Developments in Microencapsulation of Food Ingredients"*, Drying Technology, 23, 1361-1394.

Espinosa-Andrews H., Bez-Gonzlez J.G., Cruz-Sosa F., and Vernon-Carter E.J., (2007), *"Gum Arabic-Chitosan Comples Coacervation"*, Biomacromolecules, 8 (4), 1313-1318.

Ghaderi R., Sturesson C., Carlfors J., (1996), *"Effect of Preparative Parameters on the Characteristics of Poly(D,L-Lactiide-co-glycolide)Microsphaeres Made by the Double Emulsion Method"*, International Journal of Pharmaceutics, 141, 205-216.

Fernandez-Uusuno R., Calvo P., Remunan-Lopez C., Vila-Jato J.L., Alonso M.J., (1999), *"Enhancement of Nasal Absorption of Insulin Using Chitosan Nanoparticles"*, Pharmaceutical Research, 16 (10), 1576-1581.

Gan Q., Wang T., Cochrane C., McCarron P., (2005), *"Modulation of Surface Charge, Particles Size and morphological Properties of Chitosan-TPP Nanoparticles Intended for Gene Delivery"*, Colloids and Surfaces B: Biointerfaces, 44, 66-73.

Gan Q., Wang T., (2007), *"Chitosan Nanoparticles as Protein Delivery Carrier-Systematic Examination of fabrication Conditions for Efficient Loading and Release"*, Colloids and Suefaces B: Biointerfaces, 59, 24-34.

Guliyeva, U., Oener, F., Oezsoy, S., et al. (2006) *Chitosan microparticles containing plasmid DNA as potential oral gene delivery system*. Eur.J.Pharm.Biopharm. *62*, 17-25.

Hahn K.S., Oh J.E., miyamoto H., Shimobouji T., (2006), *"Sustained Release Formulation of Erythropoietin using Hyaluronic Acid Hydrogel Crosslinked by Michael Addition"*, International Journal of Pharmaceutics, 322, 44-51.

Heller J., Baker R.W., Gale R.M., Rpdin J.O., (1978), *"Controlled Drug Release by Polymer Dissolution. I. Partial Easters of Maleic Anhydride Copolymers- Properties and Theory"*, J. Applied polymer Science, 22, 1991-2009.

Herrero E.P., Martin Del Valle E.M., Galan M.A., (2006), *"Development of a New Technology for the Production of Microcapsules Based in Atomization Process"*, Chemical Engineering Journal, 117, 137-142.

Hillery A.M.,(2001), *" Advanced Drug Delivery and Targeting: An Introduction"*, in Hillery A.M., Lloyd A.W., Swarbrick J., *"Drug Delivery and Targeting for Pharmacists and Pharmaceutical scientists"*, Taylor & Francis, London, UK.

Jalil R., Nixon J. R., (1990), *"Biodegradable Poly(lactic acid) and Poly(lactide-co-glycolide) Microcapsules: Problems Associated with Preparative Techniques and Release Properties"*, J. Microencapsulation, 7 (3), 297-325.

Jelkmann W., (1992), *"Erythropoietin: Structure, Control of Production, and Function"*, Physiological Reviews, 72, 449-489.

Katchedler I., Hoffman A., Goldberger A., Friedman M., (1997), *"Modeling of Drug Release from Erodible Tablets"*, J. Pharmaceutical Sciences, 86 (1), 110-115.

Kilonzo P., Margaritis A., Yu J.T., Ye Q., (2007), *"Bioethanol Production from Starchy Biomass by Direct fermentation Using Saccharomyces Diastaticus in Batch free and Immobilized Cell Systems"*, International Journal of Green energy, 4, 1-14.

Kwok K.K., Groves J.M., Burgess J.D., (1991), *"Production of 5-15 µm Diameter algnate-Polylysine Microcapsules by an Air-atomization Technique"*, Pharmaceutical Research, 8 (3), 341-344.

Lai, P. H., Everett, R., Wang, F. F., Arakawa T., Goldwasser E (1986), *"Structural characterization of human erythropoietin"*. J .Bioogical .Chemistry, 261, 3116-3121

Lee P.I, (1980), *"Diffusional Release of Solute from a Polymeric Matix- Approximate Analytical Solutions"*, J. Membrane Science, 7, 255-275.

Lee K.Y., Kwon I.C., Kim Y.H., Jo W.H., Jeong S.Y., (1998), *"Preparation of Chitosan Self-Aggregates as a gene Delivery System"*, J. Controlled release, 51, 213-220.

Lee J.H, Park T.G., Choi H.K., (2000), *"Effect of Formulation and Process Variables on the Characteristics of Microsphere for Water-Soluble Drugs Prepared by W/O/W Double Emulsion Solvent Diffusion Method"*, International Journal of Pharmaceutics, 196, 75-83.

Li D.X., Oh Y., Lim, S., Kim J. O., Yang H. J., Sung J. H., Yong C. S., Choi H., (2008a) *"Novel Gelatin Microcaapsule with Bioavailability Enhancement of Ibuprofen using Spray-Drying Technique"*, International Journal of Pharmaceutics, 355, 277-288.

Li X.M., Xu Y.L., Chen G.G., Wei P., Ping Q.N., (2008b), *"PLGA Nanoparticles for the Oral Delivery of 5-fluorouacil Using High Pressure Homogenization-Emulsification as the Preparation Method and in Vitro/in Vivo Studies"*, Drug Development and Industrial Pharmacy, 34, 107-115.

Lin, F. K., Suggs, S., Lin, C. H., Brown J.K, Smalling R., Egrie J.C., Chen K.K., Fox G.M., Martin F., Stabisky Z., (1985), *"Cloning and expression of the human erythropoietin gene"* Proceedings of the National Academy of Sciences of the United States of America, 82 (22), 7580-7584.

Liu F., Liu L., Li X., and Zhang Q.,(2007), *"Preparation of chitosan-hyaluronate double-walled microspheres by emulsification-coacervation method"*, Journal of Material Science, 18, 2215-2224.

Magdassi S., Vinetsky Y., (1996), *"Microencapsulation of Oil-in-Water Emulsions by Proteins"*, in in Benita S., *"Microencapsulation: Methods and Industrial Applications"*, Marcel Dekker , USA.

Manocha B., Margaritis A., (2008), *"Production and Characterization of gamma-Polyglutamic Acid Nanoparticle for Controlled Release of Anticancer Drugs"*, Critical Reviews in Biotechnology, 28 (1), 83-99.

Mao S., Shi Y., Li L., Xu J., Schaper A., Kissel T., (2008), *"Effects of Process and Formulation Parameters on Characteristics and Internal Morphology of Poly (D,L-Lactide-co-Glycolide) Microspheres Formed by the Solvent Evaporation Method"*, European Journal of Pharmaceutics and Biopharmaceutics, 68, 214-223.

Margaritis A., kilonzo P., (2005)," *Production of Ehtanol Using Immobilized Cell Bioreactor Systems"* in *"Applications of cell immobilization technology"*, Nedovic V and Willaert R. (Eds), Springer, Dorchet, The Netherlands. 375-495.

Mathieu F., Ugazio S., Carnelle g., Ducini Y., and Legrand J., (2006), *"Complex Coacervation of the Gelatin-Poly(acrylic acid) System"*, Journal of Applied Polymer Science, 101, 708-714.

Mayya Ks., Bhattacharyya A., and Argillier J-F, (2003),*"Micro-encapsulation by complex coacervation: influence of surfactant"*, Polymer Internation, 52, 644-647.

Merchant F.J.A., Margaritis A., Wallace J.B., Vardanis A., (1987), *"A Novel Technique for Measuring Solute Diffusivities in Entrapment Matrices Used in Immobilization"*, Biotechnology and Bioengineering, 30, 936-945.

Millman J.S., (1992), "Diffusivity Characteristics of Globular Proteins in Calcium Alginate Immobilization Matrices", (M.E.Sc thesis) The University of Western Ontario, London, Ontario, Canada.

Miyake T., Kung C. K. H., Goldwasser E. (1977), *"Purification of human erythropoietin"*, J. Biological Chemistry, 252 (15), 5558-5564.

Mocini M., Leone T., Tubaro M., Santini M., and Penco M., (2007),*"Structural, Production and Function f Erythropoietin: Implications for Therapeutical Use in Cardiovascular Disease"*, Current Medicinal Chemistry, 14, 2278-2287.

Morlock M., Koll H., Winter G., Kissel T., (1997), *"Mocroencapsulation of rh-Erythropoietin, Using Biodegradable Poly(D,L-Lactide-co-Glicolide): Protein Stability and the Effects of Stabilizing Excipients"*, European Journal of Pharmaceutics and Biopharmaceutics, 43, 29-36

O'Donnell B.P.., McGinity W.J., (1997), *"Preparation of Microspheres by Solvent Evaporation Technique"*, Advanced Drug Delivery Reviews, 29, 25-42.

Pilkington P.H., Margaritis A., Mensour N.A., (1998a), "*Mass transfer Characteristics of Immobilized cells Used in Fermentation Processes*", CRC Crit. Rev. Biotech., 18 (2), 237-255.

Pilkington P.H., Margaritis A., Mensour N.A. Russell I., (1998), "*Fundamentals of Immobilized Yeast Cells for continuous Beer Fermentation: A Review*", J. Inst. Brew., 104, 19-31.

Pistel k.F., Bittner B., Koll H., Winter G., Kissel T., (1999), "*Biodegradable Recombinant Human Erythropoietin Loaded Microspheres Preparaed from Linear and Star-Branched Block Copolymers: Influence of Encapsulation Technique and Polymer Composition on Particle Characteristics*", J. Controlled release, 59, 309-325.

Prata A.S., Menut C., Leydet A., trigo J.R., and Grosso R.F.,(2008), "*Encapsulation and release of a fluorescent probe, khusimyl dansylate, obtained from vetiver oil by complex coacervation*", Flavor and Fragrance Journal, 23, 7-15.

Rao B.S., Sharma P.C.,(1997), "*Use of Chitosan as a biomaterial: Studies on its safety and Henostatic Potential*", J. Biomedical Materials research, 34, 21-28.

Romanowski R.R., Sytkowski A.J., (1994), "*Molecular Structure of Human Erythropoietin*", Hematology/Oncology Clinics of North America, 8 (5), 885-894.

Sadek P., (1996) "The HPLC Solvent Guide", John Wiley & Sons, USA.

Sah H., Chien Y.W., (2001), "Rate Control in Drug Delivery and targetin: Fundamentals and Applications to Implantable Systems", in Hillery A.M., Lloyd A.W., Swarbrick J., "*Drug Delivery and Targeting for Pharmacists and Pharmaceutical scientists*", Taylor & Francis, London, UK.

Sieomann J., Peppas N.A., (2001), "*Modeling of Drug Release Systems Based on Hydroxypropyl Methylcellulose (HPMC)*", Advanced Drug Delivery Reviews, 48,139-157.

Sinha V.R., Singla A.K., Wadhawan S., Kaushika R., kumria R., Bansal K., Dhawan S., (2004), "*Chitosan microspheres as a Potential Carrier for Drugs*", International Journal of Pharmaceutics, 274, 1-33.

Szepesi G., (1992), "*How to Use Reverse-Phase HPLC*", VCH Publishers, USA.

Takeuchi M., Inoue, N., Strickland, T. W., Kubota m., Wada M., Shimizu R., Hoshi S., Kozutsumi H., Takasaki S., Kobata A., (1989), " *Relationship between sugar chain structure and biological activity of recombinant human erythropoietin produced in Chinese Hamster Ovary cells*" Proceedings of the National Academy of Sciences of the United States of America, 86, 7819-7822.

Tamilvanan S., Sa B., (1999), *"Effect of Production Variables on the Physical Characteristics of Ibuprofen-Loaded Polystyrene Microparticles"*, J. Microencapsulation, 16 (4), 411 – 418.

Thies C., (1994), *"A Survey of Microencapsulation Processes"*, in Benita S., *"Microencapsulation: Methods and Industrial Applications"*, Marcel Dekker, USA.

Tsifanskt M..D., Yeo Y., Evgenov O.V., Bella E., Benjamin J., Kohane D.S.,(2008) , " Microparticles for Inhalation Delivery of Antipseudomonal Antibiotics", The American Association of Pharmaceutical Scientists Journal, 10 (2), 254-260.

Vander Meer P, Voors A.A., Lipsic E., Van Gilst H.W., van Velduisen D.J., (2004) *"Erythropoietin in Cardiovascular Diseases"*, European Heart Journal, 25, 285-291.

Viseras C., Cela R., Barraso C.G., Perez-Bustamante J.A., (1987), *"Influence of Temperature in Reverse-Phase High Performance Liquid Chromoatograohy with Gradient Elution"*, Analytica Chimica Acta, 196, 115-122.

Walsh G., *"Biopharmaceuticals- Biochemistry and Biotechnology."* 2^{ed} Ed. (2003) John Wiley.

Weinbreck F., de Vries r., Schrooyen P., and de Kruif C.G., (2003), *"Complex coacervation of Whey Protiens and Gum Arabic"*, Biomacromolecules, 4 (2), 293-303.

Weiland-Berghausen S., Schote U., Frey M., Schmidt F., (2002), *"Comparison of Microencapsulation Technique for the Water-Soluble Drugs Nitenpyram and Clomipramine HCl"*, J. Controlled Release, 85, 35-43.

Wells L.A., Sheardown H.,(2007), *"Extended release of high pI Proteins from Alginate Microspheres via a novel Encapsulation Technique"*, European Journal of Pharmaceutics and Biopharmaceutics, 65, 329-335.

Xu Y., Du Y., (2003), *"Effect of Molecular Structure of Chitosan on Protein Delivery Properties of Chitosan Nanoparticles"*, International Journal of Pharmaceutis, 250, 215-226.

Zhao H., Gagnon J., Häfeli U., (2007), *"Process and Formation Variables in the Preparation of Injectable and Biodegradable Magnetic Microspheres"*, Biomagnetic Research and Technology, 5 (2), 2-12.